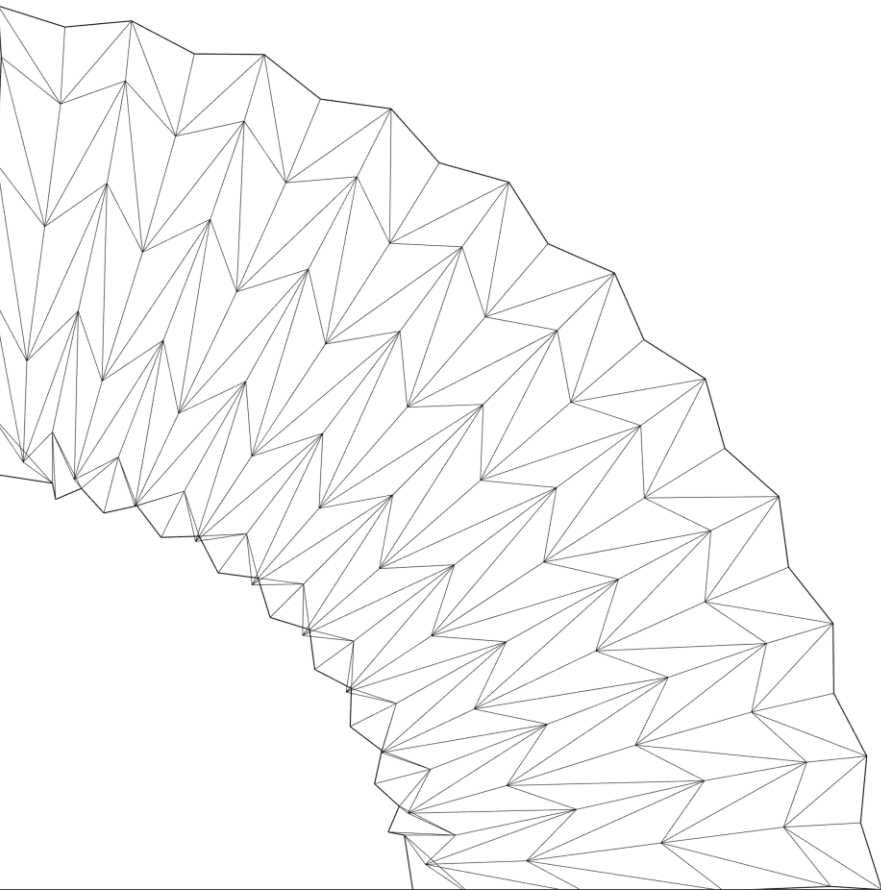

Adaptive Forms: Origami Geometry in Responsive Architecture



ALMA MATER STUDIORUM - UNIVERSITÀ DI BOLOGNA

SCHOOL OF ENGINEERING AND ARCHITECTURE

DEPARTMENT OF ARCHITECTURE

SECOND CYCLE DEGREE IN BUILDING ENGINEERING-ARCHITECTURE

MASTER'S THESIS

in

Architectural Design and Composition III

Adaptive Forms: Origami Geometry in Responsive Architecture

CANDIDATE:

Parisa Kazemi

SUPERVISOR:

Prof. Alessio Erioli

Academic Year 2024/25

Session III

Table of Contents

01 Introduction	4
<i>01 Introduction</i>	5
2 Conceptual Framework	6
<i>2.1 Introduction to Responsive Architecture</i>	7
<i>2.2 Approaches to Responsiveness in Architecture</i>	12
<i>2.3 Responsiveness Through Kinetic Mechanisms</i>	13
03 Origami: Geometry, Mechanics, and Design Potential	16
<i>3.1 Origami Origin</i>	17
<i>3.2 Origami Technical Terms</i>	18
<i>3.3 Origami Tessellation</i>	21
<i>3.4 Origami Application in Design</i>	25
04 Case Studies	26
05 Design Process	49
<i>5.1. Exploration of Origami Folds and Geometries</i>	50
<i>5.2 Parametric Modelling and Simulation Process</i>	71
<i>5.3 Patterns Behaviour</i>	74
<i>5.4 Deformation in members</i>	96
<i>5.5 Conclusion</i>	102
06 Design Implementation	103
<i>6.1 Integration into Real-World Applications</i>	104
<i>6.2 Selected Case Studies</i>	104
<i>6.3 Form Finding through Clustering</i>	108
<i>6.4 Design Strategies for Responsiveness and Adaptation</i>	110
<i>6.5 Possible Applications</i>	111
<i>6.6 Material and Construction</i>	113
<i>6.7 Imaginary Scenario of Application</i>	117
07 Conclusion	119
References	121

01 | Introduction

01 Introduction

Architectural environments have long demonstrated a need for greater flexibility, prompting numerous attempts over the past decades to create buildings capable of adjusting to changing climatic, spatial, and programmatic conditions. The introduction of digital tools, computational design, and emerging technologies has expanded the possibilities of responsive architecture, offering new materials, smart systems, and innovative structural solutions. While many of these approaches have been implemented in both temporary installations and large permanent buildings, their broader applicability often remains restricted. High technological complexity, elevated costs, and reliance on rigid mechanical components limit the scalability and accessibility of most responsive systems. In contrast, origami-based design offers a materially efficient, low-cost, and geometrically intelligent alternative—one that has the potential to introduce responsiveness not only in advanced prototypes, but also in everyday architectural environments. Within this context, the thesis proposes origami geometry as a promising pathway toward more adaptable and widely implementable architectural systems. To explore this potential, the thesis investigates how origami principles can be translated into architectural strategies that enable controlled transformation.

Origami offers a unique combination of structural flexibility, spatial modulation, and formal precision, allowing surfaces to fold, expand, or reorient in response to external conditions. By examining key folding typologies, computationally modelling deployable patterns, and developing physical prototypes, the research seeks to identify how origami mechanisms can support movement at architectural scales without relying only on actuators. The focus lies on understanding the relationship between geometric patterning, kinematic behaviour, and functional performance, establishing a design methodology for adaptive surface systems.

Through this investigation, the thesis ultimately engages with the broader question of what it means for architecture to be responsive. Responsiveness is not simply the capacity to move; it is the ability of a system to meaningfully adjust its form, performance, or orientation in relation to environmental stimuli or user interaction. Origami-based geometries offer a pathway toward such responsiveness by embedding adaptability into the structure itself, enabling transformations that are lightweight, efficient, and inherently programmable. By demonstrating how folding logics can support dynamic modulation of space, light, airflow, or enclosure, the thesis aims to contribute to a shift toward more adaptable architectural environments—spaces capable not only of accommodating change but actively participating in it.

2| Conceptual Framework

2.1 Introduction to Responsive Architecture

2.2 Approaches to Responsiveness in Architecture

2.3 Responsiveness Through Kinetic Mechanisms

2.1 Introduction to Responsive Architecture

Norbert Wiener In his book *Cybernetics*, first published in 1948, established the theoretical foundations for the multidisciplinary field of cybernetics. the study of controlling the flow of information in systems with feedback loops, whether biological, mechanical, cognitive, or social. At the core of his theory is the message, sent and responded to, where the quality of communication determines the system's ability to maintain equilibrium.(Wiener, 2019) Applied to architecture, cybernetic principles define roles, hierarchies, and feedback mechanisms within a building, transforming it into a performative, adaptive system capable of responding intelligently to changing conditions.(Herdt, 2021)

In the early 1960s, Gordon Pask, and other cyberneticians made advancements toward understanding and identifying the field of interactive architecture by formulating their theories on the topic. Pask's conversation theory informed much of the original development in interactive architecture, basically establishing a model by which architects interpreted spaces and users as complete feedback systems. Cybernetic theory continued to be developed into the late sixties and early seventies by the likes of Warren Brody, Nicholas Negroponte, Charles Eastman, Andrew Rabeneck, and others, who expanded upon the earlier ideas of Wiener and Pask. Cedric Price was perhaps the most influential of the early architects to adopt the initial theoretical work in cybernetics, expanding it into the architectural concept of anticipatory architecture. John Frazer extended Price's ideas in positing that architecture should be a "living, evolving thing." (Fox, 2016)

When speaking of Cedric Price, it is impossible to ignore the Fun Palace; a system designed in conjunction with the theatre producer Joan Littlewood. In Fun Palace all the components are constantly moved by a crane system that allows the complete transformation of the complex. (Hernández Vargas, 2015) The design focused on a simple open structure rather than an enclosed monument capable of quick responses to the user's desires.(Schmidt and Austin, 2016)

2| Conceptual Framework

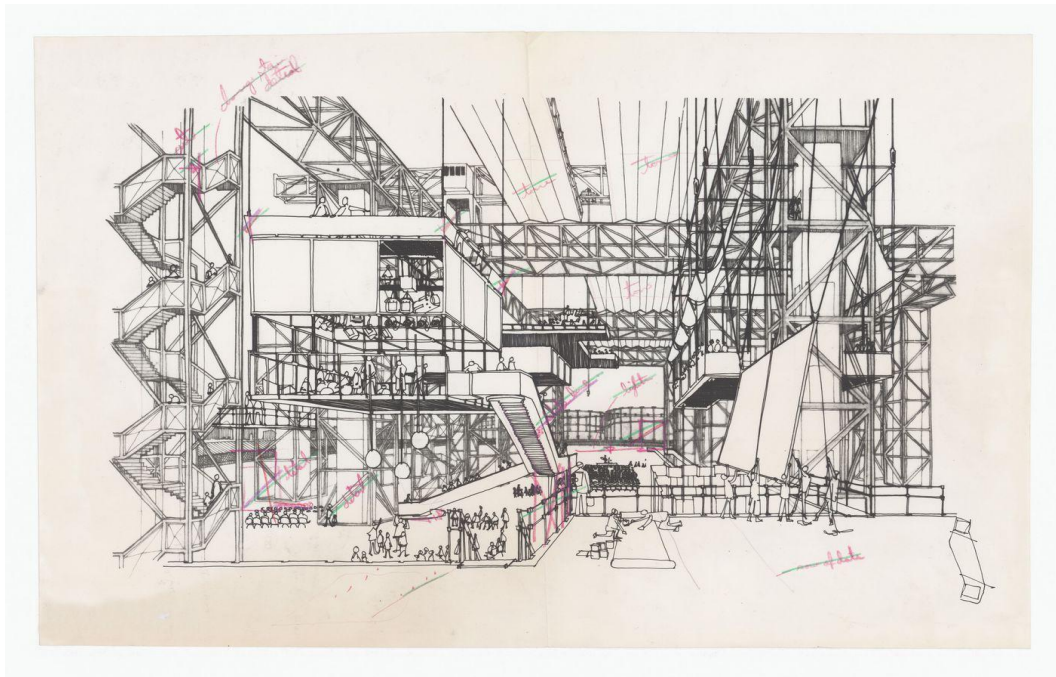


Fig.2.1: Perspective drawing of Cedric Prices “Fun Palace.”(Price, 1960-1964)

To materialize the dynamics within the Fun Palace, Joan Littlewood invited Gordon Pask to be part of the project team who would later become a central figure of the cybernetic committee. In 1976, ten years after the rejection of the proposal for the Lea Valley, Price officially ended the Fun Palace project. This decision was because the project was originally planned to have a ten-year life cycle after which technological advancement and variations in social requirements would render it obsolete. (Hernández Vargas, 2015)

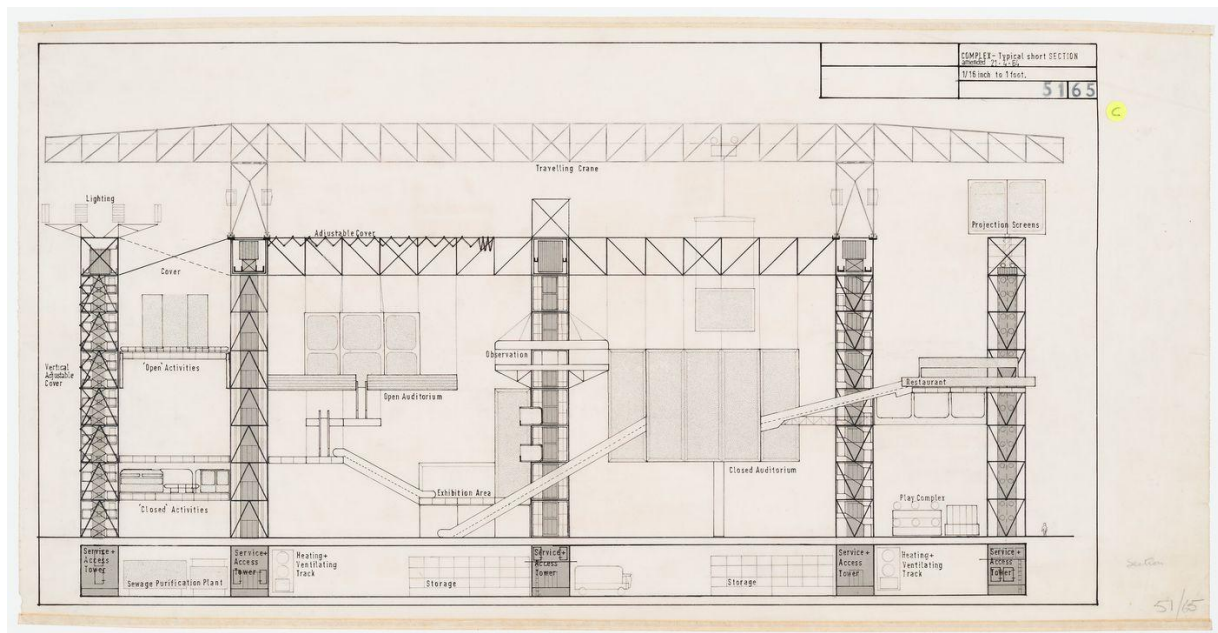


Fig. 2.2: Section drawing of Cedric Prices “Fun Palace.” (Price, 1964)

2| Conceptual Framework

Cedric's next project The Generator was developed in collaboration with John and Julia Frazer and Cristiano Ceccato and explored a reconfigurable complex that accommodate company activities, cultural events, and artist residencies composed of 150 cubes of 3.6 meters that are subdivided and grouped in standard modules project is configured on a tartan grid of 4 × 4 meters, composed of a 3.6 meters module plus a 0.3 meters separation. This tartan type fabric had already been used in the structural system of the Fun Palace;¹⁵ designed under the guidance of Frank Newby (Fig. 03). (Mathews, 2007)

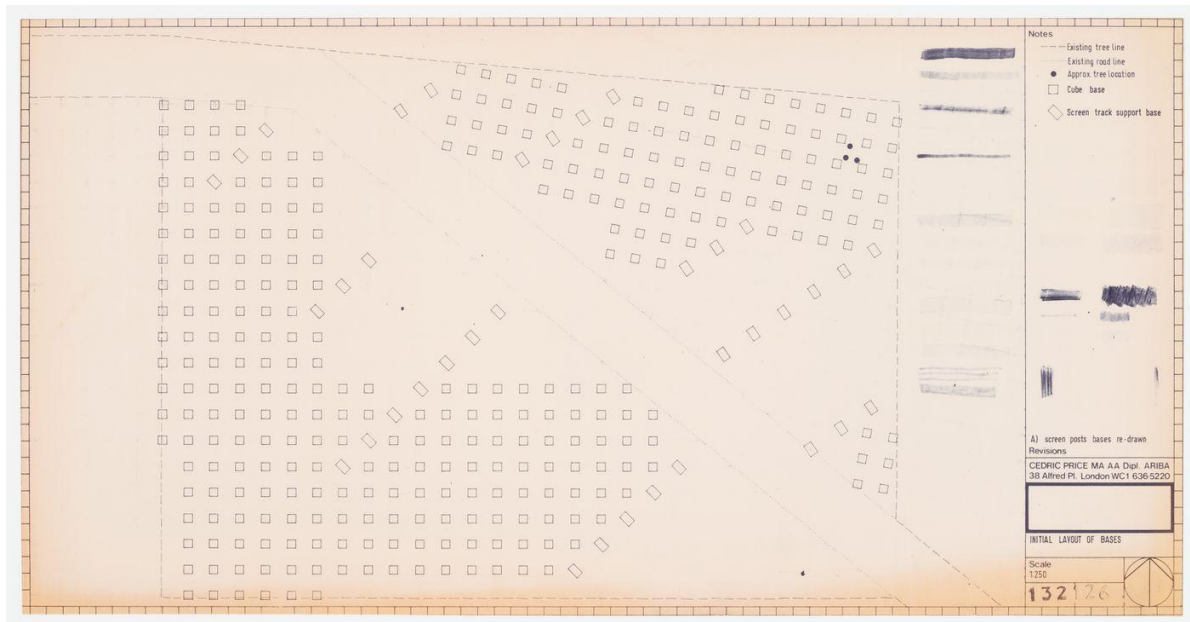


Fig. 2.3 Generator project, White Oak Plantation, Yulee, Florida: grid layout, Menu 23 and External Spaces (Price, 1976-1979)

While the Generator seems to be a much simpler project, its control and transformation system is much more complex and arrives at a level of definition far superior to that of the Fun Palace, even though neither of the two projects possesses a specific plan. (Hernández Vargas, 2015)

In John Frazer's words: "The real difficulty with the Fun Palace was not that no-one knew what it might look like, but that it was never clear how it would be controlled and who would have the fun of controlling all the gantries and moving parts. However, the GENERATOR offers a clear programme of how, and why change is produced and how these variations might affect the environment." (Hardingham, 2003)

2| Conceptual Framework

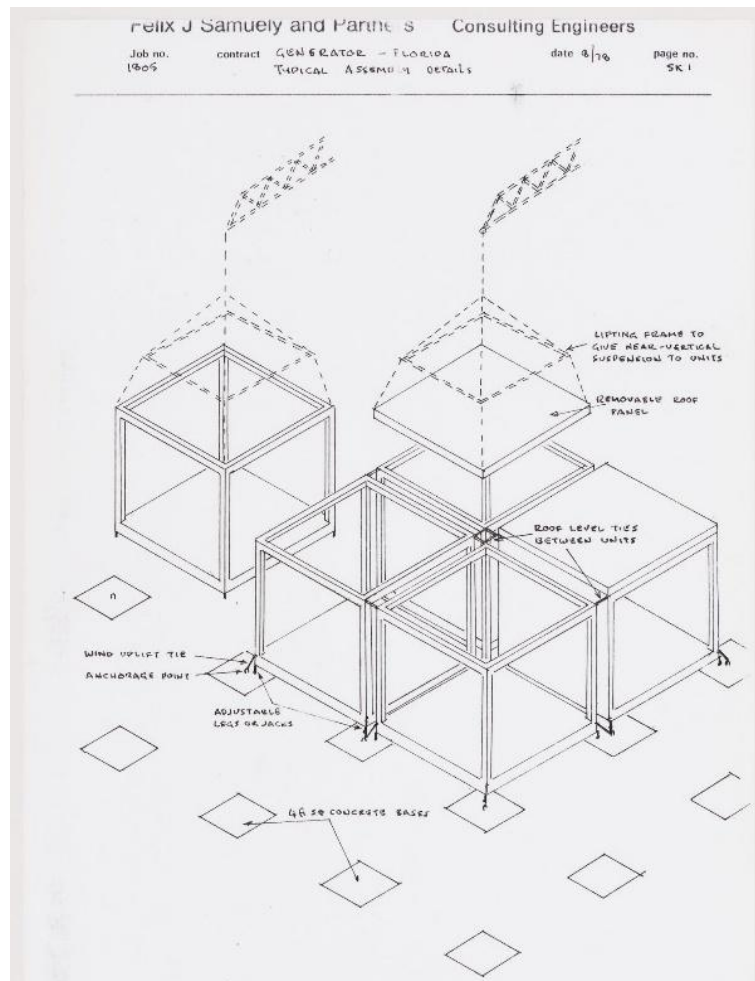


fig.2.4 Generator: Axonometric showing typical assembly details. (Price, 1978)

Published as the first intelligent building, the Generator is in fact, the first project that precisely addresses a dynamic building capable of interacting with project users. (Hernández Vargas, 2015) Beyond enabling users, both Price and the Frazers intended for the system itself to suggest its own reconfigurations, introducing a form of non-human agency within the built environment. (Liu Cheng, 2023) The system could generate unsolicited proposals for new arrangements—responding not only to user input and patterns of activity but also activating a built-in “boredom” mechanism that triggered reconfigurations when no changes occurred for some time. Conceived as a heuristic program, it was intended to refine its strategies over time, learning from experience and adjusting its organizational logic based on user feedback. (L, 2008)

Although the Generator Project was never realized, it stands as the first clear example of an architectural experiment concerned with bidirectional communication between human and non-human agents, positioning it as a foundational precursor to later concepts of architectural intelligence. (Liu Cheng, 2023)

Aside from the more visionary theorists mentioned above and a number of architects attempting to project them into an architectural horizon, the notion of intelligence in the context of interactive environments revolved around a central control system for

everything; these systems were called “smart environments.”(Fox and Kemp, 2009) In the 1990s there were “smart home” and “smart workplace” projects being initiated at every turn that relished the newly available technologies. For the first time, wireless networks, embedded computation, and sensor effectors became both technologically and economically feasible to implement by computer science. (Fox, 2016) The interactive architecture workshop at the Bartlett School of Architecture was initiated in the early 1990s as a pioneering forum for actual architectural pursuits under the guidance of Stephen Gage. In the late 1990s, the long-standing exploration of kinetics in architecture was revisited, based on the idea that performance could be enhanced by utilizing newly available computational data and processing to enable physical adaptation. Architecture began re-examining traditional kinetic aesthetics, integrating technological advancements, notably driven by Robert Kronenberg, who organized a series of exhibitions and conferences on transportable environments. concepts of motion, stasis, and order were questioned, redefined, and reshaped by the new possibilities and strategies introduced by technological innovations, especially those related to mobility and transportation in contemporary nomadic cultures. The renewed focus on adaptable architecture was propelled by the evolving ways in which humans interact with the built environment, influenced by technological progress. (Fox and Kemp, 2009)

William Zuk and Roger Clark state in their book *Kinetic Architecture* that “our present task is to unfreeze architecture, to make it a fluid, vibrating, changeable backdrop for the varied and constantly changing modes of life. An expanding, contracting, pulsating, changing architecture would reflect life as it is today and therefore be part of it.”(Zuk and Clark, 1970)

2.2 Approaches to Responsiveness in Architecture

Architectural responsiveness can be realized through a range of design strategies, each enabling buildings to sense, interpret, and adapt to changing conditions in ways appropriate to both the type of stimulus and the scale of the structure. Depending on these parameters, responsiveness may be expressed as morphological transformations, adaptive environmental control, or active spatial reconfiguration. The principal approaches through which responsiveness is typically achieved include:

- **material-based systems:** Material-based responsiveness now increasingly leverages programmable, architected materials that dynamically adjust their form or behaviour in response to environmental stimuli, without relying on complex mechanical systems. For example, advanced architected materials can be “encoded in time,” meaning they evolve after fabrication in response to heat, humidity, or chemical changes, demonstrating built-in temporal adaptability.(Xia, Spadaccini and Greer, 2022)
- **environmental and cybernetic systems:** Architectural responsiveness grounded in environmental and cybernetic systems is based on feedback-driven control, where buildings sense, interpret, and adapt to their surroundings in real time. This paradigm draws on cybernetic theory that already in chapter 2.1 of this thesis was covered.
- **computationally driven systems:** Computationally driven responsive systems employ digital models, algorithmic logic, and real-time data processing to adapt building behaviour. These systems often combine parametric design with machine learning and multi-agent simulation to interpret environmental and occupancy inputs, enabling adaptive responses in lighting, shading, ventilation, or spatial layout.(Karakoç and Çağdaş, 2021)
- **mechanical or kinetic systems:** Mechanical or kinetic responsiveness in architecture refers to systems that physically move—through actuators, hinges, sliding or rotating components, and other mechanical mechanisms—to adapt to environmental conditions or user requirements. Kinetic architecture is fundamentally concerned with motion, in which parts of a building, such as façades, walls, or roofs, are designed to translate, rotate, or deform in a controlled and purposeful manner. This approach not only enables functional adaptability but also creates dynamic spatial experiences.(Akgün, Erkarıslan and Kavuncuoğlu, 2022) In the following chapter, this thesis will examine kinetic and mechanically driven systems in greater detail, exploring their design principles, typologies, and applications in responsive architecture.

2.3 Responsiveness Through Kinetic Mechanisms

The ability to not only monitor but also physically control environments is unveiling important implications and applications. There is great potential for dynamic architecture that arises from understanding what a space or object is currently doing and how it can aid in promoting or accommodating a specific task. Some of this understanding relates to dynamically changing architectural elements or spatial layouts that address desires to have public or private space, to optimize thermal, visual, lighting, and acoustic conditions, and to promote sharing or collaboration in space. (Fox and Kemp, 2009)

Robert Kronenberg defines kinetic Architecture as “systems as buildings or building components with variable mobility, location, and/or geometry.”(Kronenburg, Lim and Chii, 2003) While kinetic architecture’s modern roots are split between the utopian visions of Sant’Elia’s futurism and Leonidov’s constructivism and expressionism, its conceptual roots lie in the portable structures of prehistoric times. Kinetic architecture encapsulates the ability to change its shape and location – from the scale of a component to the entire building – in response to changing conditions. The strand grows from the creative desire for unlimited architectural freedom.(Schmidt and Austin, 2016)

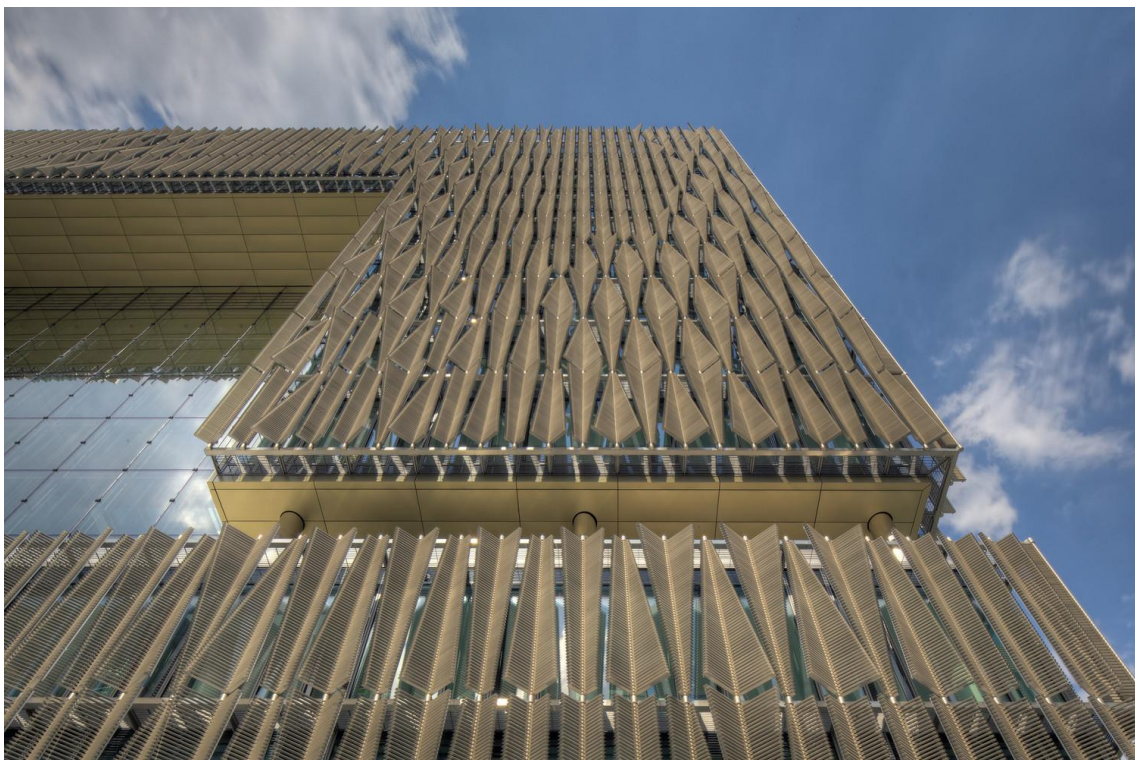


Fig2.5: Q1, ThyssenKrupp Quarter Essen Kinetic facade element({ArchDaily}, 2013)

2| Conceptual Framework

Kinetic principles have been explored across a wide range of architectural programs and scales, illustrating how movement can serve functional, environmental, and experiential goals. The most impressive ones have been applied as responsive facades. The responsive facades act as a filter between the interior and the exterior, which control the shade, sunlight, ventilation and even the view. The well-known examples of the responsive facades applied in architecture are the Al Bahr Towers in Abu Dhabi, the Arab World Institute in Paris, the Q1 Thyssenkrupp Headquarter in Essen, the Kiefer Technic Showroom in Bad Gleichenberg and the Thematic Pavilion EXPO 2012 in Yeosu.(Some of the buildings mentioned here are examined in greater depth in Section 4 as case studies within this thesis.)(Maden, 2019) On the other hand, responsive structures used for roofs, shelters or canopies also offer various functional and spatial solutions in architecture. Mostly preferred in temporary buildings, pavilions, exhibitions, sports venues and recreation facilities, these structures can transform from one configuration to another in response to changing environmental conditions or spatial and functional have potentials for compact storage and transportability. (Maden, 2019)

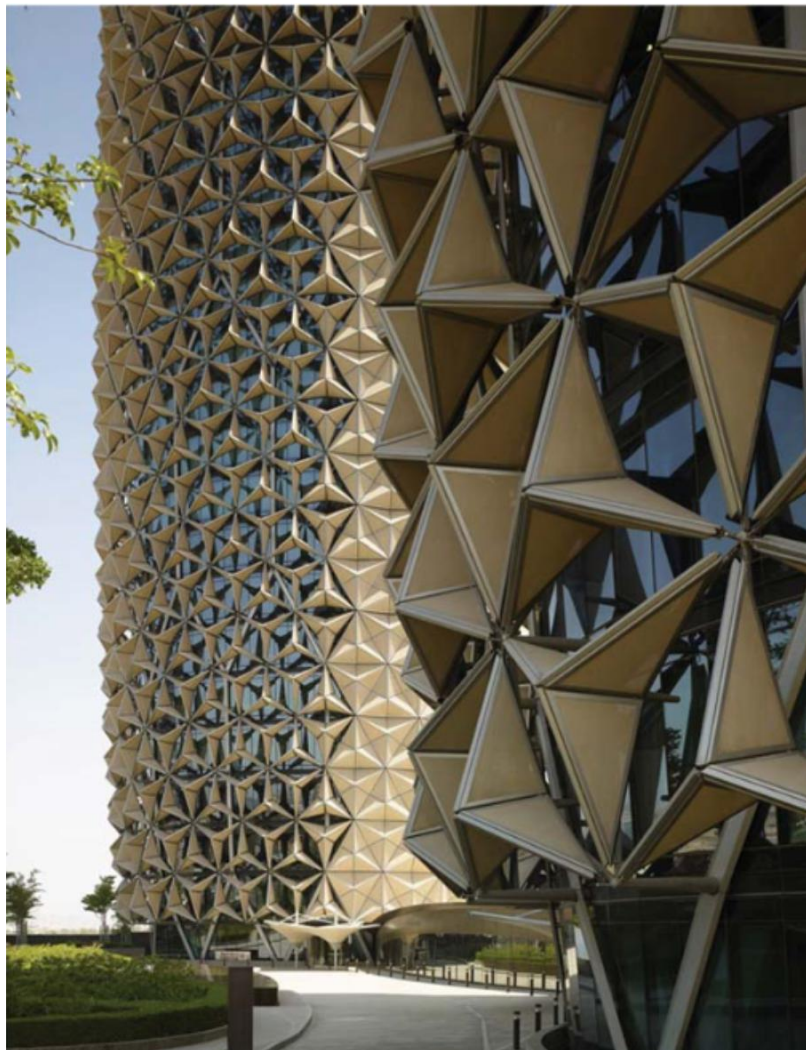


Fig.2.5 The Façade elements of the Al-Bahr Towers as seen from the outside(Karanouh and Kerber, 2015)

2| Conceptual Framework

The kinetic mechanisms include two types: spatial-real movement and non-spatial-material deformation. The former presents basic movement—folding, sliding, rolling, expanding and transforming—by changing the axis, strength and direction of kinetic elements. The latter uses smart materials driven by their molecules' ability to change form, function or appearance.(Megahed, 2016) In the kinetic architecture literature, the most prevalent interactive behaviour (IB) is structural adaptive behaviour achieved through folding mechanisms. Many kinetic systems use linkages—such as Watt-I linkages (with one degree of freedom), spherical linkages, or more complex multi-joint linkages—to achieve smooth folding and unfolding.(Lee and Ostwald, 2021) These mechanisms allow for large-scale transformations like roof openings, façade modulation, or deployable structures. In addition, some designs incorporate origami-inspired folding or curved crease folding, enabling elegant and efficient shape changes without heavy mechanical systems.(Lee, Ostwald and Kim, 2021)

While a wide variety of approaches exist to achieve kinetic behaviour, the focus here has been on folding mechanisms due to their simplicity, efficiency, and versatility in design. By establishing the principles and examples of mechanical and fold-based motion, this discussion lays the groundwork for the following section, where the thesis will delve more deeply into origami-inspired geometries and their application in creating adaptable, dynamic architectural structures.

03| Origami: Geometry, Mechanics, and Design Potential

3.1 Origami Origin

3.2 Origami Technical Terms

3.3 Origami Tessellation

3.4 Origami Application in Design

3.1 Origami Origin

The term *origami* refers to the commonly known ancient art of paper folding. It finds its roots in the composition of the Japanese words *oru*, which means “fold,” and *kami*, which means “paper.”(Meloni *et al.*, 2021)

Origami used to be, and still sometimes is, said to originate in the second century in China. Some say origami started in the Heian period (794-1185) in Japan. The origin of origami in Japan is thought to be ceremonial wrappers as represented by *noshi*. *Noshi* was originally a form of folded wrappers for *noshi-awabi*. Another example is a pair of paper butterflies known as *ocho* and *mecho*.(Fig3.1) *The samurai warriors of the Edo period (1603–1868) were supposed to fold wrapping paper in a specific way according to what was inside when they sent a gift.*(Hatori, 2011)

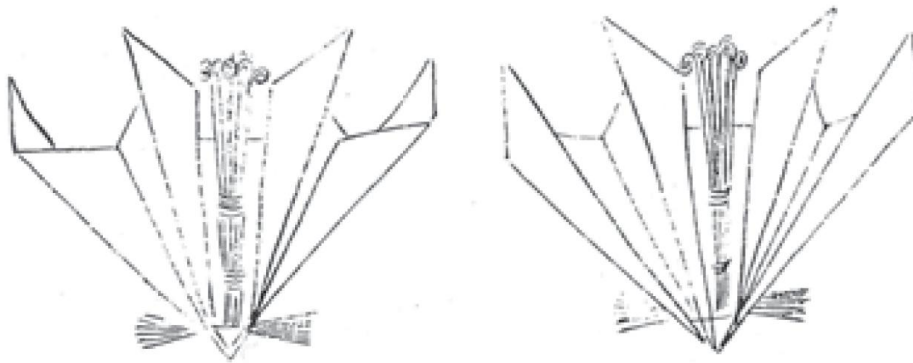


Fig 3.1: Ocho and mecho illustration (Hatori, 2011)

In contrast, the origin of Western origami is thought to be baptismal certificates folded in a “double blintz,” that is, folding all the four corners of a square to the center and repeating the same folds on the smaller square. The most typical European origami model is perhaps the little bird called *pajarita* in Spain and *cocotte* in France. Another popular model in Europe is the boat. Vicente Palacios argued that the boat is recorded in an edition of *Tractatus de Sphaera Mundi* published in Venice in 1490 and Also well-known is the hat, which John Tenniel has depicted in artwork for Lewis Carroll’s *Through the Looking Glass* published in 1872 , Although both the boat and the hat are made from rectangular sheets of paper, most of the European traditional models are made from square sheets. (Lang, Wang-Iverson and Yim, 2016)

in the 1860s and 1870s, the European education system was introduced and adopted in Japan. As a result, European origami was imported to Japan as a part of the kindergarten curriculum. In addition, as people travelled internationally, Japanese origami spread over the Western world. The state of origami as we know it today has been developed as a consequence of such a cultural exchange. (Hatori, 2011)

3.2 Origami Technical Terms

Attempts have been made regarding fixing the technical terms of origami worldwide, mostly from the Western world. On the Origami-L email list for folders, such a proposal or two (or more) have been made. Lang presents a long list of origami technical terms in the appendix of his seminal book on the mathematical foundations of origami design. However, such attempts have hardly been made in Japan. (Tateishi, 2016)

This part of the thesis introduces the key concepts of origami geometry that form the basis for understanding how folding systems behave and operate in architectural design.

- **Fold angle:** it is intended the dihedral angle between two consecutive faces divided by a crease at any moment of the folding motion. The dihedral angle is an angle between two planes in a third plane, which is perpendicular to the intersection line between the former two planes. To measure the fold angle, we can measure the actual angle between the two planes from surface to surface, or we can measure the angle between their normal vectors. In the former case, the fold angle of a flat-foldable origami with one single linear crease goes from 180° (unfolded flat configuration) to 0° (folded configuration) or from 180° to 360° depending on the mountain/valley assignment. In the latter, the fold angle goes from 0° (unfolded flat configuration) to $\pm 180^\circ$ (folded configuration). (Foschi, 2022)
- **Rigid-Foldability** An origami pattern is rigid-foldable when it can be folded and unfolded without bending, stretching, intersecting or cutting the faces. This kind of origami structure is not like paper origami, because the faces must be infinitely rigid (Osorio, Paio and Oliveira, 2023)
- **Mountain and valley** two types of folds: mountain folds (which form a ridge) and valley folds (which form a trough). (Lang, 2011)

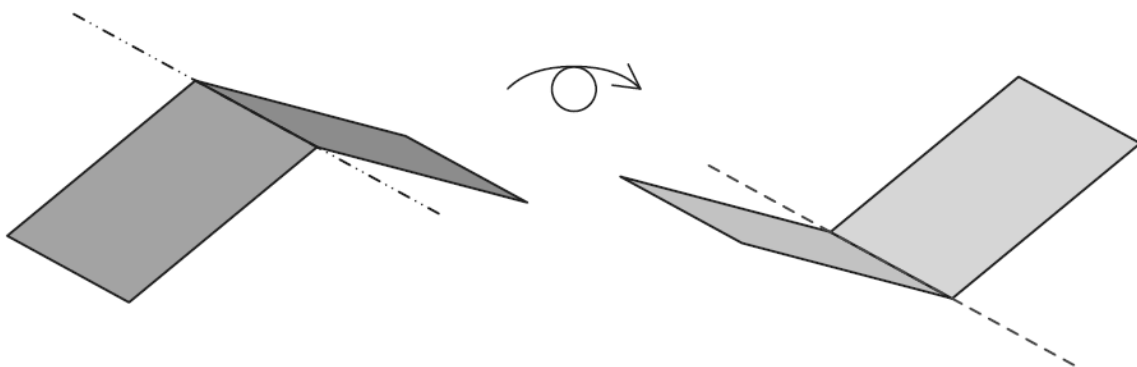


Fig3.2: A mountain fold is the same as a valley fold turned over. (Lang, 2011)

- **Crease:** On the other hand, perhaps there are *three* types of fold: valley folds, mountain folds, and unfolds. If we fold the paper in half and unfold it, we will be left with a line on the paper—a crease—which is also a type of fold. Creases are sometimes merely artifacts, leftover marks from the early stages of folding, but they can also be useful tools. Creases can provide reference points (“fold this point to that crease”) and in the purest style of folding (no measuring devices, such as rulers, allowed) creases, folded edges, and their intersections are the only things that can serve as reference points. Creases are also commonly made in preparation for a complex manoeuvre. (Lang, 2011)

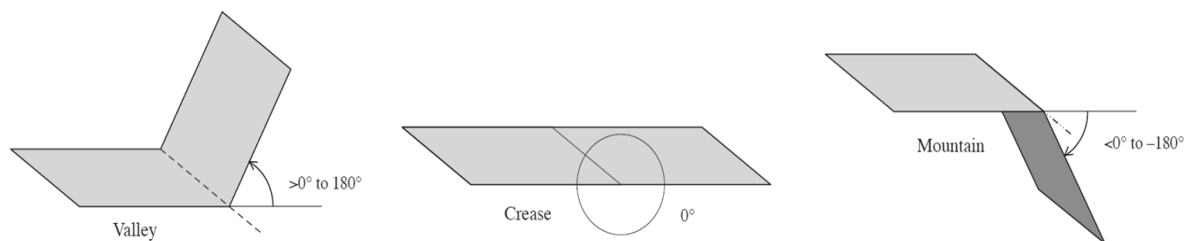


Fig3.3: Valley folds, Creases, and mountain folds are all part of a continuum. (Lang, 2011)

- **Base and Preliminary Fold:** a geometric form with the same general shape and/or number of flaps as the desired subject.” there are four shapes known for hundreds of years in Japan and they are often called the four *Classic Bases* of origami and are named for the most famous models that can be folded from them: the Kite, Fish, Bird, and Frog Base. The Classic Bases are not the only bases in regular use. There are a few other candidates for standard bases: the so-called Preliminary Fold (a precursor to the Bird and Frog Bases), the Waterbomb Base (obtainable from the Preliminary Fold by turning it inside-out), the Cupboard Base (consisting of only two folds), and the Windmill Base (also known as the Double-Boat Base in Japan). The Preliminary Fold was named Fold rather than Base by Harbin since it was a precursor to other bases, a somewhat artificial distinction that has stubbornly persisted in the English-speaking origami world. (Lang, 2011)

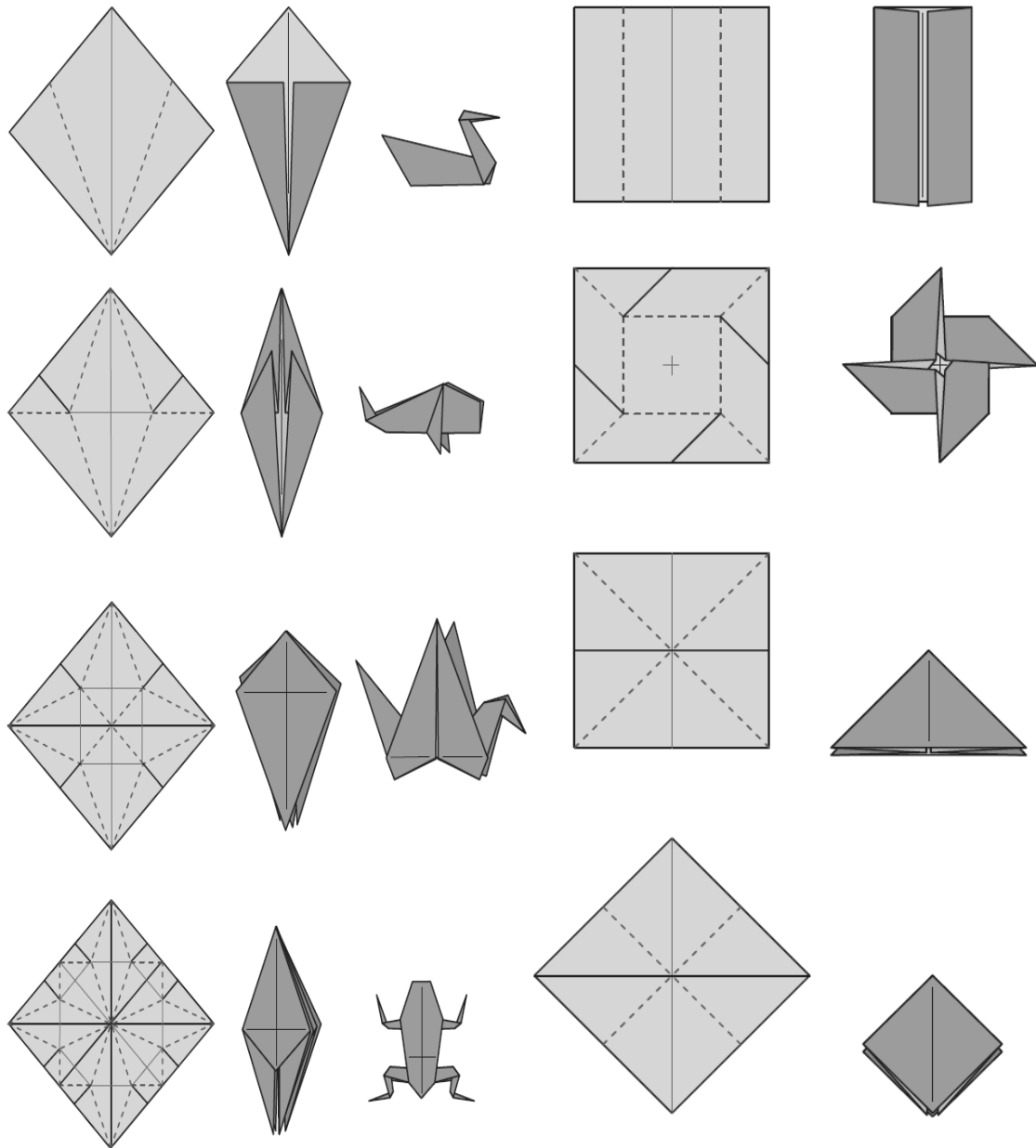


Fig3.4: Left Column: Four origami Bases | Right Column: Preliminary Fold(Lang and Hull, 2011)

3.3 Origami Tessellation

Origami tessellations are foldable paper models that take advantage of repeated patterns in the geometry of their crease patterns. It involves folding a sheet of paper into repeated geometric patterns that tessellate (i.e., tile) the plane, commonly through pleats, twists, and grid-based designs. (Xing and You, 2023) Tessellations can serve as deployable surfaces, material metamaterials, and architectural skins, thanks to their capacity for folding, unfolding, and reconfigurability. (Osorio, Paio and Oliveira, 2023)

The field's modern foundations were laid by **Shuzo Fujimoto**, whose *Twist Origami* book series introduced fundamental twist-based molecules such as triangle, square, and hexagon twists. (Fujimoto, 1978)

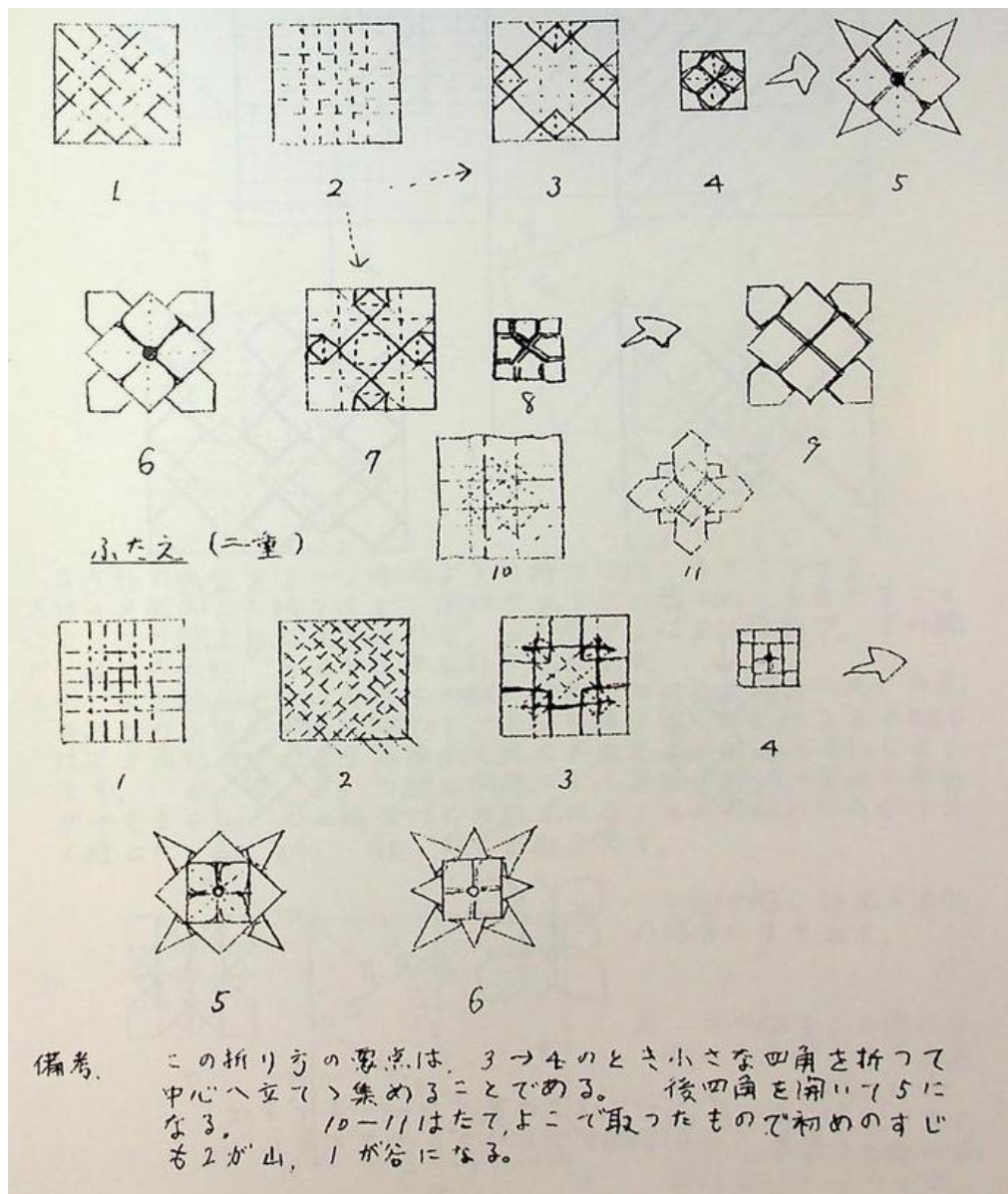


Fig3.5: Fujimoto's hand-written notes (Fujimoto, 1978)

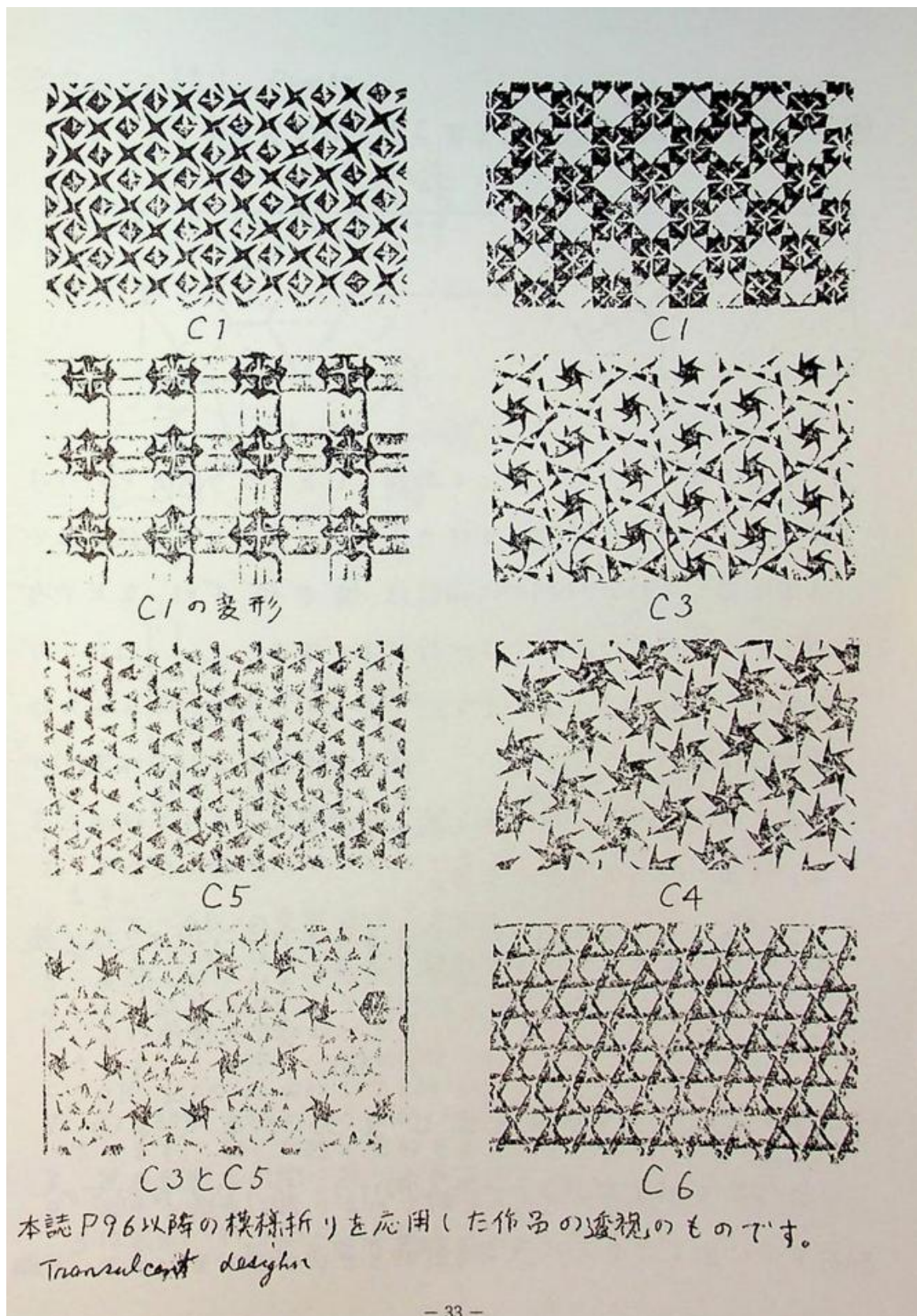


Fig3.6: Fujimoto's Tessellations from his book (Fujimoto, 1978)

In the 1960s and 1970s, **Ron Resch** significantly advanced the field by combining artistic folding with computational modelling, ultimately influencing engineering and architectural applications. In more recent decades, **Eric Gjerde** has helped systematize tessellation design for a broad audience: his book *Origami Tessellations: Awe-Inspiring Geometric Designs* offers both historical context and step-by-step crease patterns.(Osorio, 2014)



Fig3.7: Pre-show assembly of my basic Triangle fold by Ron Resch(Resch, 1967)

In addition, research by **Tomohiro Tachi**—particularly his work on *freeform origami tessellations*—has extended and generalized Resch’s early explorations into fully three-dimensional, continuously varying tessellating surfaces, enabling new possibilities for deployable structures, adaptive geometries, and mechanical metamaterials.(Tachi, 2013)

Together, these contributions illustrate how origami tessellation has developed into a rich and interdisciplinary field at the intersection of geometry, materials science, computation, and architectural design. This synthesis of artistic intuition and mathematical precision continues to shape contemporary research and applications, In Section 5 of this thesis, several iconic tessellation patterns were examined in greater detail, and the geometric principles that govern their behaviour were analysed.

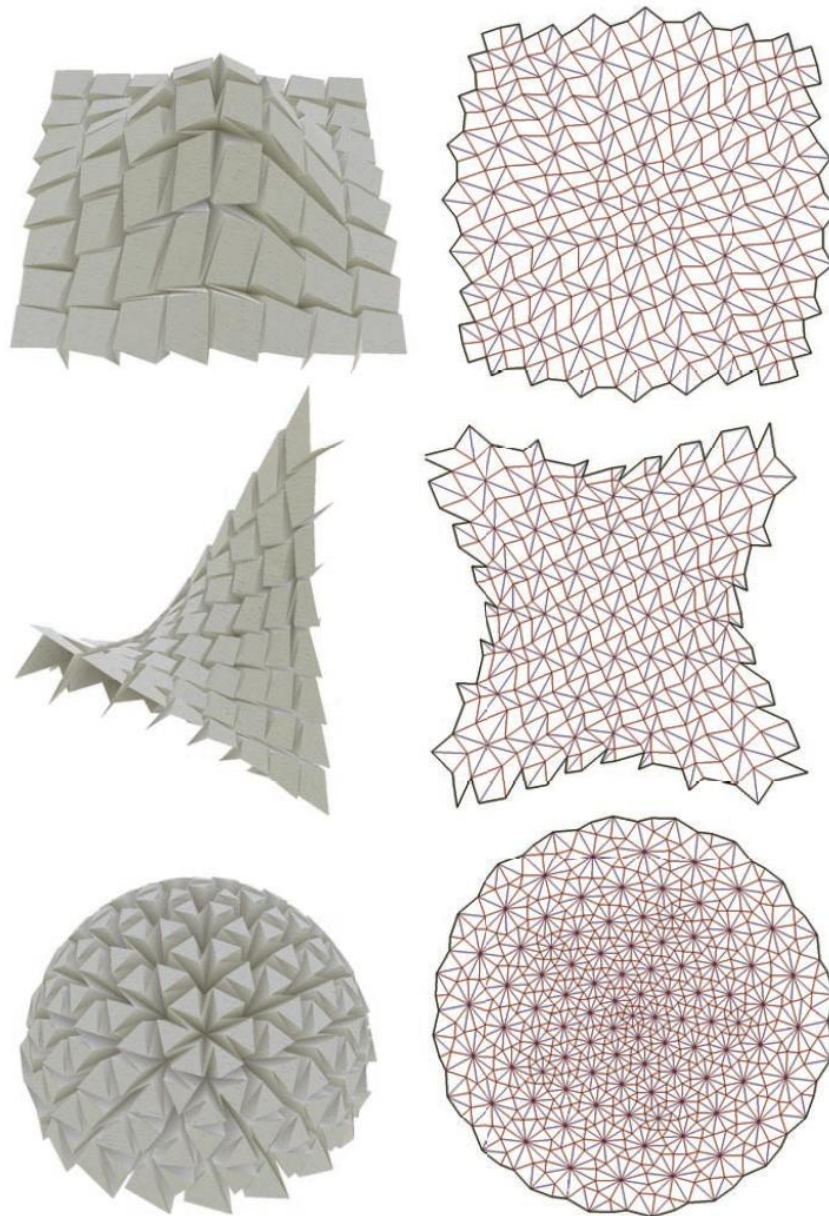


Fig3.8: Tomohiro Tachi’s work on Ron Resch’s tessellation(Tachi, 2013)

3.4 Origami Application in Design

Although origami has existed for centuries, and it became a powerful source of inspiration for designers, engineers, and architects. What began as a traditional art of paper folding has evolved into a sophisticated design strategy capable of solving complex spatial, structural, and functional challenges. Today, origami principles appear in an astonishing range of fields—from architecture and product design to biomedical devices and aerospace engineering—demonstrating how a simple fold can unlock entirely new ways of thinking about form, movement, and material efficiency.

Indeed, the fields in which origami principles are applied are remarkably diverse, but they can be broadly categorized into several key areas:

- **Permanent Architecture:** Historically, architectural projects that drew inspiration from origami primarily used folding as a formal, geometric, and static concept. Buildings such as the American Concrete Institute Building (Minoru Yamasaki, 1958), the USFA Cadet Chapel (Walter Netsch Jr., 1962, Skidmore, Owings & Merrill), and the Miami Marine Stadium (Hilario Candela, 1963) exemplify this approach, where folds functioned as geometric devices to articulate form, structure, and rhythm while remaining materially rigid. In these cases, origami-inspired folds were primarily structural motifs, embedded in planar surfaces or roof forms, with the fold's logic residing largely at the level of shape and geometry. A transitional example is the Art Tower Mito, where origami principles were applied more structurally, integrating the fold into the building's support system rather than merely its aesthetic envelope. In more recent projects, such as Poly International Plaza, Beijing (2016, Skidmore, Owings & Merrill), origami continues to inspire form and static geometry, demonstrating that folding logic still informs large-scale architectural massing and roof articulation even in contemporary design. In contrast, a separate approach—discussed in Section 2.3—applies origami primarily to façades and kinetic surfaces, where the fold becomes a dynamic, performative mechanism rather than a static structural or geometric element.
- **temporary architecture:** In temporary architecture, origami principles are leveraged to create deployable, lightweight, and structurally efficient systems that can be easily transported and reconfigured. The classical Miura-ori fold, first introduced by Kōryō Miura in 1985 for packaging large membranes in space, provides a powerful geometric logic for compact storage and rapid deployment.(Miura and Kenkyūjo, 1985) Research in composite origami structures, such as the work by O'Neil, DeLeo, Yasuda, and colleagues, demonstrates that bellows-like origami modules, made with composite materials, can offer high stiffness and mechanical behaviour ideal for temporary shelters or relief structures.(O'Neil *et al.*, 2018)
- **Installation and Performance**
- **Furniture and Interior design**
- **Fashion, Robotics**
- **Industrial Design**

04| Case Studies

This chapter presents the case studies examined as part of the research. The selected projects are organised into two main groups according to their approach to responsiveness and their relevance to the development of adaptive surface systems.

Group A: Responsive Architectural and Performative Projects (Case Studies 1–8)

The first group comprises eight projects that demonstrate responsiveness at an architectural or performative level. The analysis of these projects serves two primary objectives:

- To clarify the concept of responsiveness in architecture—specifically, to understand how responsive strategies influence spatial behaviour, environmental adaptation, and dynamic performance.
- To broaden the perspective on structural, material, and technical strategies that enable responsive behaviour within built systems.

Particular attention is given to the relationship between responsiveness and material systems, including construction details and kinetic mechanisms. While these projects do not necessarily employ folding principles, they establish an essential conceptual and technical foundation for the thesis, which ultimately focuses on origami-based adaptive systems.

Group B: Origami-Inspired, Folding-Based Responsive Projects (Case Studies 9–19)

The second group includes projects that rely primarily on folding mechanisms or origami-inspired design strategies. These case studies are central to understanding the current state of origami applications in architecture, spanning both theoretical investigations and built implementations.

This group encompasses permanent, large-scale architectural works as well as research-oriented prototypes and studies originating from disciplines outside architecture. Incorporating examples from engineering, product design, and material science allows the thesis to:

- Draw insights from parallel explorations of folding and deployable systems,
- Identify transferable principles with architectural potential, and
- Explore opportunities for adapting non-architectural folding strategies into architectural contexts.

1. URBAN IMPIRINT

2019, NEW YORK
Nassia Inglessis, Studio INI

-Application: Temporary installation(Performative)

-Geometry: Semi-close Space (Box Shape)
two parallel hexagonal cut surfaces, positioned at the top and bottom.

-Mechanism of movement: Passive
Mechanical, Rotational Vertical movement.

-Type of movement: Sequentially Transitioning, Interlinked Surfaces Pieces

-Actuation: Passengers weight, Pulley System

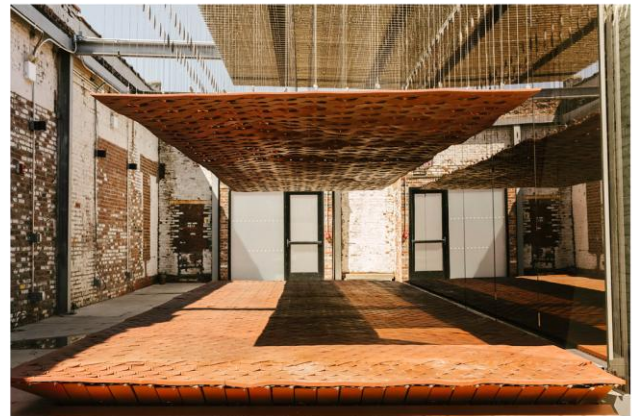
-Aim of movement: User Response

-Covered Area : Flexible

-Movement time : Immediately

-Material and Construction:

The rubber and concrete surfaces are composed of a grid of water-jet-cut patterns, coordinated with laser-cut double-steel elements, a spring bed, and an overhead pulley system.



2. GREEK PAVILION

2018, LONDON
Nassia Inglessis, Studio INI

-Application: Temporary installation(Performative)

-Geometry: Close Space(Surface)
Two vertical surface constructed from small bricks, connected at the top and bottom boundaries

-Mechanism of movement:

-Type of movement: Passive, Mechanical, Rotation
Serial Revolute, Interlinked Element (Woven straw effect)

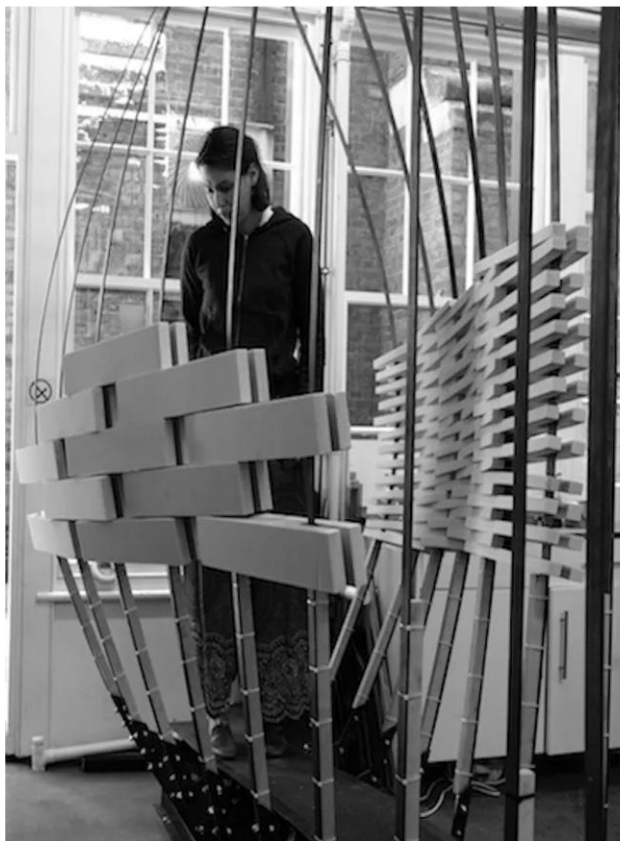
-Actuation: Passengers Weight,Pulley System

-Aim of movement: User Response

-Covered Area : 17m Pathway

-Movement time : Immediately

-Material and Construction:
A steel spring skeleton integrated with members made of recycled plastic, In work with spring bed



3. HYGROSKIN PAVILION

2 0 1 3 , F R A N C E
Achim Menges Architect
Oliver David Krieg, Steffen Reichert

-Application: Pavilion

-Geometry: Close Space(Box), Voronoi

-Mechanism of movement: Passive
Material Properties

-Type of movement: Automaticlly or Locally controlled

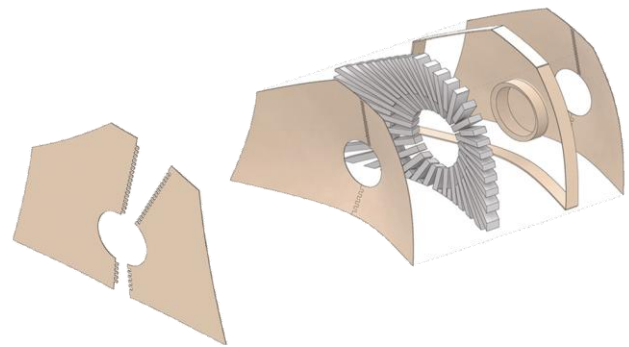
-Actuation: Moisture (Pinecone effect)

-Aim of movement: Climate Responsive Apertures (Light and Ventilation)

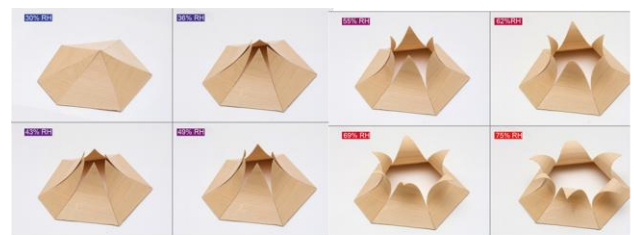
-Covered Area : 5.7*4.2*3 meters

-Movement Time: Variable (Base on the environment)

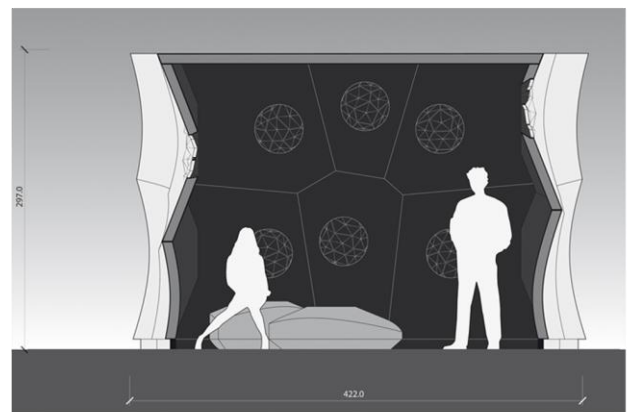
-Material and Construction:
Multilayer Modules of Double Layered Skin Plywood and
Sandwich Panel, Robotic Fabrication.



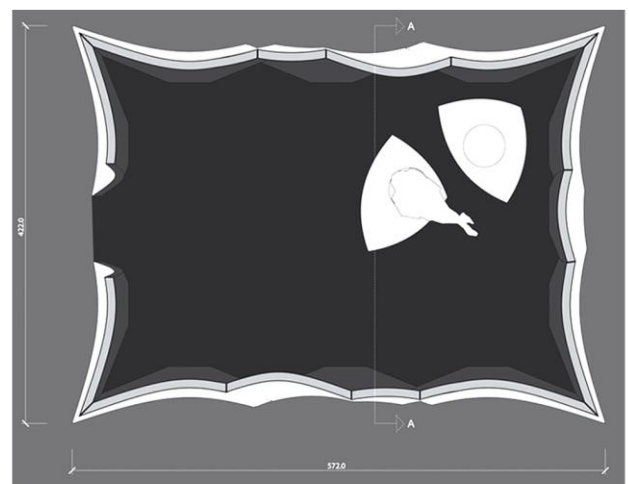
Material Layer Axonometric



Apertures reaction in different moisture level



Section View



Top View



4. SHIVER HOUSE (V1,2)

2019, FINLAND
2022, FRANCE
NEON STUDIO

-Application: Pavilion

-Geometry: Pinecone leaves elements

-Mechanism of movement:
Passive, Mechanical, Rotation and Vibration

-Type of movement: Passive
Centrally and Locally Controlled

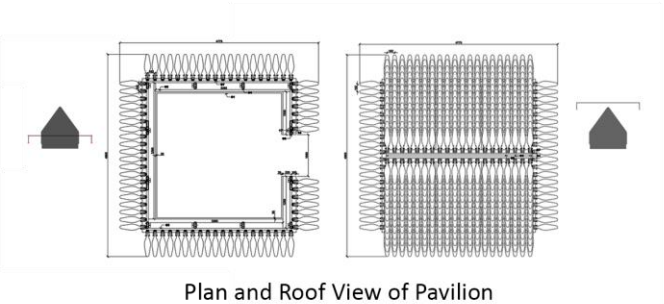
-Actuation: Air flow, Moisture

-Aim of movement:
Climate Response(Air Flow, Ligh), Visual Diversity

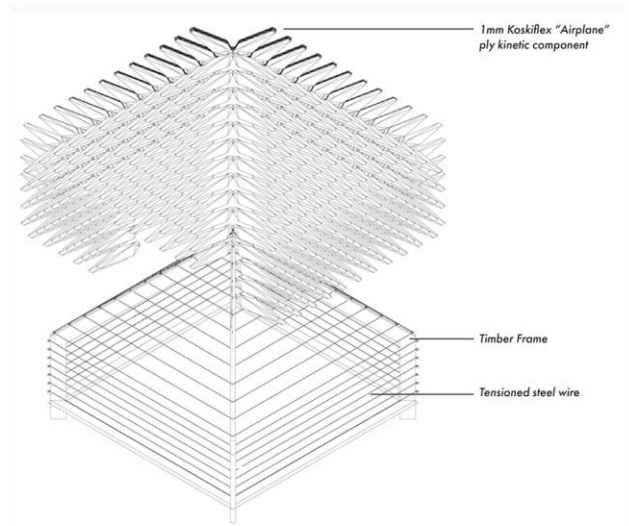
-Covered Area : Flexible
Different versions of the project were constructed in various size

-Movement Time: Immediately
The speed of movement directly dipent of environment

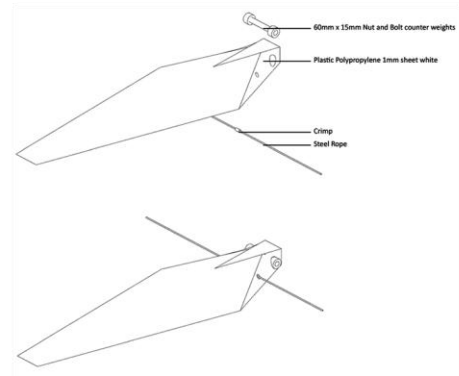
-Material and Construction:
Shingles Airplane Plywood, V2 Polycarbonate,
Timber Structure which supports a number of rows of tensioned Steel Wire



Plan and Roof View of Pavilion



Exsonometric view of structure and surface elements



Facade Elements Connection Details



5. HYPOSURFACE

2001, BIRMINGHAM
Mark Goulthroe. dECOi

-Application: Temporary installation

-Geometry: Open Surface, Triangular tessellation

-Mechanism of movement: Active
Mechanical, Rotation and Horizontal move

-Type of movement: Central and local
Controlled Unconnected Element

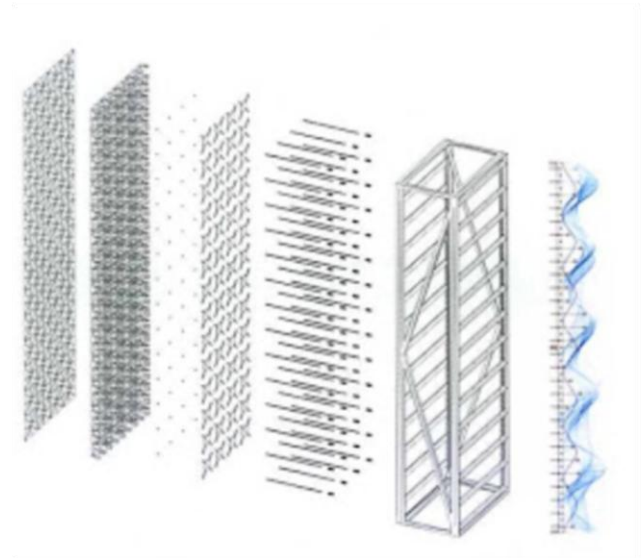
-Actuation: Sensor (data collection)
Pneumatic Pistons (data response)

-Aim of movement: User Response

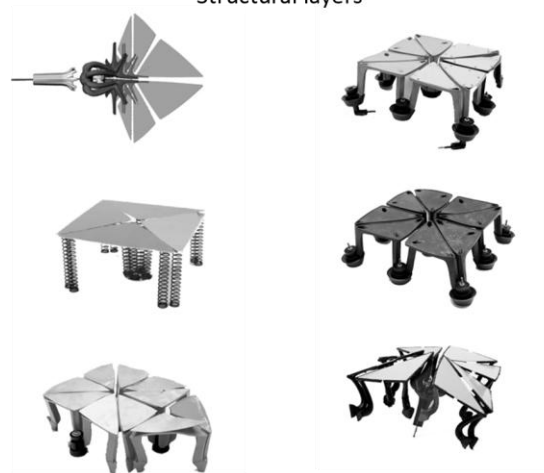
-Covered Area : 10*3 meters(Possible variation)

-Movement time : Immediately

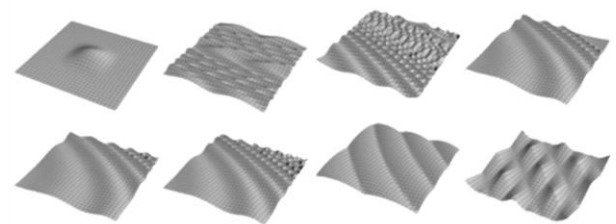
-Material and Construction:
Triangular Metal Surface with Modular Frame, a Matrix of
Pneumatic Pistons, Series of Rubber 'Squids', and a Surface
of bi-polar Metallic Facets.



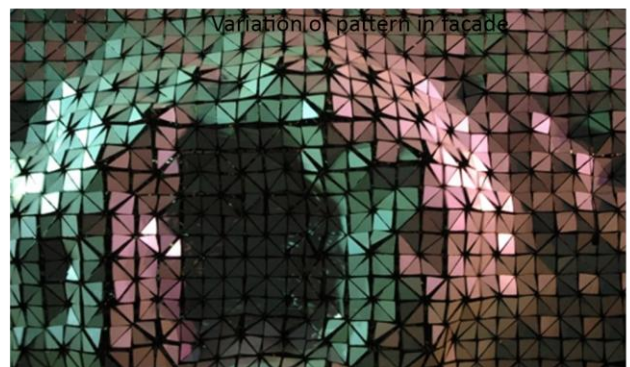
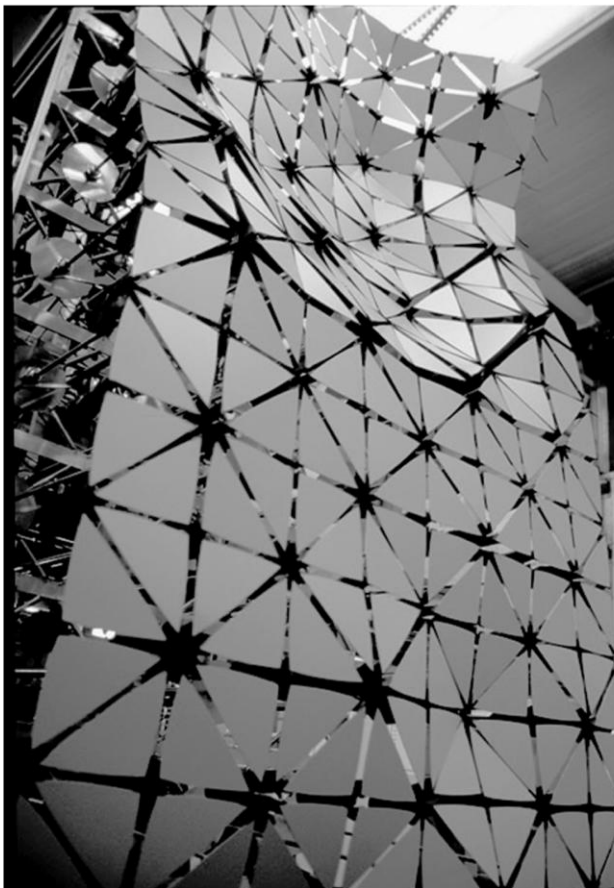
Structural layers



Arms that provide movement and connection of elements to structural parts



Variation of pattern in facade



6. THEMATIC PAVILION

2012, SOUTH KOREA
SOMA Lima Studio

-Application: Building Facade(Permanent)

-Geometry: Surface, Rectangular Strip

-Mechanism of movement: Active, Bending Deformation

-Type of movement: Centrally and locally controlled, Unconnected Element-

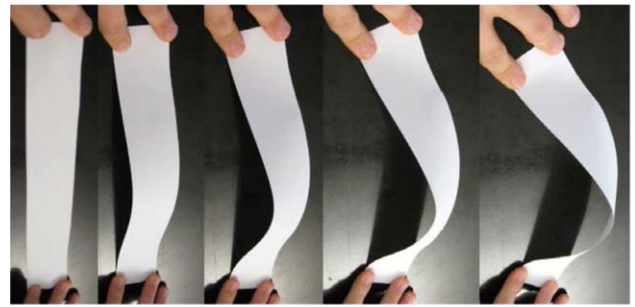
-Actuation: Sensors (data collection)
Screw spindle driven by a servomotor induces pressure

-Aim of movement: Environment Response (Light)

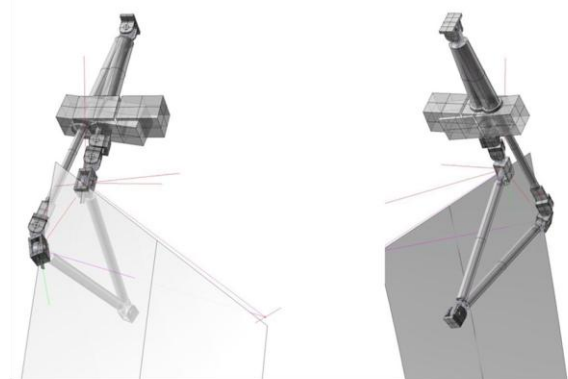
-Covered Area : 10*3 meters(each strip)

-Movement time : Immediately

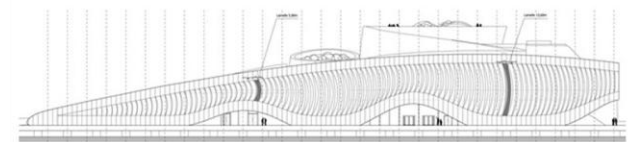
-Material and Construction:
Lamellas of Glassfibre-reinforced polymers GFRP, two hinged corners and screw spindles driven by a servomotor that control the buklung



Strips Movement Mechanism



Jonis Screw Spindles



7. SIMONS CENTER

2010, NEW YORK
Hoberman Associates

-Application: Building Facade (Permanent)

-Geometry: Flat Surface (Variable Pattern)

-Mechanism of movement: Active
Mechanical, Sliding

-Type of movement: Centrally Controlled

-Actuation: Electronic engines induce movement (Computer Program)

-Aim of movement: Climate-Response (Light)
User-Response (View and privacy)

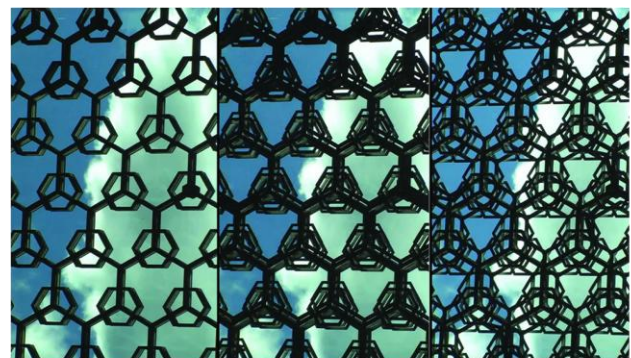
-Covered Area : 124sq/m facade

-Movement Time: Controllable

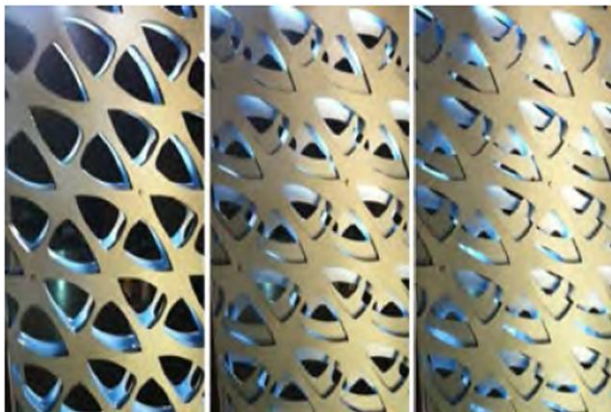
-Material and Construction: Light Metal Surface, Laser Cut, Metal Structural Frames



Different Layer of Facade



Diversity of geometry in movement process



4



Constructuion, Layer Fixing



8.MADINAH HARAM PIAZZA

2010, SAUDI ARABIA
Peter Katcha ,SEFAR® STUDIO

-Application: Shader Elements

-Geometry: Radially symmetric

-Mechanism of movement: Active
Mechanical, Deployable, Folding

-Type of movement: Locally Controlled

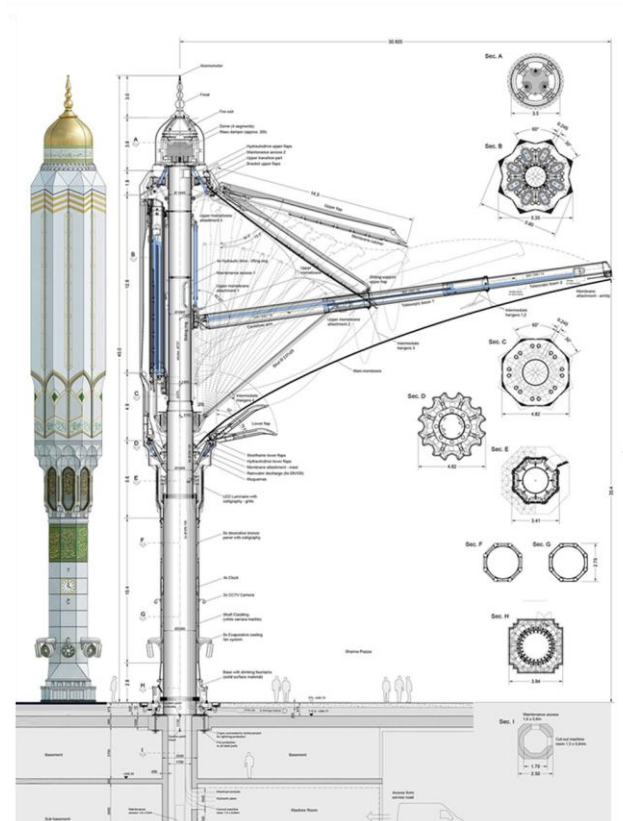
-Actuation: Electronic Engines

-Aim of movement: Climate Comfort
Shading, Rain Protection, Create Semi-Close Space

-Covered Area : 625m², 25 x 25 m Spans

-Movement Time: Complete Opening 3min

-Material and Construction:
PTFE (Fabric High Tolerance UV), Light Metal Arms and Columns.



Detail of metal arm in open position with connection and column section



9. AL-BAHAR TOWER

2013, ABU DHABI
AHR Architects
Aedas Architects

-Application: Building Facade (Permanent)

-Geometry: Triangular Tessellation

-Mechanism of movement: Active
Origami Rigid Folding

-Type of movement: Locally Controlled, Unconnected Element

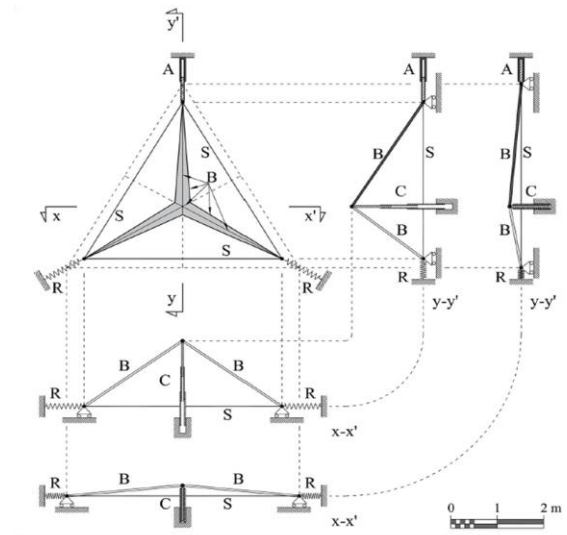
-Actuation: Sensors (data collection)
Electronic Pistons (data response)

-Aim of movement: Climate-Responsive Apertures/Shading system
(light-control mechanism)

-Covered Area : Each unit is a hexagon with side lengths of 6 m

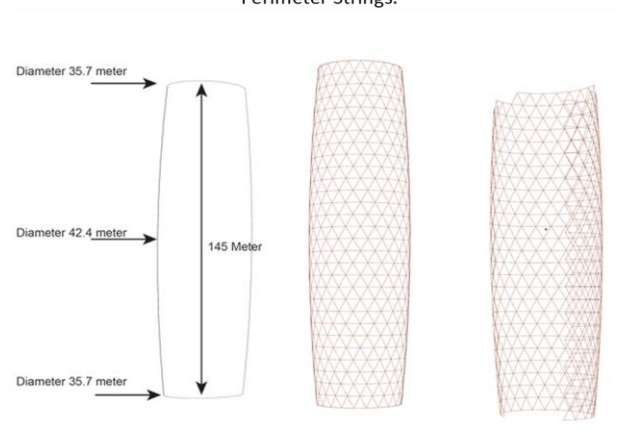
-Material and Construction:

PTFE-coated glass-fibre mesh with self-cleaning properties,
combined with double-layer plywood and sandwich panels,
manufactured using robotic fabrication



Schematic views of the Move Mechanism; top view and mid-plane sections (in two different configurations):

A: Linear Actuator; B: Bars; C: Telescopic Collar; R: Elastic Restraints; S: Perimeter Strings.



10. RESONANT CHAMBER

2011, MICHIGAN
Kathy Velikov, RVTR Studio

-Application: Acoustic Panels

-Geometry: Open Surface, Triangular Tessellation

-Mechanism of movement: Active
Mechanical, Origami Folding

-Type of movement:
Locally controlled, Interconnected Elements

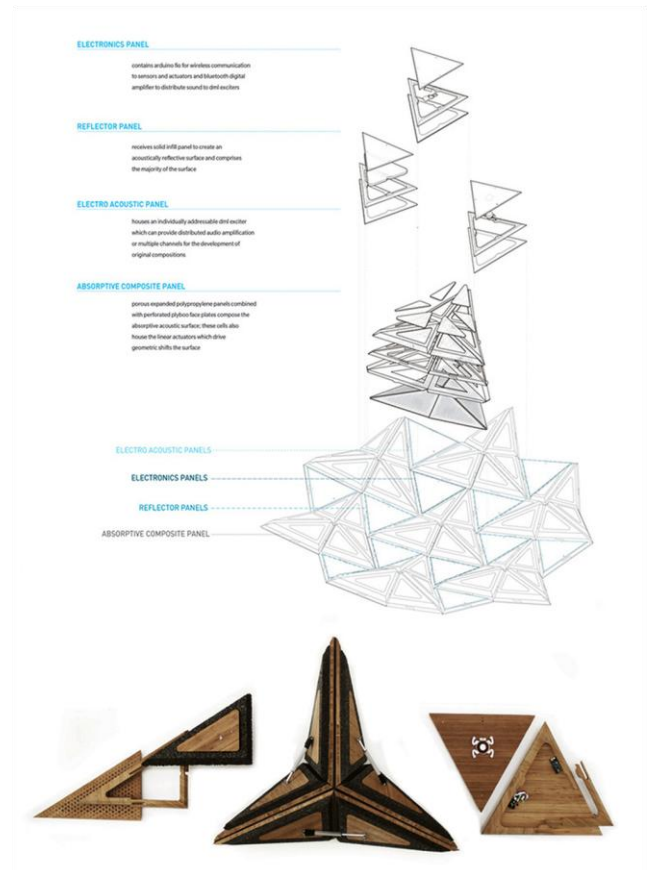
-Actuation: Sensors (data collection)
Electricity induce rotation in hinges (data response)

-Aim of movement: Acoustic Response

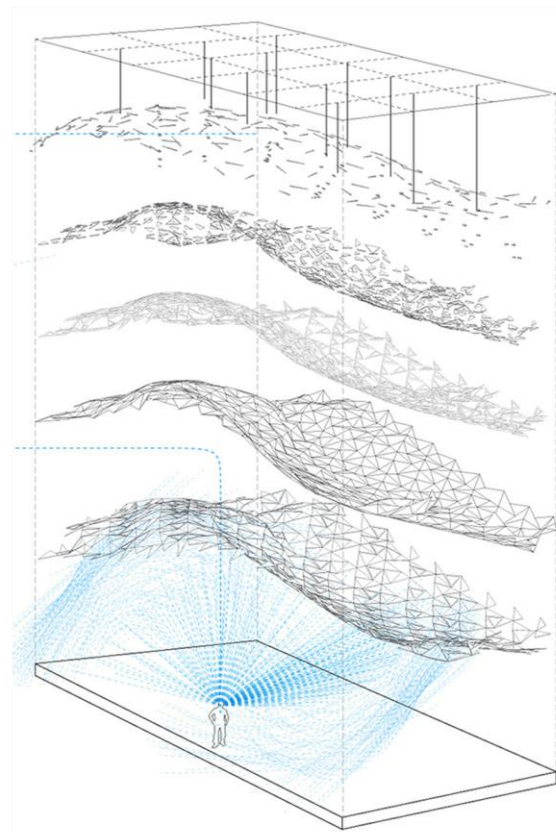
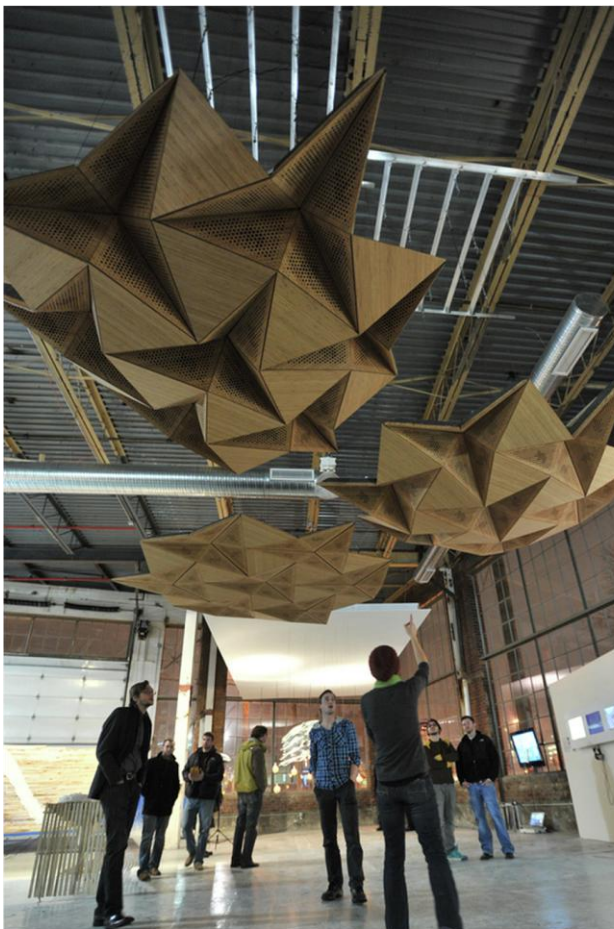
-Covered Area : Triangular Unit 50cm Boarder size

-Movement Time: Variable

-Material and Construction:
Porous Expanded Polypropylene (PEPP) Panel, Central Electrical Panel, Acoustic Materials



Modules Materials and Layers Demonstration



Panels Construction Levels

11. KIEFER TECHNIC SHOWROOM

2007, AUSTRIA
Ernst Giselbrecht + Partner

-Application: Building Facade

-Geometry: Rectangular elements

-Mechanism of movement: Active
Mechanical, Sliding, Folding

-Type of movement:
Centrally or Locally Controlled, Possible to be Programmed

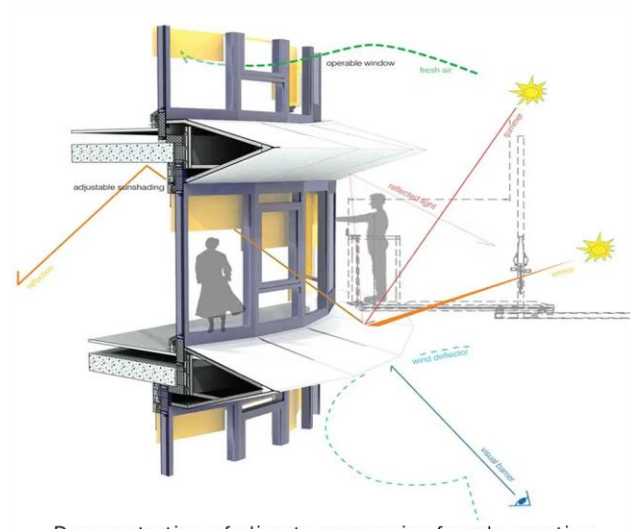
-Actuation: Sensors(data collection),
Electronic engines (data response)

-Aim of movement:
Climate Response (Light and Shading Control)

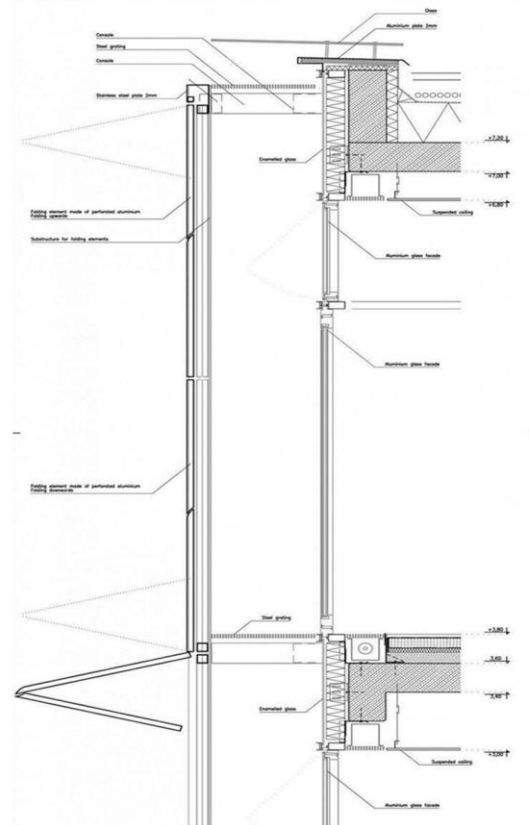
-Covered Area : Unit Rectangles in 6*4 meters

-Movement Time: Variable

-Material and Construction:
Folding Elements made of Perforated Aluminium, Metal Support Network, Sliding Aluminium Chassis



Demonstration of climate responsive facade reaction



Section view of facade shaders.



Different configuration of facade movement.

12. F L E C T O F O L D

2018, STUTTGART
UNIVERSITY of STUTTGART

-Application: Temporary Installation

-Geometry: Surface, Recangular Elements

-Mechanism of movement: Active
Material Properties, Folding Mechanism

-Type of movement: Active
Centrally and Locally Controlled

-Actuation: Sensore (data collection)
Electronic Integrated Pneumatic Cushion (data response)

-Aim of movement: Climate Response (Ligh), Visual Diversity

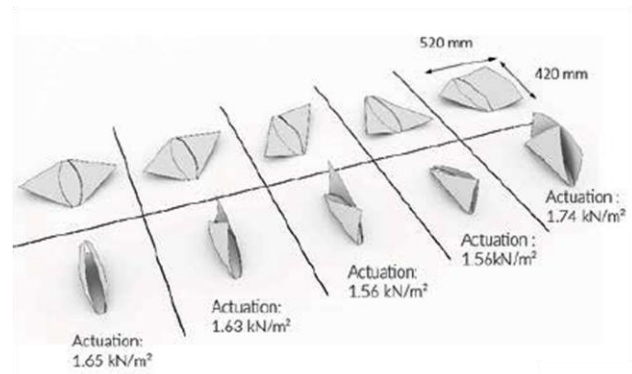
-Covered Area : Unit Size: 50 × 50cm

-Movement Time: Immediately

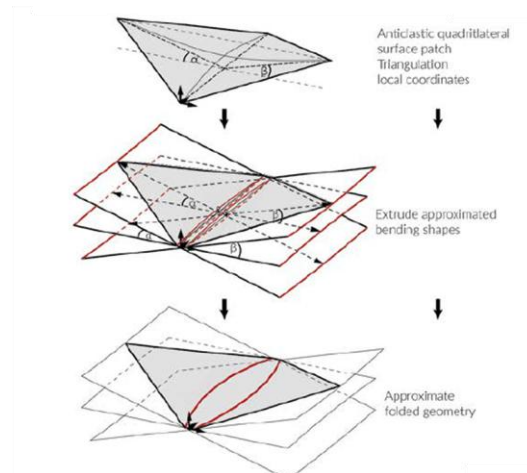
-Material and Construction:
Units Materialy-graduated FRP (Fiber Reinforced Polymer) on a base of Steel Sub-Structure



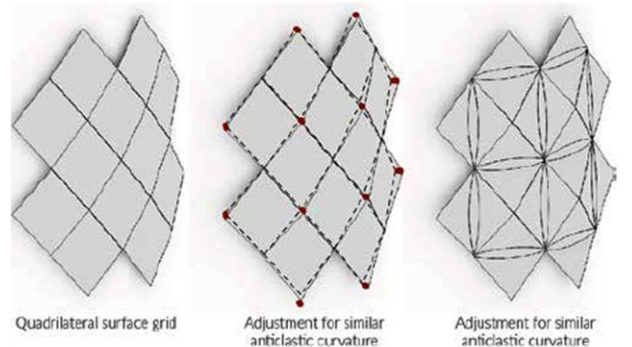
Mechanism of leaf folding used in design



Unit Geometry and Dimention



Translation of folding Mechanism into Quadrilateral Patches



Tessellation of Global Geometry



13. TRANSLATED GEOMETRIES

2014, SPAIN
IAAC Institut

-Application: Temporary Installation

-Geometry: Triangular Tessellation

-Mechanism of movement: Active, Origami Folding

-Type of movement:
Chained movement or Separated Unit and Nodes control

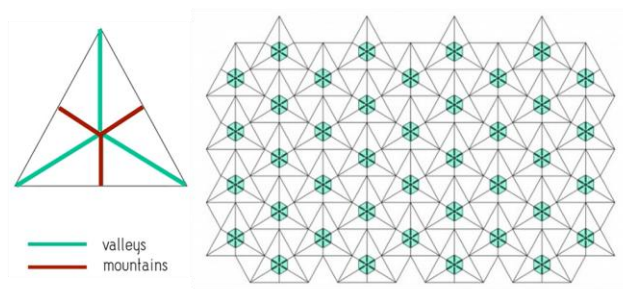
-Actuation: Heat flow (60-70°C)

-Aim of movement: Space Creation, Visual Diversity

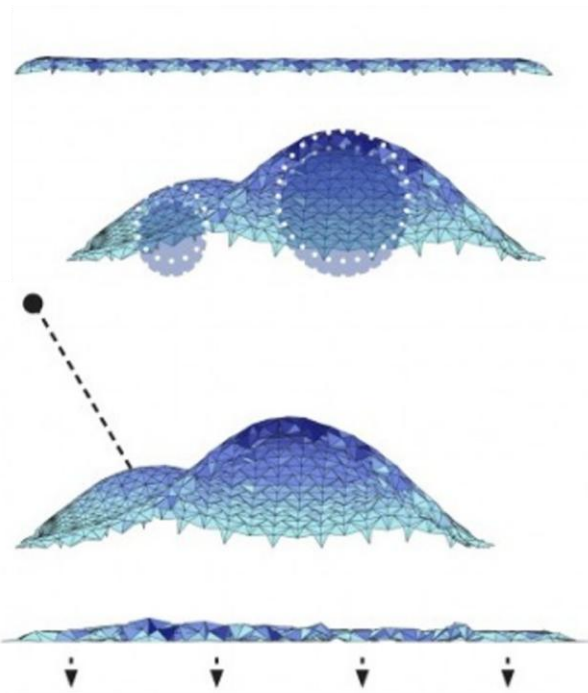
-Covered Area : Less Than 2m²

-Movement Time: 3min(to reaching to require heat)
2min (to stablizing the shape)

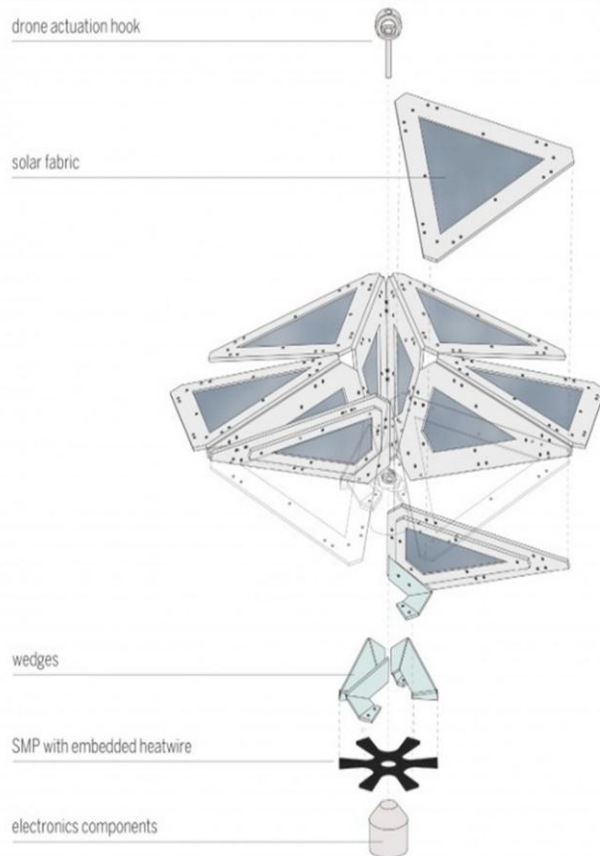
-Material and Construction:
Shape Memory Polymer (SMP) in hexagoal nodes, reglar hinges in other joints, , Wooded covering members, Solar Fabric.



Tessellation Geometry



Mechanism of Heating and Shape Change



14. RIGID ORIGAMY

2010, SINGAPORE
Tomohiro Tachi

-Application: Temporary Installation

-Geometry: Flat Surface

-Mechanism of movement: Passive, Origami Folding

-Type of movement: Chained movement

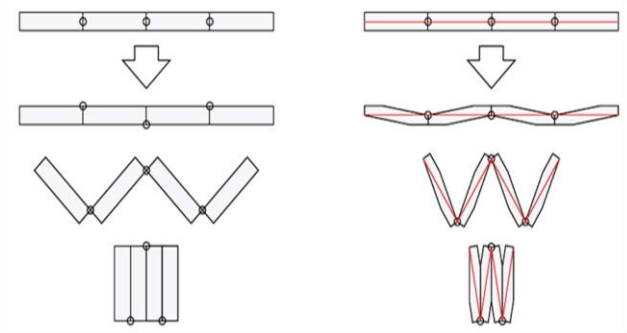
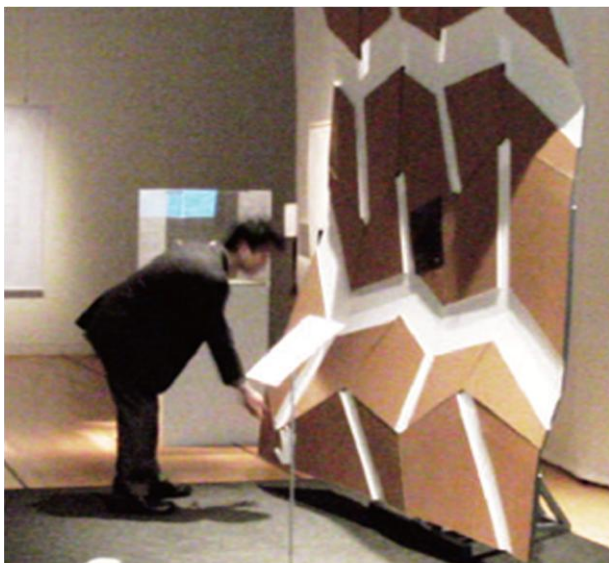
-Actuation: Mechanical force

-Aim of movement: Space Creation, visual Diversity

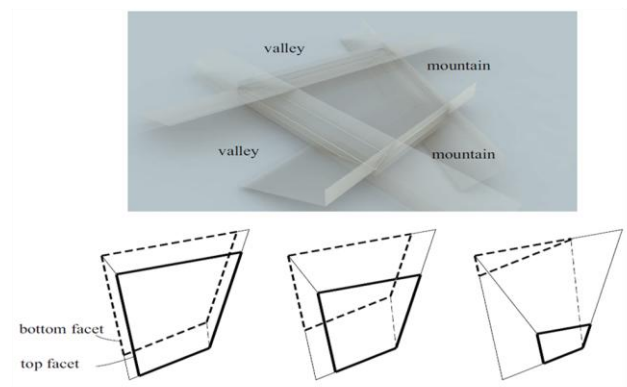
-Covered Area : Variable (Expanded Surface)

-Material and Construction:

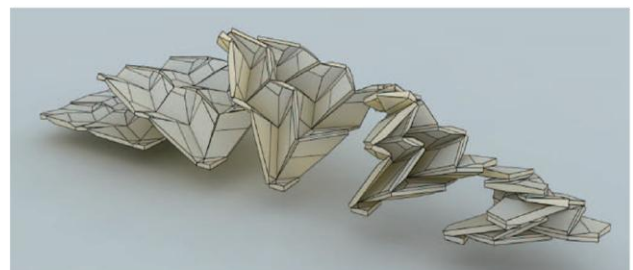
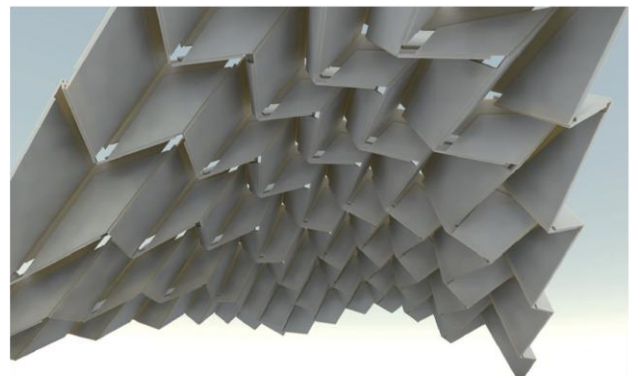
Double-walled cardboards (each of which is 10 mm thickness) sandwiched by a cloth.



Two approaches for enabling thick panel origami. (a) Axis-shift. (b) The proposed method based on trimming by bisecting planes. Red path represents the ideal origami without thickness.



Trimming the volume by bisecting planes of dihedral angles between adjacent facets.



A quadrilateral-mesh hyper model with thick tapered panels

15.SOLAR PANEL ARRAY

2014, U S A
Nasa's Jet Propulsion Laboratory
Brigham Young University, Robert Lang

-Application: Solar Panel

-Geometry: Hexagonal Surface

-Mechanism of movement: Active
Origami and a mixture of different styles of Solid Folds

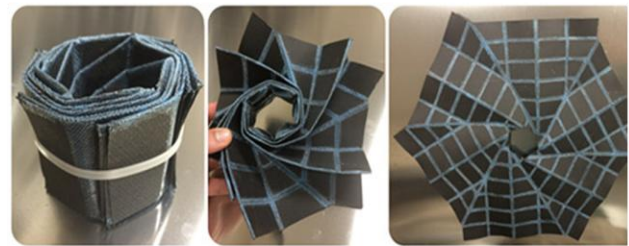
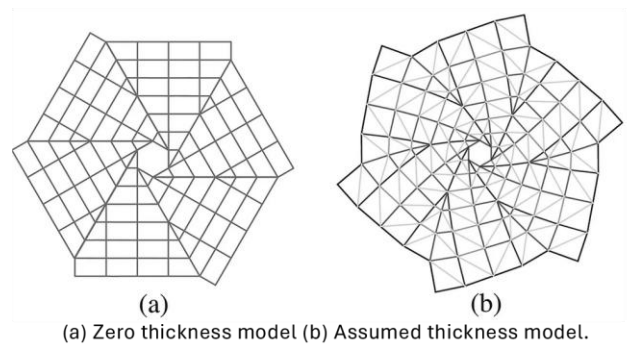
-Type of movement: Chained movement Expansion

-Actuation: Pneumatic actuation
Centripetal Acceleration, Stored Strain Energy, Thermal Activation. Motor-Driven Perimeter Truss

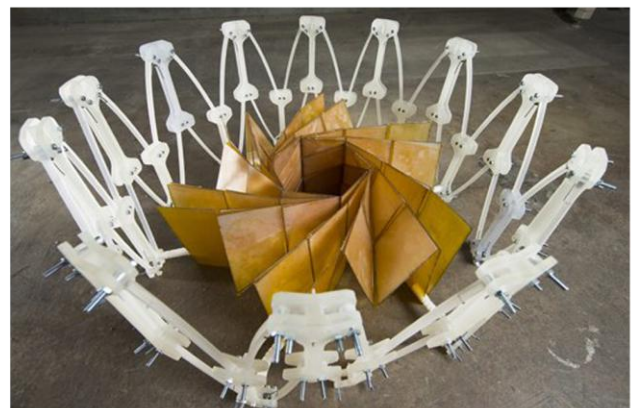
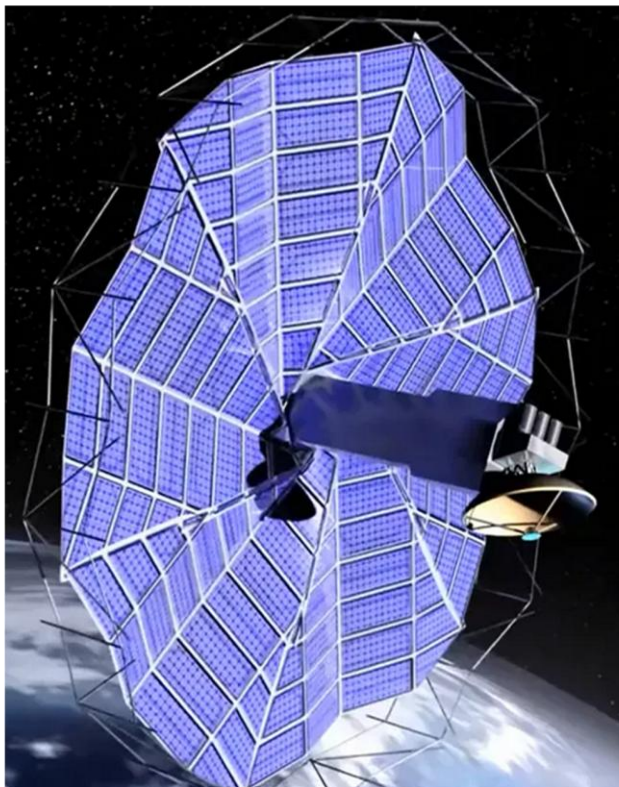
-Aim of movement:
Compact Panels for easing Space Launch.

-Covered Area :
A 1/20th scale prototyping model with 1.25 meter deployed and 0.136 stowed

-Material and Construction:
Membrane backing to connect the solar panels enable rigid foldability: valley folds with a gap of 10 to 14 times of the solar thickness.



Example of the design that accounts for the thickness of the solar panels.

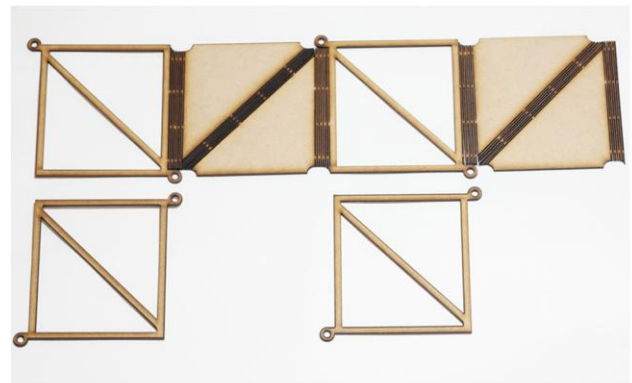


Origami-inspired solar array with a motor-driven perimeter truss

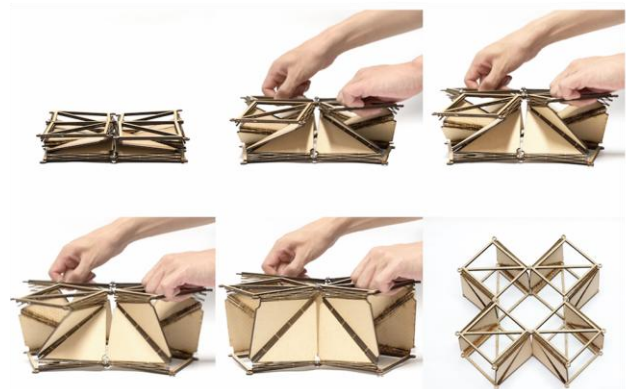
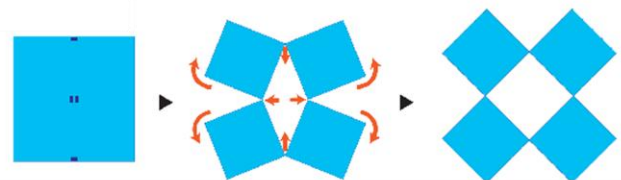
16.NOVEL STRUCTURE

2018, JAPAN
Digital Nature Group

- Application: Temporary Installation
- Geometry: Voxels, made of Triangular elements
- Mechanism of movement: Passive, Origami Solid Folding
- Type of movement: Chained movement
Expansion in X, Y axes
- Actuation: Mechanical, Axial Force
- Aim of movement: Solid reaction in direction and
- Covered Area : Variabl
- Movement Time : Immediatel
- Material and Construction: Laser cut MDF, Bolted Joints



Unit Members



Mechanism of expansion



Solid reaction in Vertical force, Flexible in horizontal forces

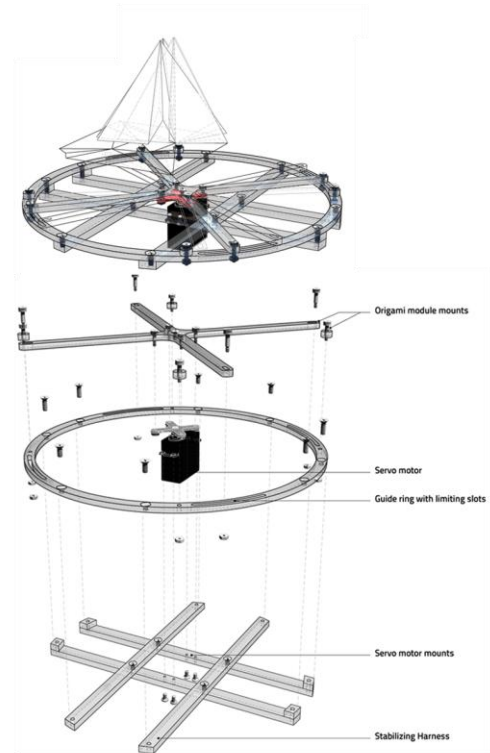


Voxel Joints

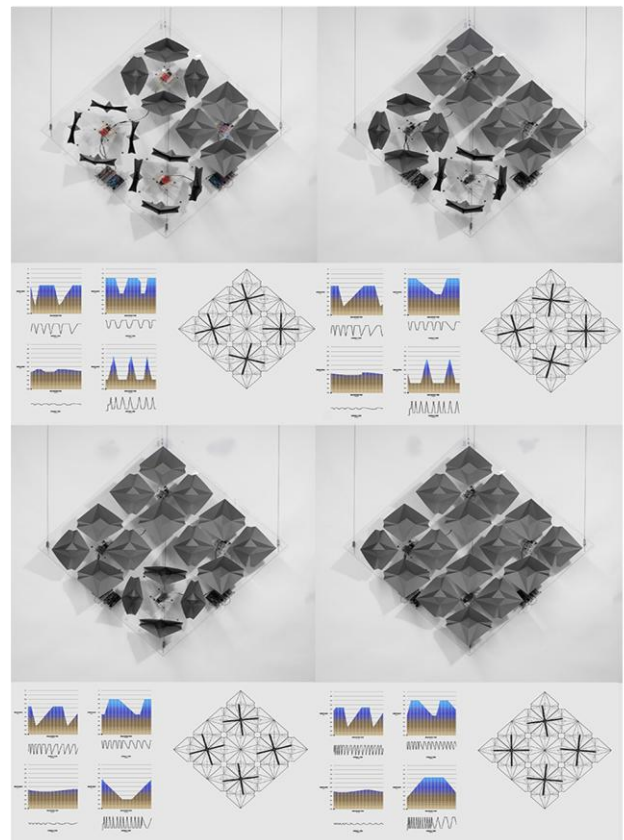
17.AUXETIC ORIGAMI SURFACE

2011, USA
Amir Shahrokhi
Yale School of Architecture

- Application: Temporary Installation
- Geometry: Diamond shape
- Mechanism of movement: Active, Origami Folding
- Type of movement: Seorated units deformation
- Actuation: Electricity
- Aim of movement: Response to Light Level
- Covered Area : Vriable Surface Area
Each Unit about 30*30cm
- Movement Time : Less than 10sec Reaction
- Material and Construction:
Laser-cut Plaxiglass with Scissor Mechanism in work with
Stainless-Steel Hardwar , Modules in Carton.



Exploded axonometric of the actuation mechanism.



Sequential activation of the AOS. Below each photo is visualization of the AOS digital interface showing the light readings for the past 10 seconds and the state of each motor.

18.RESPONSIVE PATTERN

2015, U S A
M o s t a f a A l a n i

-Application: Building facade

-Geometry: Radially Symmetric, Star Shape

-Mechanism of movement: Active
Mechanical, Origami Folding

-Type of movement: Separated Units Control

-Actuation: Sensors (data collection)
Electronical Motors (data response)

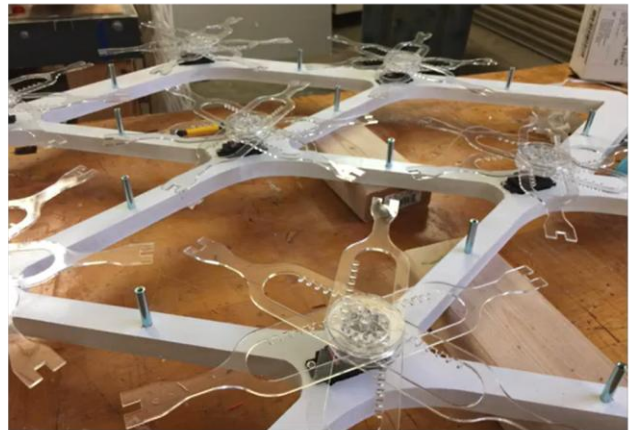
-Aim of movement: Environmental Responsive (Light)

-Covered Area : Unit Size 50 × 50cm

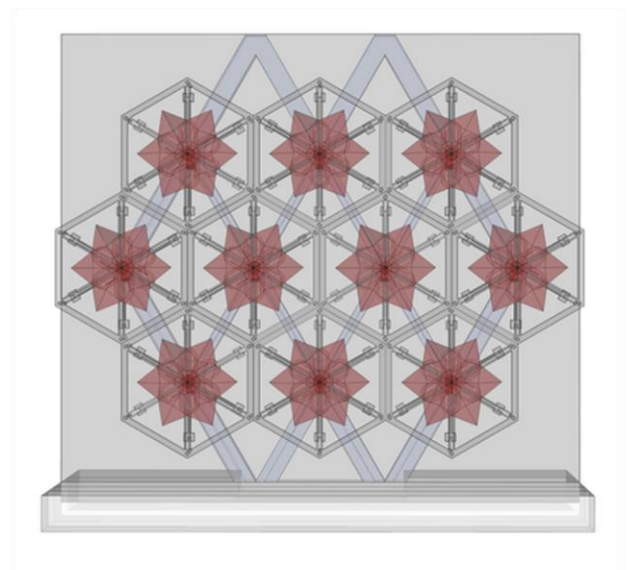
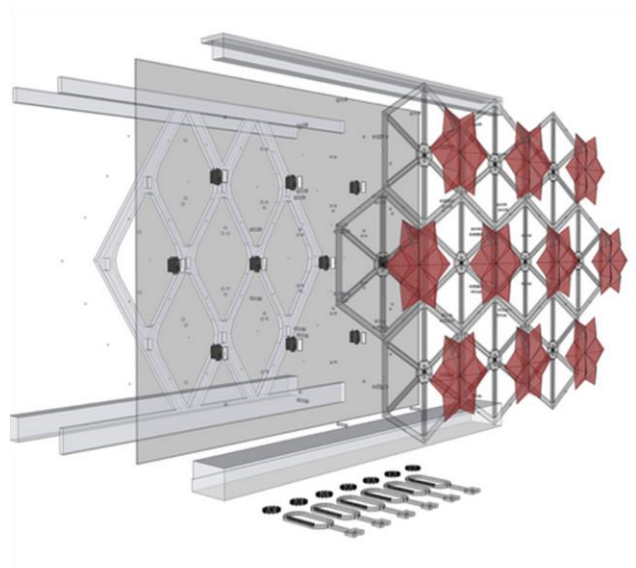
-Movement Time : Les than 10sec

-Material and Construction:

Support Structure : CNC'edMDF used to hold individuals,
Modules Support : CNC'ed Plexiglass, Cover of module:
Cartons



Structural Support System



Exploded View of Surface Members



19. TRANSFORMABLE METAMATERIAL

2015, U S A
School of Engineering and Applied
Sciences, Harvard University

-Application: Multipurpose
(photovoltaic panels, shelters, pavilions)

-Geometry:
A unit cell by extruding the edges of a cube in the direction
normal, a 3D structure with 24 faces connected by 36 edges
of same length

-Mechanism of movement: Active
Mechanical, Origami Folding

-Type of movement: Chained Movement

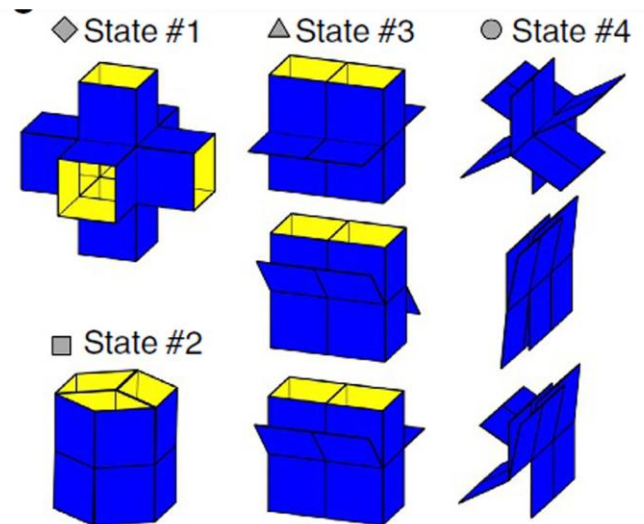
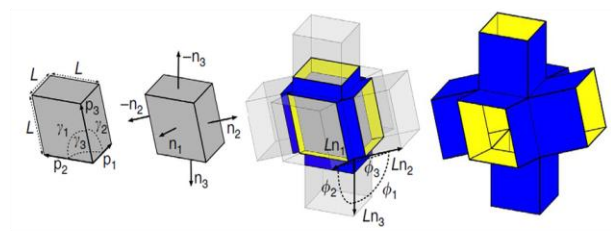
-Actuation:
Inflatable Air Pockets in Hinges, Mechanical Hand Pressure

-Aim of movement:
Changing the Function and Quality of Space

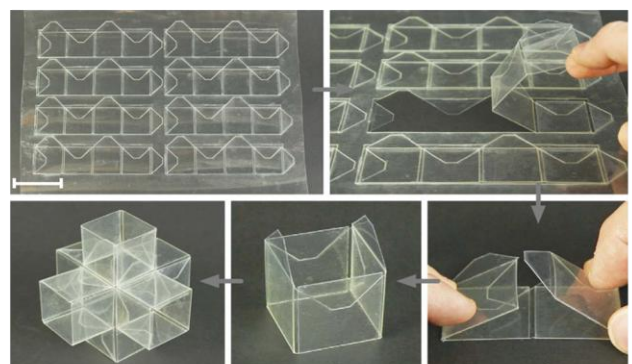
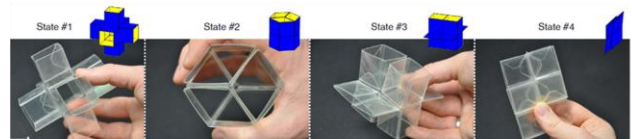
-Covered Area : Unit cells with $L=30\text{mm}$

-Movement Time : Less than 10sec

-Material and Construction:
The unit cells were fabricated from thin polymeric sheets
using an efficient stepwise layering and laser-cutting tech-
nique. Slight cut to form hinges



The possible shapes of the extruded cube unit cell.



Fabrication and deformation of a single extruded cube unit cell and the corresponding mechanical metamaterial.



The table presents the final comparative overview of all case studies and categorises them into two groups: **passive responsive systems** (shown in green) and **active responsive systems** (shown in violet). The horizontal axes organise the projects according to material type and year of development, allowing a chronological and material-based reading of responsiveness strategies. The vertical axis represents the scale of application, illustrated through stepped extrusions:

- One-step extrusion: research projects
- Two-step extrusion: installations and performance pieces
- Three-step extrusion: furniture-scale works
- Five-step extrusion: pavilions
- Highest-step extrusion: large-scale buildings

This overall comparison provides a comprehensive understanding of which technologies have been most effectively implemented within responsive design and highlights the fields in which responsiveness has been most actively explored. This diagram therefore serves as an essential synthesis, offering clear insights into the current state of responsiveness research and informing the design investigations that follow.

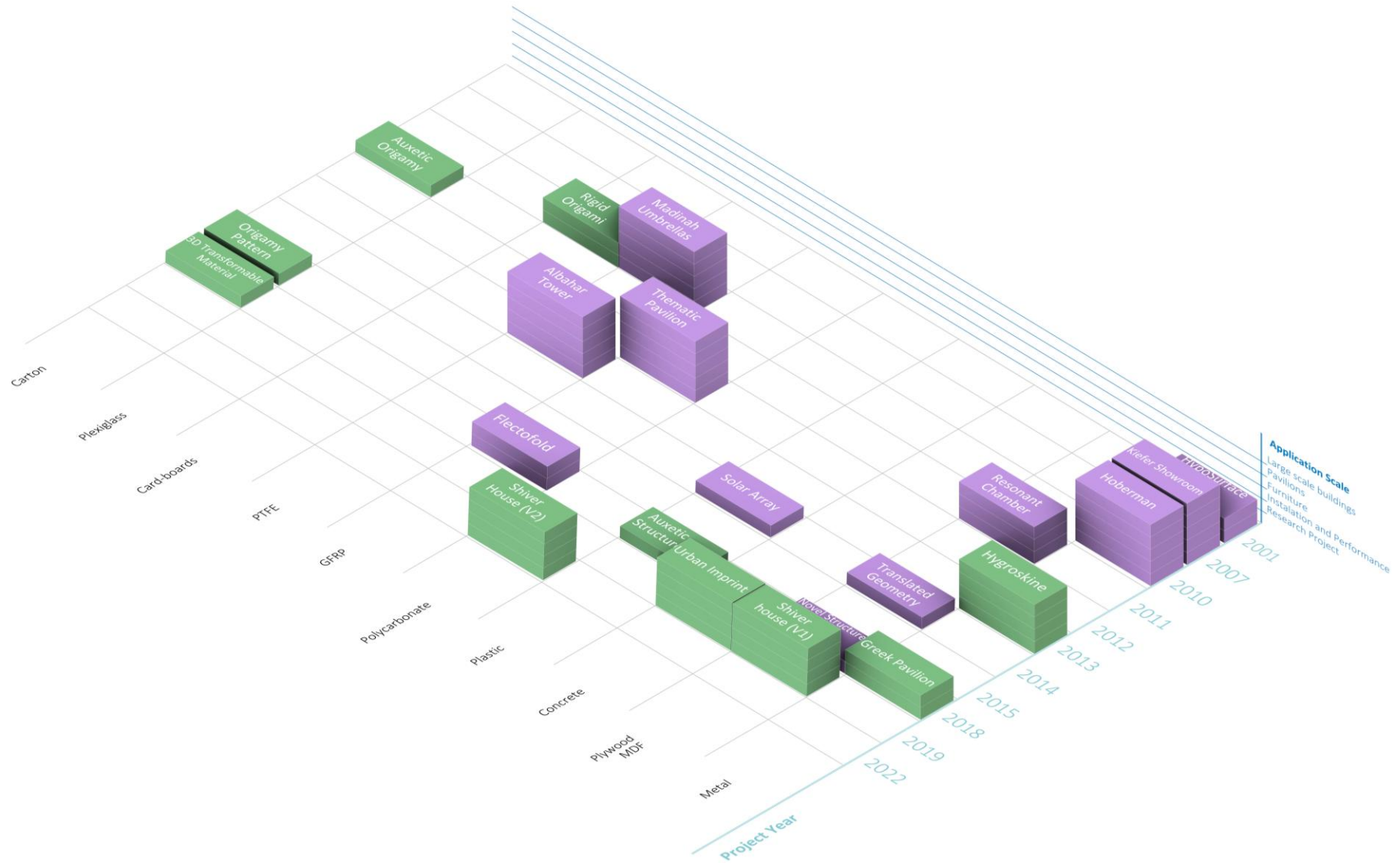


Fig 3.1: Overview of passive (green) and active (violet) responsive projects organised by material, year, and application scale.

05| Design Process

5.1. Exploration of Origami Folds and Geometries

5.2 Parametric Modelling and Simulation Process

5.3 Patterns Behaviour

5.4 Deformation in members

5.5 Conclusion

5.1. Exploration of Origami Folds and Geometries

As discussed in Section Three (Origami: Geometry, Mechanics, and Design Potential) of this thesis, the exploration of origami geometry focused on its mechanisms, various folding patterns, and their defining characteristics. This investigation considered factors such as geometric complexity, base form, folding type, aesthetic quality, and architectural applicability. While the range of potential origami patterns suitable for architectural surface design is vast and virtually unlimited, practical constraints necessitated a narrower focus. As a result, many patterns were excluded, and the preliminary analysis was limited to a selection of nine specific patterns:

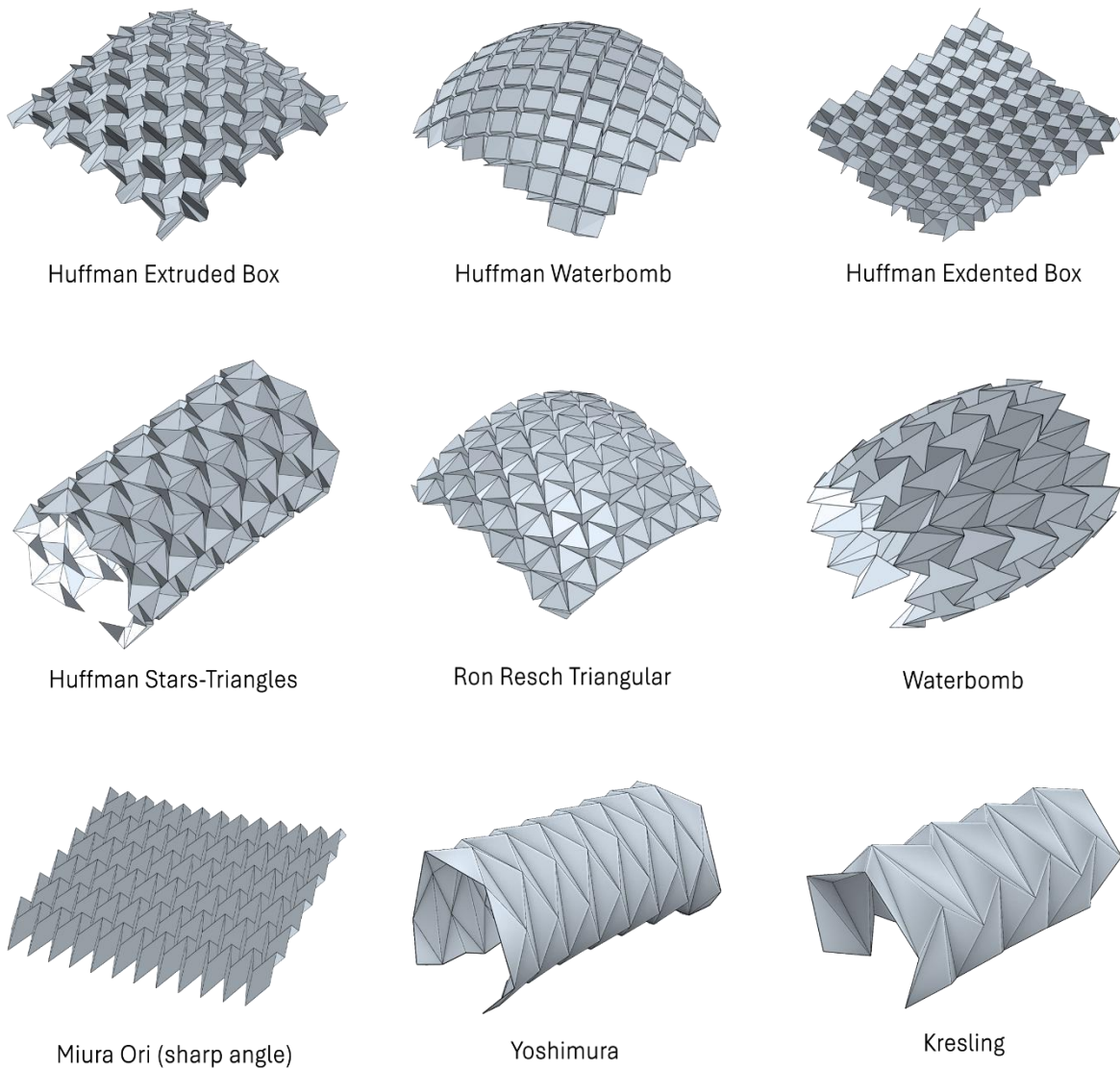


Fig 5.1: Selected patterns in 70%-folded configuration.

5.1.1 Huffman's family

David A. Huffman (1925–1999) is widely recognized in computer science for developing Huffman codes in information theory, and in the origami world as an early innovator in curved-crease folding. His origami tessellations stand out from most contemporary styles. While modern tessellations usually fold flat and are "locked" (meaning they cannot be unfolded without bending parts of the paper not marked by creases), Huffman's designs are often three-dimensional and fold rigidly, using only the crease lines without requiring extra bending. Many of his tessellation patterns are variations on each other. Two designs are considered directly related if a simple transformation connects them, and they're considered part of the same family if a series of such transformations links them. (Davis *et al.*, 2014)

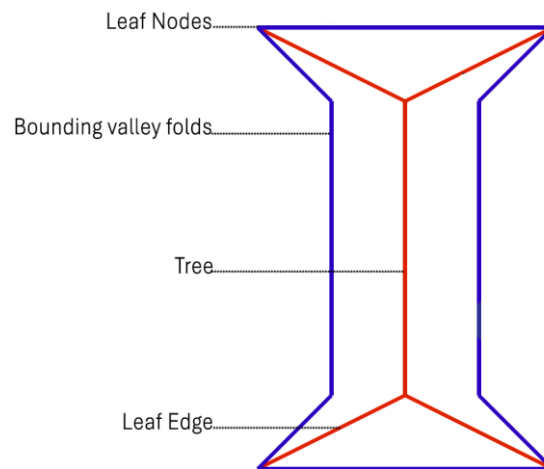
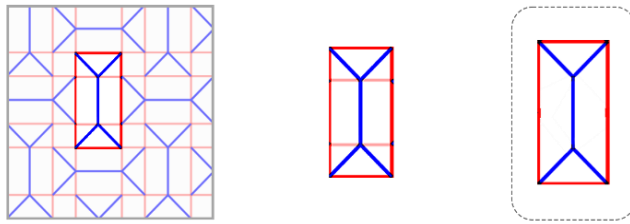


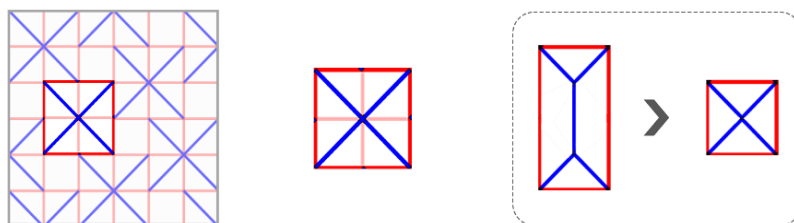
Fig 5.2: The components of repeating pattern (Davis *et al.*, 2014)

By ignoring the auxiliary creases in most of Huffman's work, we can identify a fundamental repeating unit, as illustrated in Figure 5.2. This unit typically consists of a bounding polygon and an internal tree-like structure. In transformations between tessellation designs, it is permitted to alter the bounding polygon to fit different tiling shapes, and to modify auxiliary creases as needed (Figure 5.3). However, the mountain-valley assignment of individual creases must remain unchanged, since altering them can break the structural logic of the fold. That said, it is acceptable to flip all creases at once — changing all mountains to valleys and vice versa — which results in a mirrored version of the original model. (Davis *et al.*, 2014)

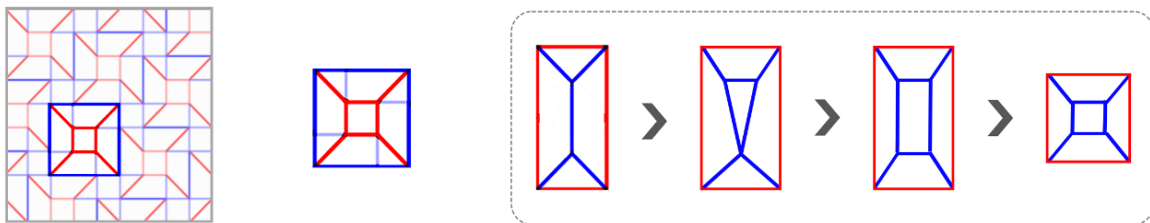
Huffman Extruded Boxes



Huffman's Waterbomb



Huffman Exdented Boxes



Huffman Stars Triangles

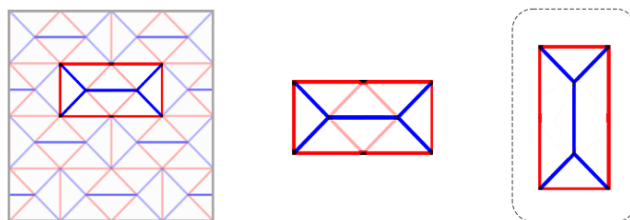


Fig 5.3: Enlargement of Nodes and Scaling of Boundaries in base unit in Different Patterns of Hoffman's Family (Mountain folds have **red** stroke, Valley folds have **blue** stroke)

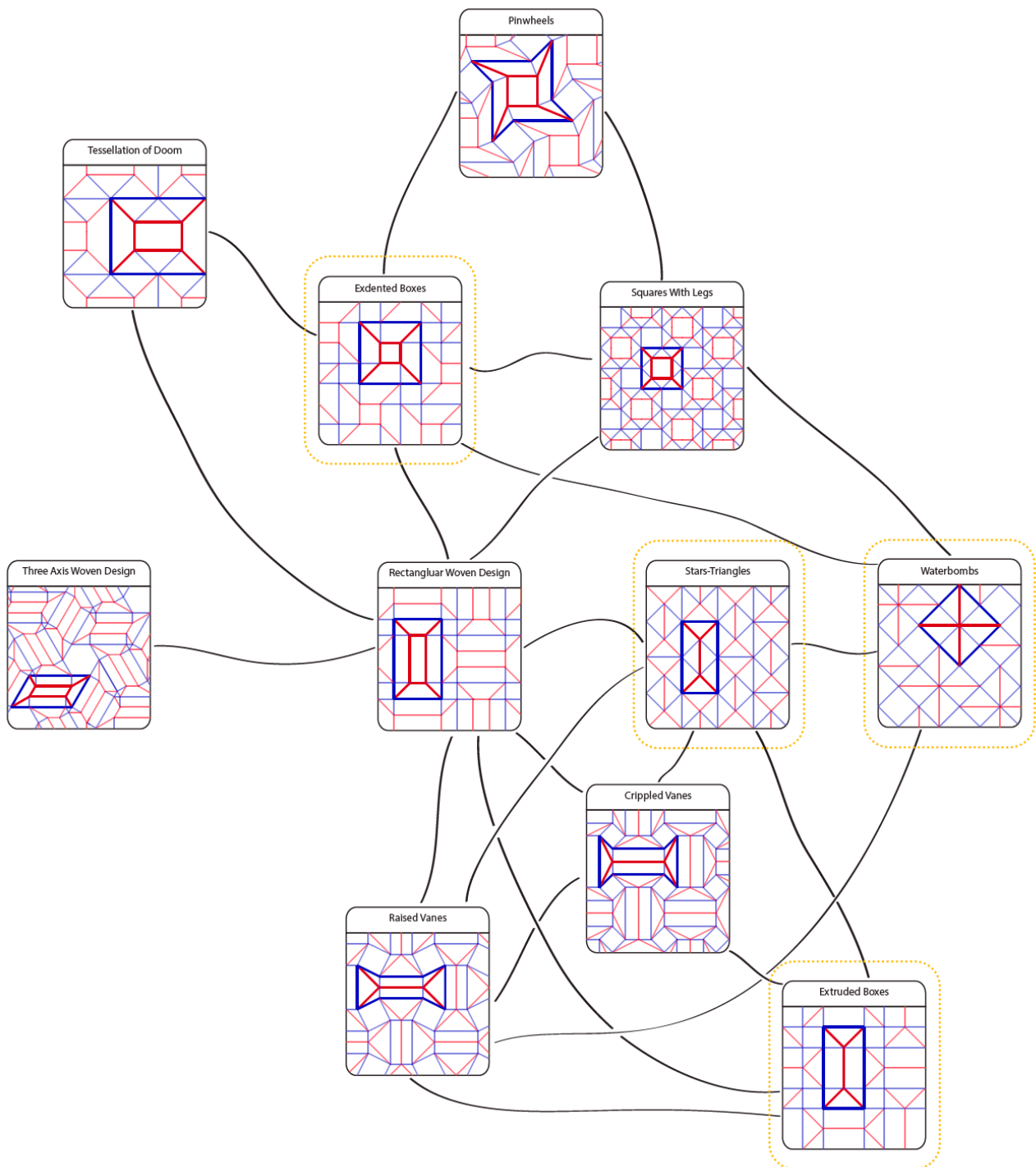
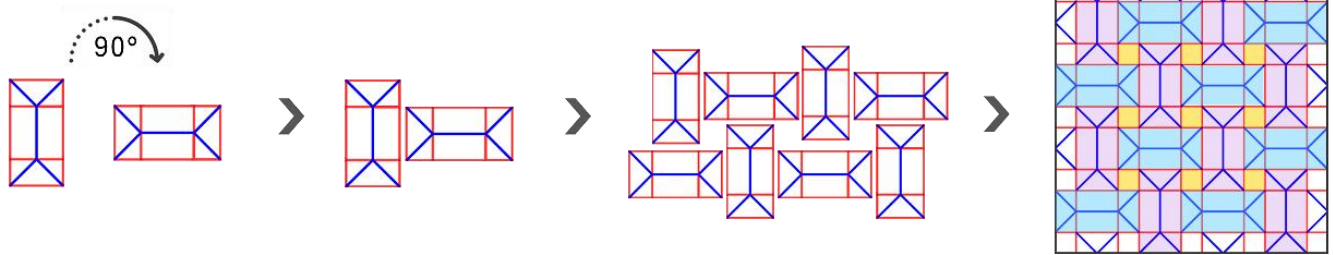


Fig 5.4: Selected patterns in the Huffman's Vanes Family Tree(Davis *et al.*, 2014)

Huffman Extruded Boxes



Geometry

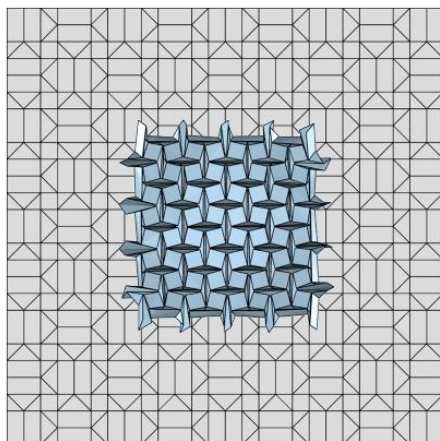
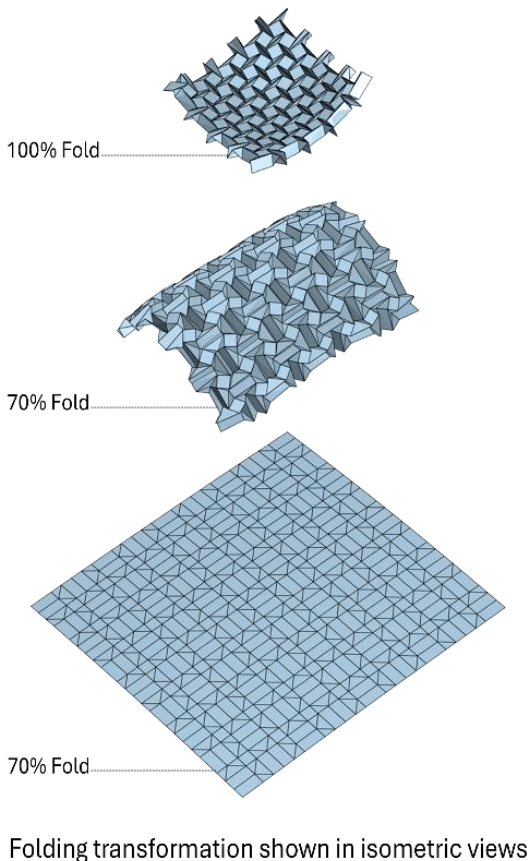
Base Unit Geometry:	Rectangular
Interior member Geometry:	Rectangular, Triangular
Crease Count per Unit:	8 Boundries, 9 Internal
Deformality Potential :	Low
Unit rotation and complexity limit geometric manipulation	

Structural | Architectural aspect

Rigidity:	High
Self -Supporting Potential:	High
Due to boxy extrusion, it holds shape well without external support	
Modularity / Tiling Efficiency:	High
Tiles well in grid patterns; strong modular repetition	
Construction Complexity:	High
Requires precision in folds and alignment for 3D extrusion	
Potential Applications:	Moderate
Shading, acoustic panels; Packaging and Storage; Facades or interior partitions; robotic limbs or grippers; Aerospace	

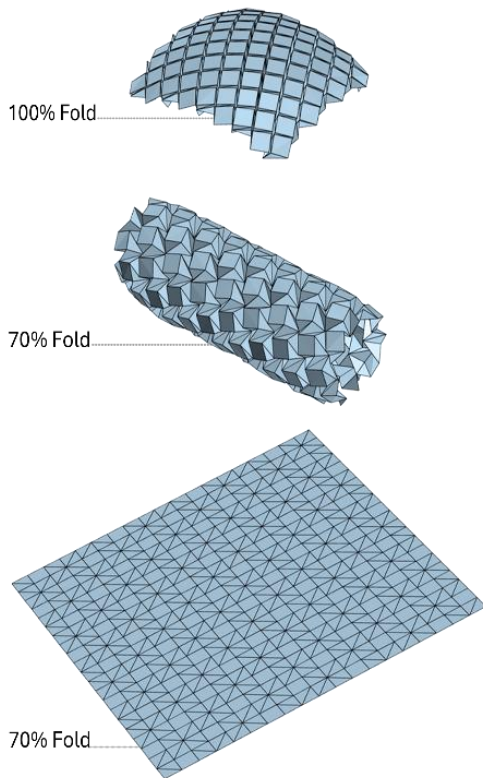
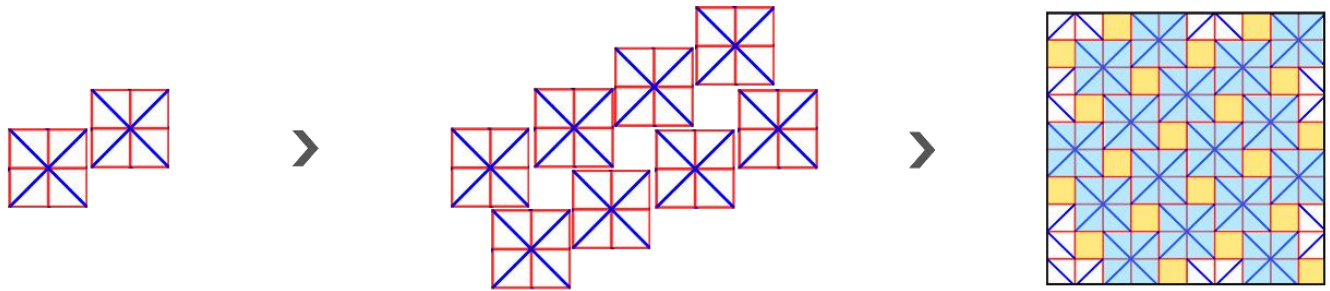
Kinetic Behaviour

Expansion/Contraction:	Planar (Multiaxial in-plane)
Primarily linear/planar with limited 3D deformation	
Folded Form - Minimum:	2D Plane
Folded Form - Maximum:	3D box structure
Area Contraction Percentage:	≈ 50%
Depends on the extrusion height and units size ratio	
Form Adaptability:	Low
Partially form change:	Low
Unit rotation and no separate rows or columns cause global movement	

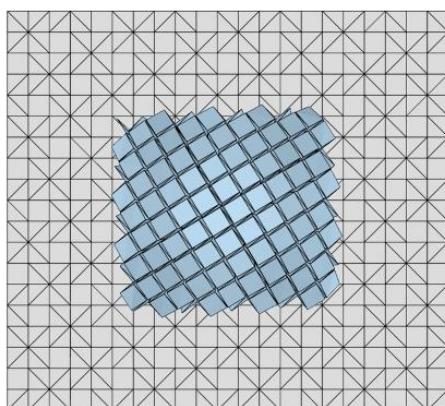


Demonstration of Area Contraction Between Flat and Fully Folded States.

Huffman Waterbomb



Folding transformation shown in isometric views



Demonstration of Area Contraction Between Flat and Fully Folded States

Geometry

Base Unit Geometry:	Square
Interior member Geometry:	Triangular, Square
Crease Count per Unit:	8 boundaries, 8 Internal
Deformity Potential:	Low
Due to the high crease density per unit hard to controll changes	

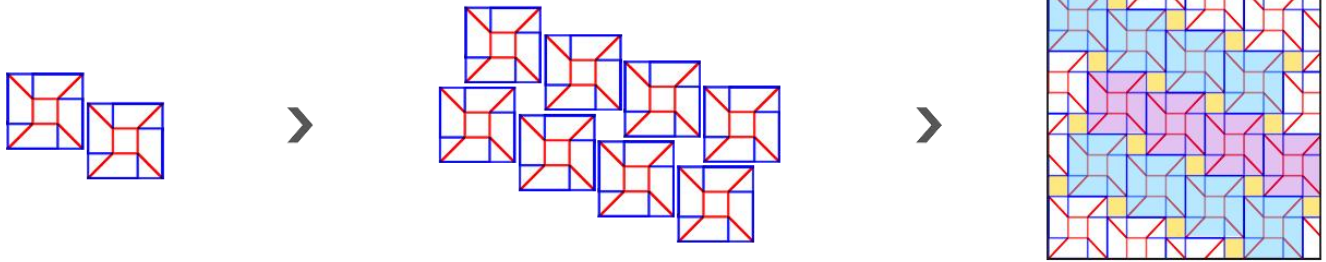
Structural | Architectural aspect

Rigidity:	Low
Self -Supporting Potential:	Low
Collapses easily without support	
Modularity / Tiling Efficiency:	High
Tesselates efficiently in grid or radial arrays	
Construction Complexity:	Moderate
Requires precise folding for correct interlocking and expansion.	
Potential Applications:	Moderate
Shading, acoustic panels; Packaging and Storage; Facades or interior partitions; robotic limbs or grippers; Aerospace	

Kinetic Behaviour

Expansion/Contraction:	3D (Out of plan)
3D deformation with dome/saddle tendency	
Folded Form - Minimum:	2D Plane
Folded Form - Maximum:	3D Box Structure
Area Contraction Percentage:	≈50%
Depends on the extrusion height and units size ratio	
Form Adaptability:	Low
Partially form change:	Low
Unit rotation and no separate rows or columns cause global movement	

Huffman Exdented Boxes



Geometry

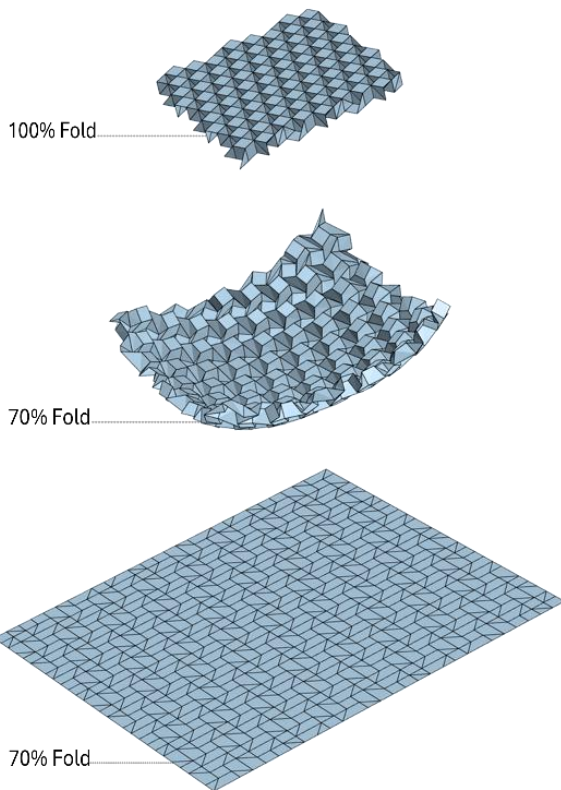
Base Unit Geometry:	Square
Interior member Geometry:	Triangular, Trapezoidal
Crease Count per Unit:	8 Boundries, 12 Internal
Deformity Potential:	Low
Due to the high crease density per unit hard to controll changes	

Structural | Architectural aspect

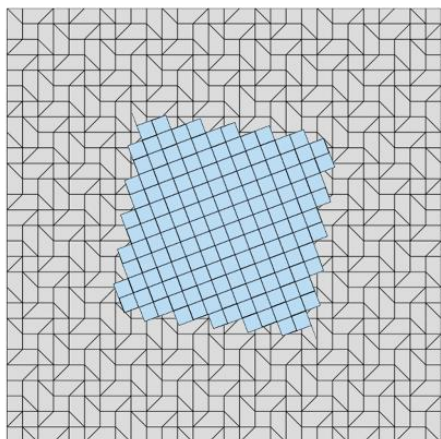
Rigidity:	Moderate
Self -Supporting Potential:	Moderate
High crease density requires added support for heavy loads	
Modularity / Tiling Efficiency:	High
Tesselates efficiently in grid or radial arrays	
Construction Complexity:	High
Requires precise folding for correct interlocking and expansion.	
Potential Applications:	Moderate
Shading, acoustic panels; Packaging and Storage; Facades or interior partitions; robotic limbs or grippers; Aerospace	

Kinetic Behaviour

Expansion/Contraction:	Planar (Multiaxial in-plane)
Primarily linear/planar with limited 3D deformation	
Folded Form - Minimum:	2D Plane
Folded Form - Maximum:	3D Box Structure
Area Contraction Percentage:	≈50%
Depends on the extrusion height and unit size ratio	
Form Adaptability:	Low
Partially form change:	Low
Unit rotation and no separate rows or columns cause global movement	

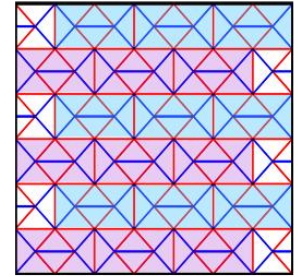
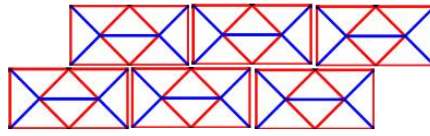
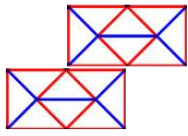


Folding transformation shown in isometric views



Demonstration of Area Contraction Between Flat and Fully Folded States

Huffman Stars Triangles



Geometry

Base Unit Geometry:

Rectagular

Interior member Geometry:

Triangular

Crease Count per Unit:

6 Boundries, 9 Internal

Deformity Potential:

Moderate

Row manipulation is possible, but high crease density requires precise fold coordination

Structural | Architectural aspect

Rigidity:

Moderate

Self -Supporting Potential:

Moderate

Forms dome-like or shell shapes; holds shape better than flat

Modularity / Tiling Efficiency:

Moderate

Tesselates efficiently in grid or radial arrays

Construction Complexity:

High

Requires precision due to complex folds and multiple crease angles

Potential Applications:

Moderate

Shading, acoustic curved panels; Packaging and Storage; Fa-cades or interior partitions

Kinetic Behaviour

Expansion/Contraction:

3D (Out of plan)

3D deformation with vault shape tendency

Folded Form - Minimum:

2D Plane

Folded Form - Maximum:

3D Vault Structure

Area Contraction Percentage:

≈50%

Depends on the extrusion height and units size ratio

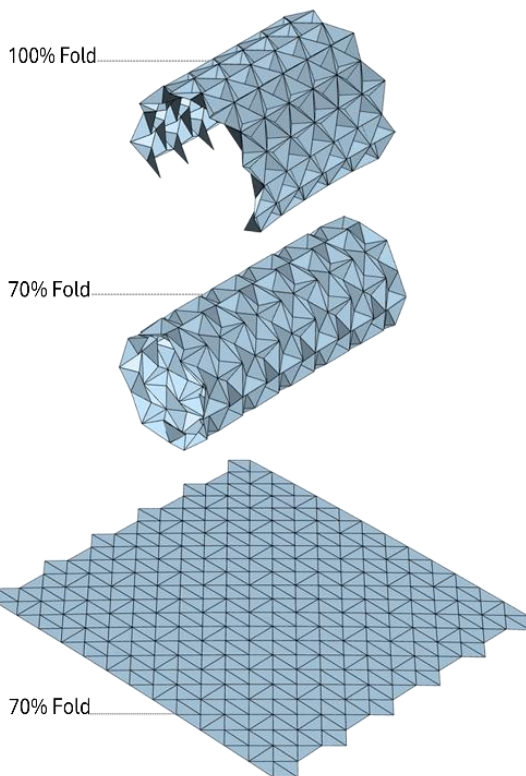
Form Adaptability:

Low

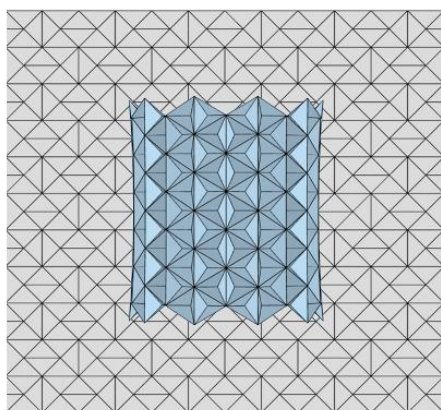
Partially form change:

Low

Strong geometric interdependency limits localized shape control



Folding transformation shown in isometric views



Demonstration of Area Contraction Between Flat and Fully Folded States

5.1.2 Ron Resch Triangular

The Resch Triangular Tessellation (RTT) is a well-known example of an origami tessellation design. It was developed and patented in the 1960s by Ronald Resch, who was an artist, computer scientist, and expert in applied geometry. This design features a repeating triangular pattern that appears consistently in both its folded and unfolded forms. (Resch, 1968)

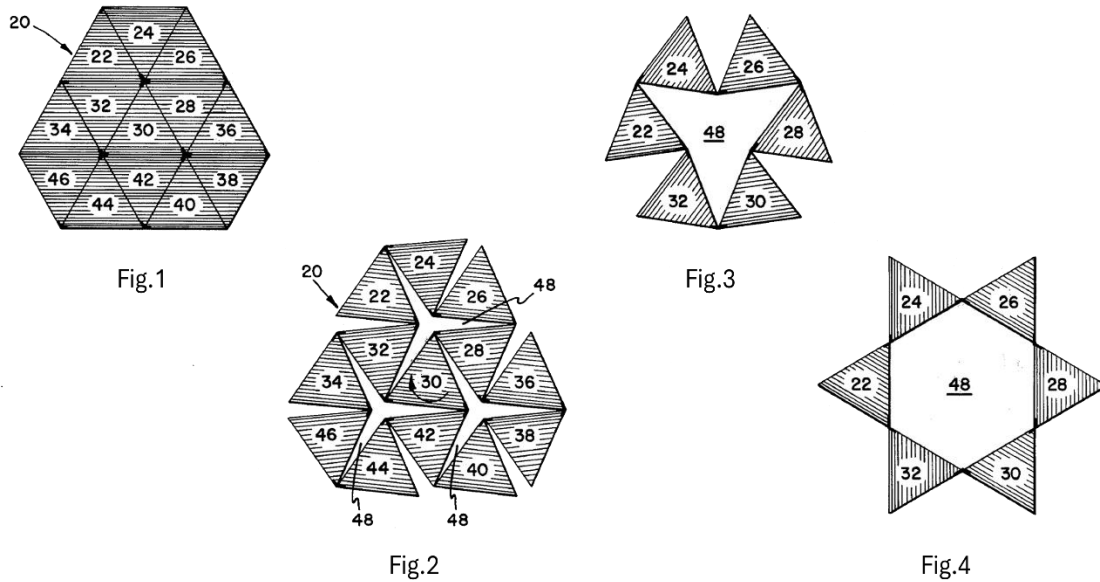


Fig. 5.5: Fig. 1: Top view of the geometric device in the closed position, showing identical equilateral triangle sections.

Fig. 2: Top view showing the device in a partially opened position between closed and fully open.

Fig. 3: Top view of a section of the device in a more advanced intermediate opening stage.

Fig. 4: Top view of a section of the device in the fully opened position. (Resch, 1976)

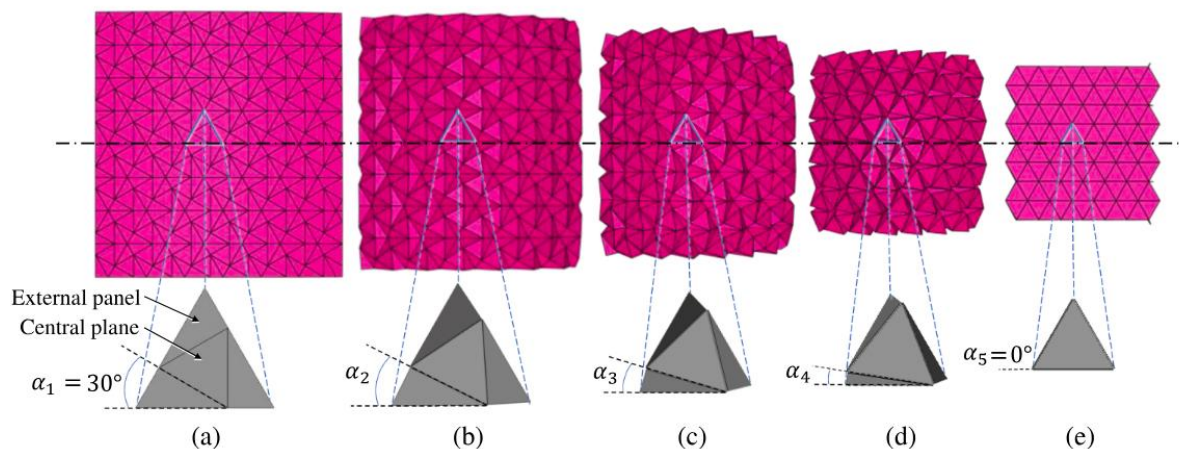
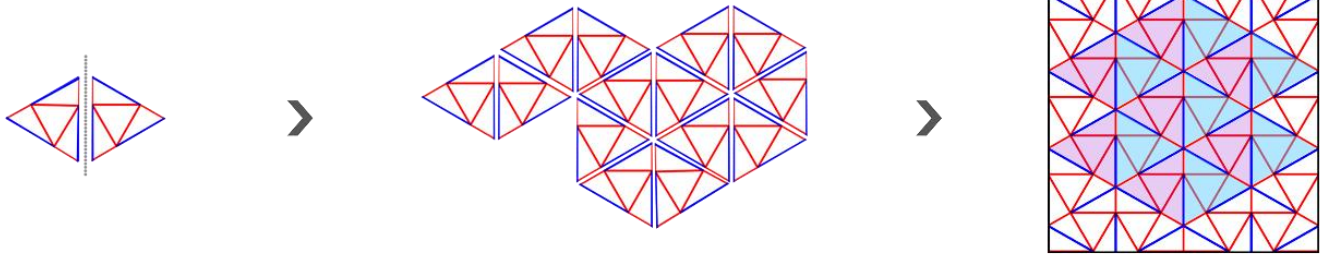


Fig. 5.6: The folding process of Ron Resch Triangular Tessellation and the twisting behaviour of the minimum unit (Haitong *et al.*, 2023)

Ron Resch Triangular



Geometry

Base Unit Geometry:	Equilateral triangle
Interior member Geometry:	Triangular
Crease Count per Unit:	6 Boundries, 3 Internal
Deformity Potential:	High
Allows localized manipulation due to triangular geometry	

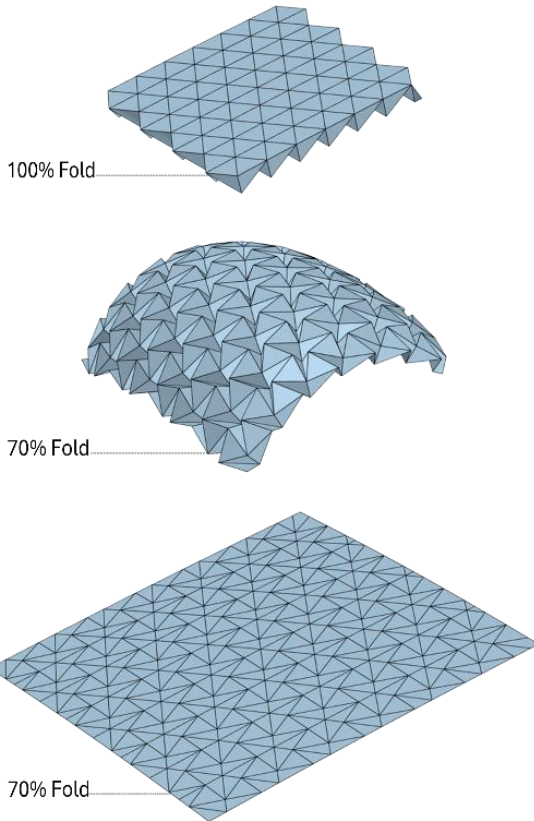
Structural | Architectural aspect

Rigidity:	Moderate
Self -Supporting Potential:	Low
Need to be reinforced unless shaped into a specific form	
Modularity / Tiling Efficiency:	High
Tesselates efficiently in grid or radial arrays	
Construction Complexity:	Moderate
Requires Precision in folds and creases; not ideal for fast production	
Potential Applications:	High
Shading, acoustic curved panels; Packaging and Storage; Fa-cades or interior partitions; Responsive skin	

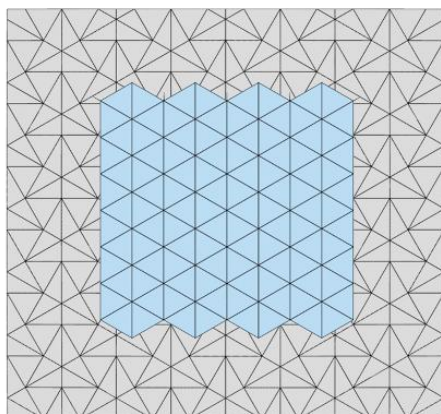
Kinetic Behaviour

Expansion/Contraction:	Planar (Multiaxial in-plane)
Articulated 3D surface reliefs without forming curved	
Folded Form - Minimum:	2D Plane
Folded Form - Maximum:	3D Box Structure
Area Contraction Percentage:	>50%
Form Adaptability:	High
Ideal for free-form, open surfaces; adapts well to multi-curved geometry	

Partially form change:	Moderate
Individual regions can buckle, pop, or fold independently	



Folding transformation shown in isometric views



Demonstration of Area Contraction Between Flat and Fully Folded States

5.1.3 Waterbomb

The waterbomb is a traditional Japanese origami model, often referred to as the “water balloon” due to its ability to be filled and burst like a toy. The six-crease waterbomb base originates from a square sheet and features two mountain folds and four valley folds radiating from a central vertex.(Chen *et al.*, 2016)

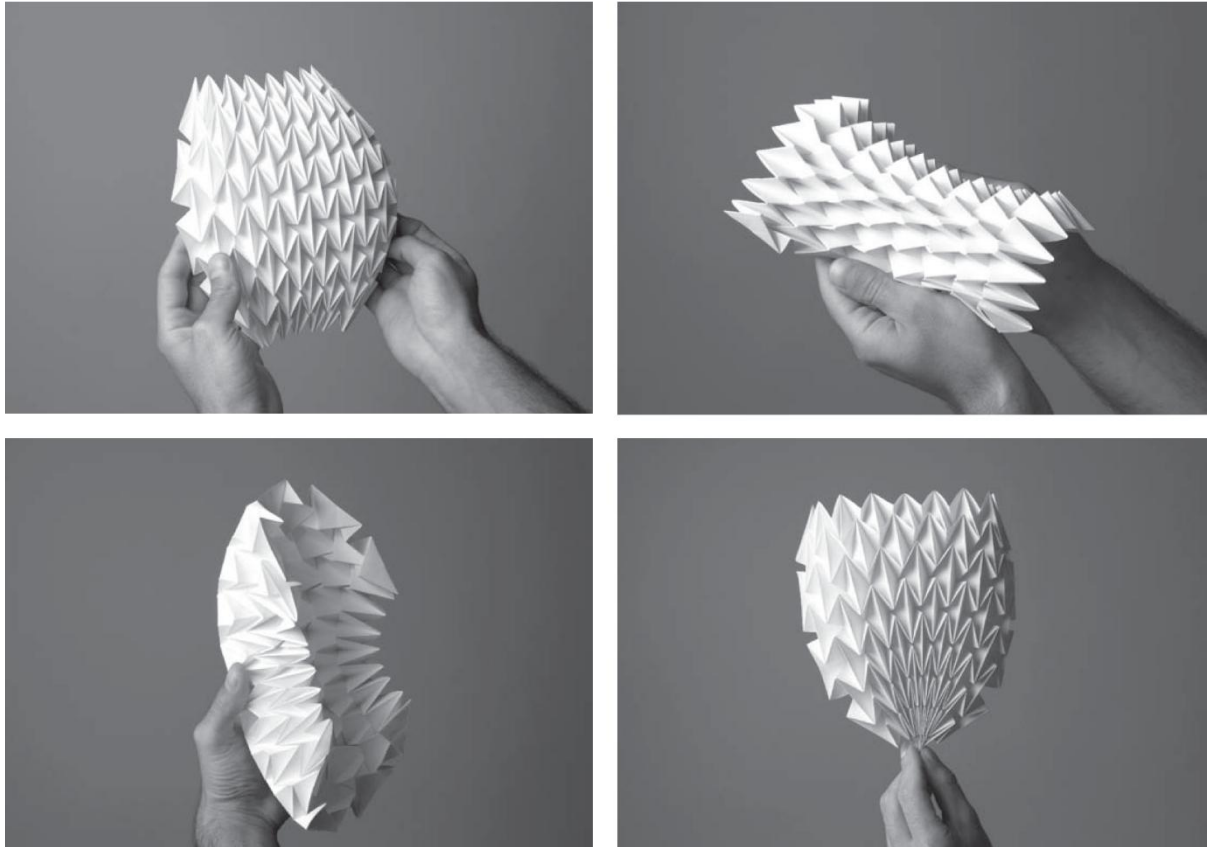
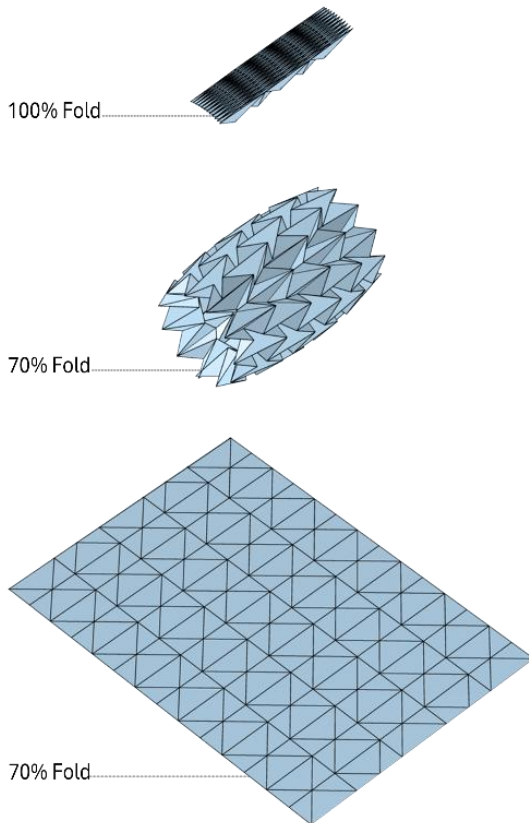
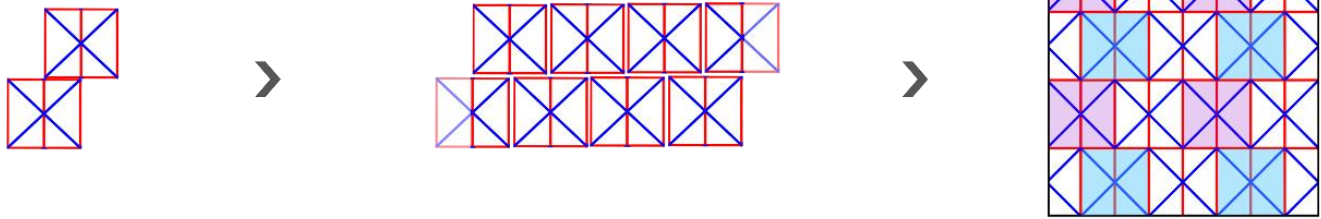


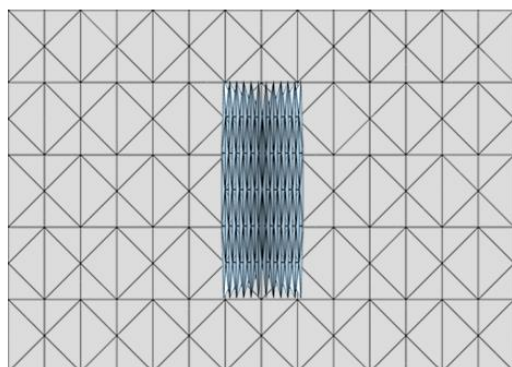
Fig. 5.7: Geometric Transformation of the Waterbomb Tessellation in Fold and Form (Jackson, 2011)

Mechanically, the waterbomb pattern functions as a spherical 6R linkage, with each vertex behaving like a mechanism composed of six rotational joints, offering up to three degrees of freedom. However, when geometric symmetry is applied—particularly in cylindrical or uniformly tessellated forms—this complex motion simplifies to a single degree of freedom, making the pattern significantly more predictable and controllable for engineered applications. Furthermore, the waterbomb configuration can demonstrate multistable behaviour, allowing it to maintain stability in multiple distinct folded states depending on its geometric parameters.(Chen *et al.*, 2016)

Waterbomb



Folding transformation shown in isometric views



Demonstration of Area Contraction Between Flat and Fully Folded States

Geometry

Base Unit Geometry:	Square
Interior member Geometry:	Triangular
Crease Count per Unit:	6 Boundries, 6 Internal
Deformity Potential:	Moderate
Adjustable row spacing, crease angle variation, limited local control	

Structural | Architectural aspect

Rigidity:	Moderate
Self -Supporting Potential:	Moderate
Needed to be paired with rigid panels or edge frames	
Modularity / Tiling Efficiency:	High
Tesselates efficiently in grid or radial arrays	
Construction Complexity:	Moderate
Requires precise alignment of creases to achieve functional fold	
Potential Applications:	Medium to High
Shading, acoustic panels; Building Skin; Packaging and Storage; Facades or interior partitions; robotic limbs or grippers; Aero-	

Kinetic Behaviour

Expansion /Contraction:	3D (Out of Plan)
Tendency to buckle and form dome-like or saddle-shaped	
Folded Form - Minimum:	2D Plane
Folded Form - Maximum:	1D vertical strip
Area Contraction Percentage:	X direction ≈100%
Assuming zero material thickness	
Y direction ≈30-40%	
Depends on the unit rows and ratio	
Form Adaptability:	High
Vault and saddle shapes from two-directional folds	
Partially form change:	Moderate
Row geometry allows local movement, but generally tends toward global behavior.	

5.1.5 Miura Ori

The Miura Ori is a well-known origami corrugation named after the astrophysicist Koryo Miura, who proposed it in 1985 as a way to pack solar panels for deployment in space.(Stachel, 2009)

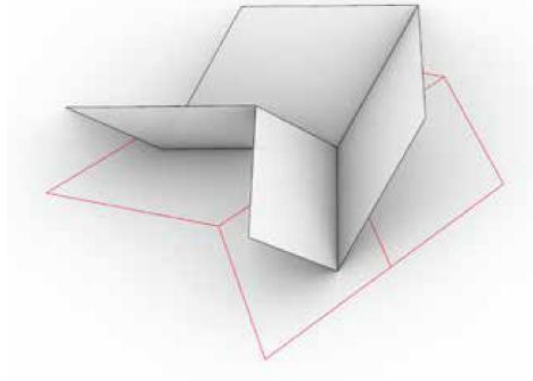


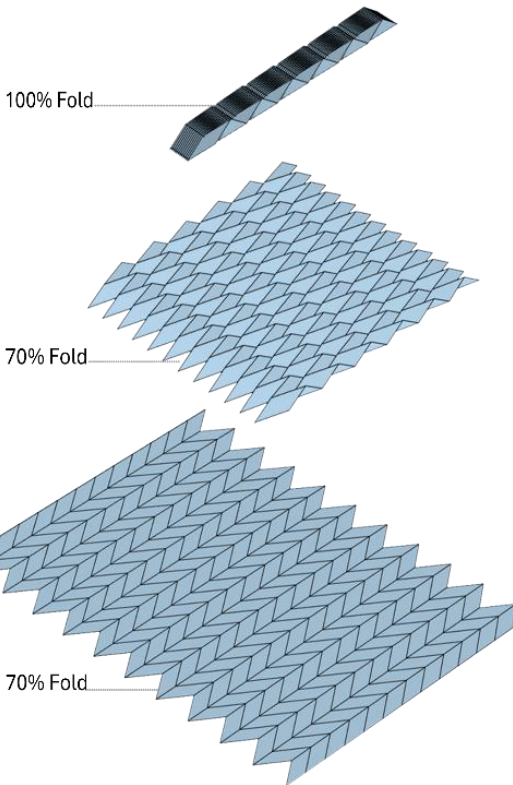
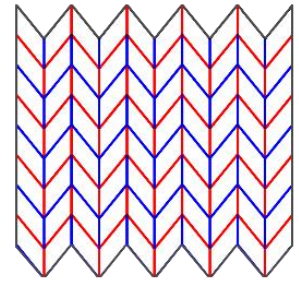
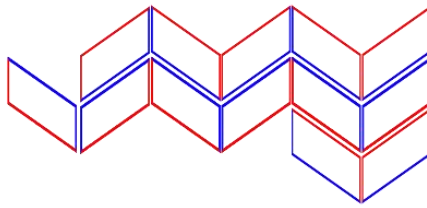
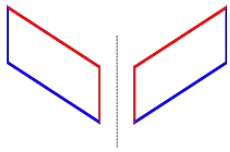
Fig. 5.8: A single module extracted from the Miura pattern clearly illustrates the folding behavior, allowing for easy identification of mountain and valley folds.(Jackson, 2011)

The Miura fold creates a tessellation of parallelograms with two types of crease directions: one with straight lines where each parallelogram is a mirror reflection of its neighbor, and another with zigzag lines where each parallelogram is a translated copy of its neighbor. Zigzag crease paths consist entirely of mountain or valley folds, alternating between paths. Straight crease paths alternate between mountain and valley folds. Importantly, the Miura fold is a type of rigid origami, meaning it can fold through a continuous motion without bending the faces, allowing it to be made from rigid materials.(Yogesh *et al.*, 2021)

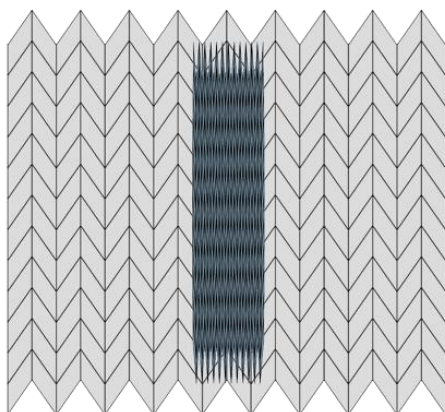


Fig. 5.9: Geometric Transformation of the Miura Ori Tessellation in Fold and Form. (Jackson, 2011)

Miura Ori



Folding transformation shown in isometric views



Demonstration of Area Contraction Between Flat and Fully Folded States

Geometry

Base Unit Geometry:	Rectangular or Parallelogram
Interior member Geometry:	-
Crease Count per Unit:	4 boundaries, No Internal
Deformity Potential:	High
Easy angle adjustment , Scalable unit across rows or column	

Structural | Architectural aspect

Rigidity:	Low
Self -Supporting Potential:	Low
Depends on fold depth, not inherently self-supporting	
Modularity / Tiling Efficiency:	High
Tessellates easily and efficiently in 2D plane	
Construction Complexity:	Low
Regular crease pattern, easy to replicate	
Potential Applications:	High
Shading, acoustic panels; Building Skin; Packaging and Storage; Facades or interior partitions; robotic limbs or grippers; Aero-space; Deployable Structures	

Kinetic Behaviour

Expansion/Contraction:	Planar + Linear
Contracts in one direction, expanding in the perpendicular one	
Folded Form - Minimum:	2D Plane
Folded Form - Maximum:	1D Narrow Strip
Area Contraction Percentage:	X Direction ≈100%
Assuming zero material thickness	
Y Direction ≈10-30%	
Depends on the unit rows number and ratio	
Form Adaptability:	High
By adjusting its geometry, highly adaptable to various forms	
Partially form change:	Moderate
Row geometry allows local movement and partial fold.	

5.1.6 Kresling

Twist buckling designs (also named “Kresling pattern”) is named after Biruta Kresling, a biologist who discovered it during her courses in the 1990's at Arts Décoratifs in Paris. (Kresling, 2012) The traditional structure of the Kresling origami is featured by only one mountain and one valley crease lines within each unit cell, which is of interest for its bistable property during the folding process. (Wang *et al.*, 2024)

The cylindrical structure of the Kresling origami enables it to provide stable nonlinear axial stiffness. Moreover, its nonlinear behaviour can be easily adjusted through small changes in geometric design, offering a wide range of configurations from monostable to multistable. (Yin *et al.*, 2024)

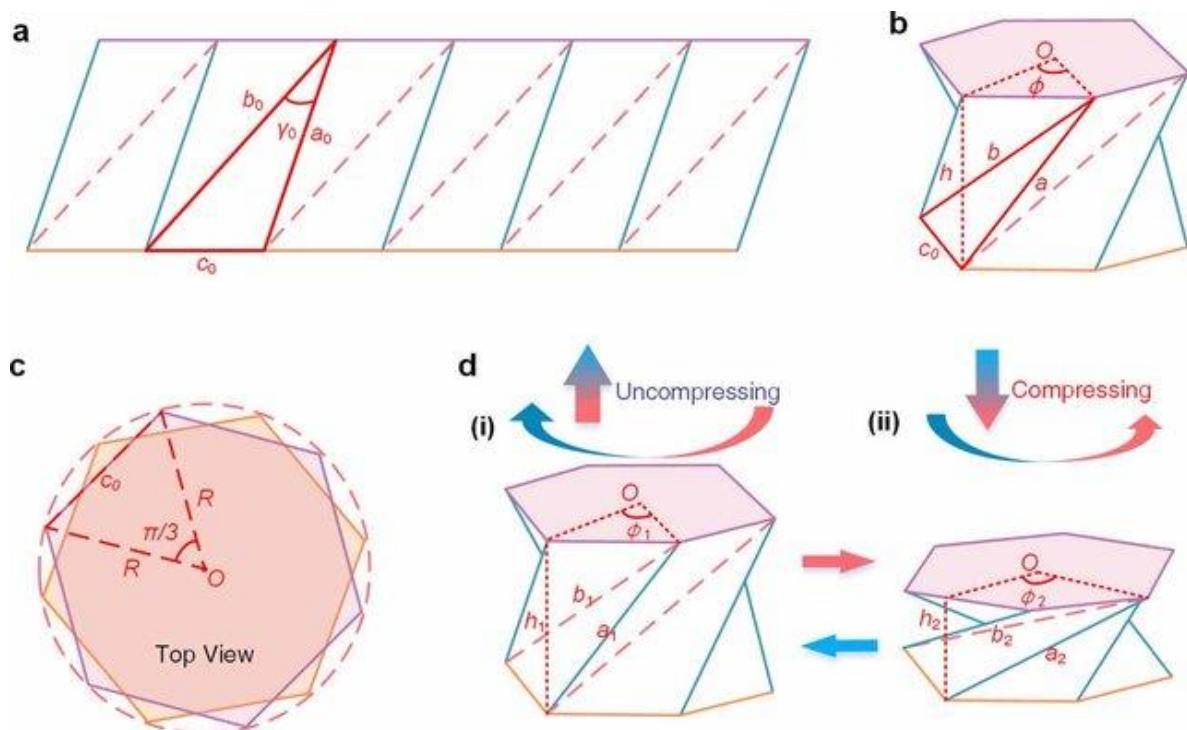
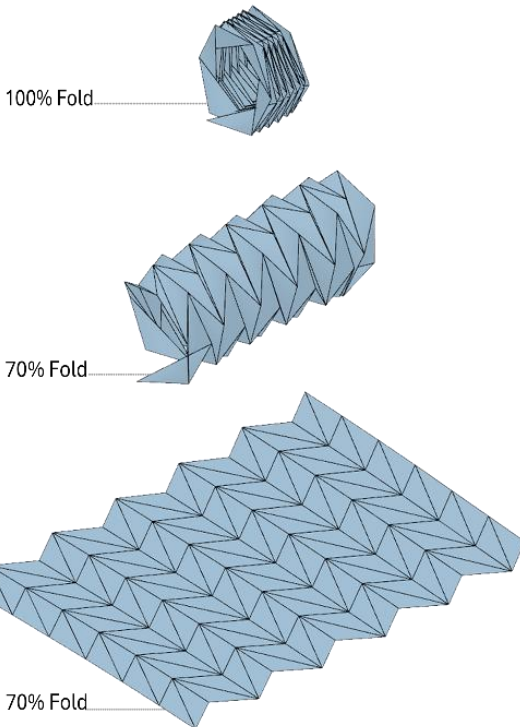
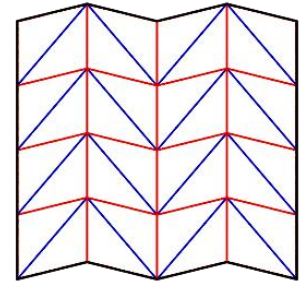
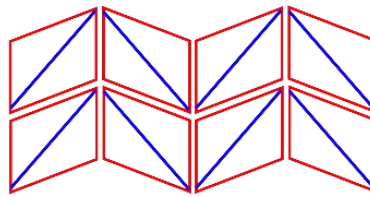
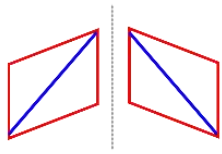
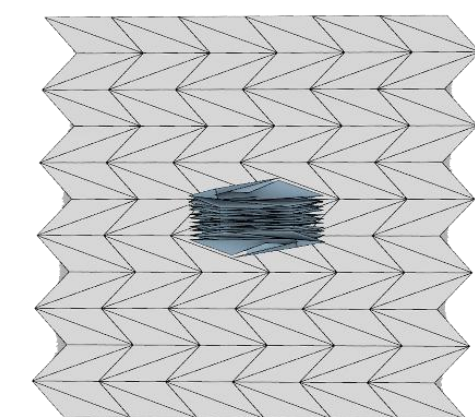


Fig. 5.10: Kresling origami configuration: (a) unfolded paper with a folding pattern for Kresling origami; (b) folded Kresling origami; (c) top view of Kresling origami; (d) configurations of Kresling origami undergoing compressing and uncompressing motion. (Yin *et al.*, 2024)

Kresling



Folding transformation shown in isometric views



Demonstration of Area Contraction Between Flat and Fully Folded States

Geometry

Base Unit Geometry:	Parallelogram
Interior member Geometry:	Triangular
Crease Count per Unit:	4 Boundries, 1 Internal
Deformity Potential:	High
Easy angle adjustment , Scalable unit across rows or column	

Structural | Architectural aspect

Rigidity:	High
Self -Supporting Potential:	High
Maintains structure due to its vault-like folded form	
Modularity / Tiling Efficiency:	High
Tessellates easily and efficiently in 2D plane	
Construction Complexity:	Low
Regular crease pattern; Easy to replicate	
Potential Applications:	High
Structural skins and facades; Energy-absorbing, Robotic and Aerospace components; Deployable structures; Furniture and product design	

Kinetic Behaviour

Expansion/Contraction:	3D; Cylindrical
Tendency to buckle and form Vault-like	
Folded Form - Minimum:	2D Plane
Folded Form - Maximum:	Flattened cylindrical shape
Area Contraction Percentage:	X Direction ≈60-70%
Depends on the unit rows number and ratio	
Y Direction ≈100%	
Assuming zero material thickness	
Form Adaptability:	Moderate
Ability to form vault; limited adaptability beyond its vertical axis	
Partially form change:	Moderate
Tendnecy to global movement; Partial change in high level of fold	

5.1.7 Yoshimura

Yoshimura buckling, named after Japanese researcher Yoshimaru Yoshimura is a triangular mesh buckling pattern that was first observed when a thin cylindrical shell was subjected to axial compression. (Yoshimura, 1955)

The pattern consists of isosceles triangles that share a common base edge, forming a repeating arrangement of rhombuses. (Sachithanandan, Uriol Balbin and Solano López, 2023) By adjusting the angles and dimensions of these individual triangles, slightly different buckling patterns can emerge, allowing for variations in the overall structure. (Yamaki and Kodama, 1976)

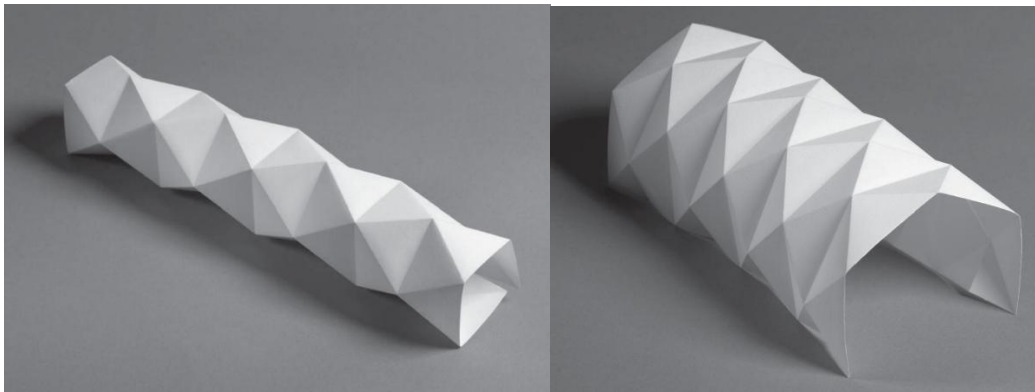


Fig. 5.11: Yoshimura model with different unit ratio (Jackson, 2011)

The pattern has more than one degree of freedom, which gives it greater flexibility in movement. Although the pattern is locally rigidly foldable for $\alpha < \pi/2$, except under specific circumstances, global self-intersection occurs before the second flat state can be reached with this fold path. (Evans *et al.*, 2015)

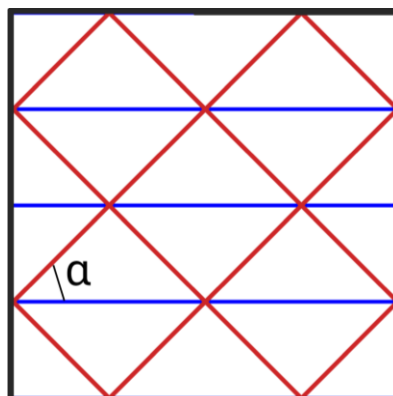
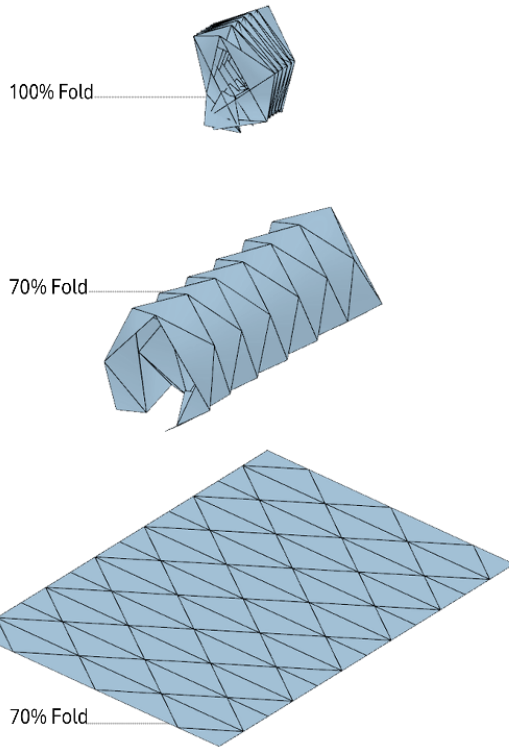
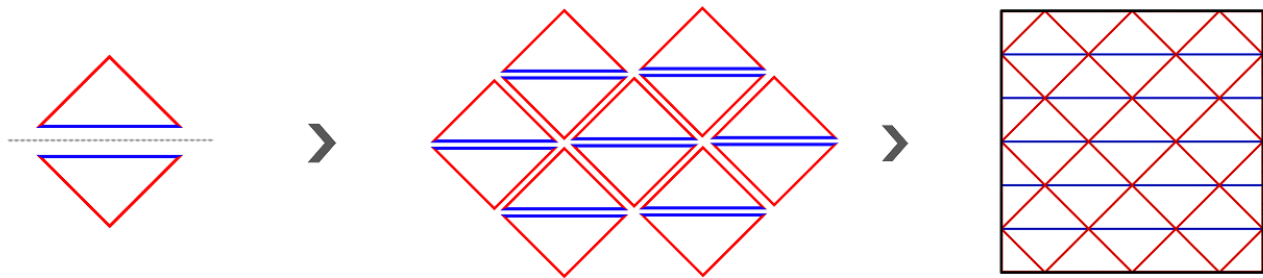
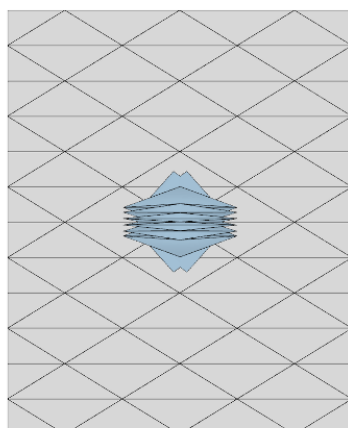


Fig. 5.12: Demonstration of α in Yoshimura pattern. (Mountain folds have **red** stroke, Valley folds have **blue** stroke)

Yoshimura



Folding transformation shown in isometric views



Demonstration of Area Contraction Between Flat and Fully Folded States

Geometry

Base Unit Geometry:	Triangular
Interior member Geometry:	-
Crease Count per Unit:	3 Boundries, No internal
Deformity Potential:	High
Easy angle adjustment ,Scalable unit across rows or column	

Structural | Architectural aspect

Rigidity:	Moderate
Self -Supporting Potential:	High
Maintains structure due to its vault-like folded form	
Modularity / Tiling Efficiency:	High
Tessellates easily and efficiently in 2D plane	
Construction Complexity:	Low
Regular crease pattern; Easy to replicate	
Potential Applications:	High
Structural skins and facades; Energy-absorbing, Robotic and Aerospace components; Deployable structures; Furniture and product design	

Kinetic Behaviour

Expansion/Contraction:	3D; Cylindrical
Tendency to buckle and form vault-like	
Folded Form - Minimum:	2D Plane
Folded Form - Maximum:	Flattened cylindrical shape
Area Contraction Percentage:	X Direction ≈60-70%
Depends on the unit rows number and ratio	
Y Direction ≈100%	
Assuming zero material thickness	
Form Adaptability:	High
Ability to form vault; Double-curved and free-form surfaces	
Partially form change:	High
Flexible in partial folds, good for gradient transformations	

5.1.8 Conclusion

After a thorough analysis of the nine selected origami patterns—each examined individually in terms of geometric structure, architectural expression, kinetic potential, and constructability—a comparative summary table was created to distil the most relevant design characteristics. This table served as the basis for selecting the most appropriate patterns for continued development in the context of responsive architectural surfaces.

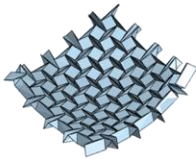

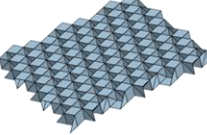



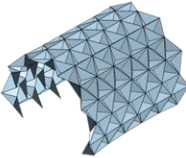

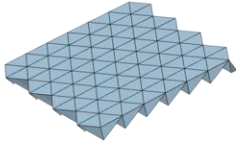
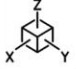
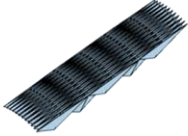

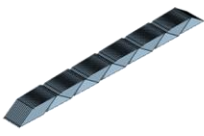

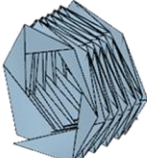

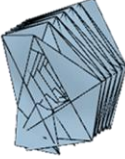

Several key criteria guided this selection. First, patterns with a high number of creases or excessive geometric complexity were excluded, as they posed challenges in fabrication and assembly. Second, recognizing the inherent rigidity of triangular geometry in structural design, patterns lacking a triangle-based structure were also removed from consideration. Flexibility in modifying the pattern—including its proportions and folding ratios—was another essential factor, as adaptability is critical in responsive design. Furthermore, particular attention was given to the area of contraction, since the objective is to use these patterns in surfaces capable of dynamic shape transformation. Patterns with higher contraction potential offer more meaningful responsiveness and versatility in architectural applications.

An additional selection criterion was the pattern's spatial performance—its ability to naturally generate enclosure-like forms, such as vaults or shells, without relying heavily on external supports. Secondary considerations included self-supporting potential, directionality of expansion and contraction, and the possibility of partial or localized folding—qualities that can influence architectural scale, interaction, and material behaviour.

As a result of this multi-criteria evaluation, three patterns were chosen for further architectural exploration: Kresling, Yoshimura, and the Six-Crease Waterbomb. These patterns demonstrated the strongest overall performance across the criteria and offer a promising balance between formal richness, kinetic responsiveness, and feasibility in construction, aligning closely with the architectural goals of this thesis.

Pattern Name	Pattern	Unit Geometry	Crease Count	Geometry Deformation	Self-supporting Potential
Huffman Extruded Box		Rectangular Triangular	17	Low	High
Huffman Exdented Box		Quadrangular Triangular Trapezoidal	20	Low	Moderate
Huffman Watetbomb		Quadrangular Triangular	16	Low	Low
Huffman Star-Triangle		Triangular	15	Moderate	Moderate
Ron Resch Triangular		Triangular	9	High	Moderate
Waterbomb		Triangular	12	Moderate	Moderate
Muir Ori		Rectangular	4	High	Low
Yoshimura		Triangular	3	High	High
Kresling		Triangular	5	High	High

05| Design Process

Construction Complexity	Architectural Applicability	Localized Form Change	Area contraction Percentage		Folded-Form Maximum	Expansion Contraction
			X	Y		
High	Moderate	Low	≈50%	≈50%		
High	Moderate	Low	≈50%	≈50%		
High	Moderate	Low	≈50%	≈50%		
High	Moderate	Moderate	≈50%	≈50%		
Moderate	High	Moderate	>50%	>50%		
Moderate	High	Moderate	≈100%	>40%		
Low	High	High	≈100%	>20%		
Low	High	High	≈70%	≈100%		
Low	High	High	≈70%	≈100%		

5.2 Parametric Modelling and Simulation Process

To gain a deeper understanding of the kinetic behaviour of the selected origami patterns and explore their architectural and formal potentials, the next stage of this thesis involved a simulation-based design process using Rhinoceros 3D®, Grasshopper®, and the Kangaroo physics plugin. This transition into digital simulation allowed for more precise parametric control and deeper analysis of how each pattern could respond to various deformation conditions in an architectural context.

Kangaroo is a real-time physics engine plugin within the Grasshopper environment, which uses Verlet's implementation (particle-spring model) to enable simulation of material behaviour and interaction with environmental forces. In this case, it was used to simulate how the origami patterns react to shape change and movement, acting as a tool to observe and control their transformation potential.

The first step in the workflow was to create the origami pattern modelled as a parametric system on a flat rectangular base surface in Grasshopper. The next step involved introducing a target geometry—a vault-shaped curve—to serve as a reference form (Fig 5.13). This target curve became the benchmark test standard for all simulations. The flat origami pattern was pulled toward this vault-like target form using Kangaroo, effectively simulating how the pattern folds, adapting to new spatial constraints and conditions.

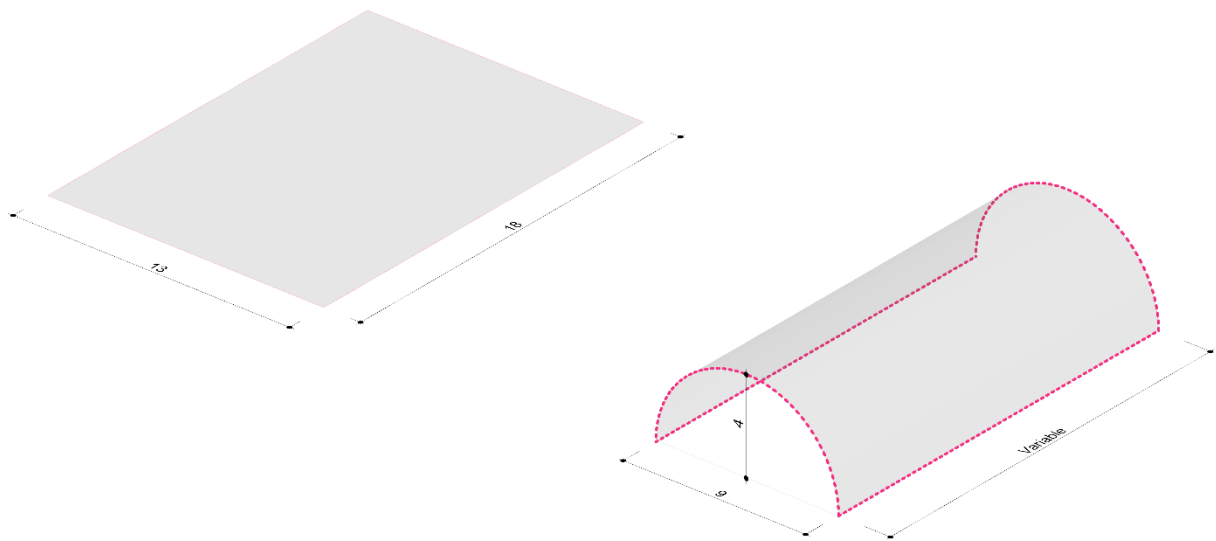


Fig 5.13: From left to right: Base surface for origami patterns, Target curve as reference form for our change process.

At this stage of the process—when both the origami pattern and the target surface are defined within the parametric environment—it is essential to identify and define the key variables and factors that influence and measure the design outcome. The following parameters were established:

- **Fold Intensity:** the degree of folding applied to the origami surface. It ranges from 0.001 (indicating a nearly flat surface) to 0.99 (indicating a fully folded state). By adjusting this value, the extent of deformation and the surface's responsiveness to the target geometry could be modulated.
- **Target Deformation Strength:** determines how strongly the origami surface conforms to the vault-shaped target geometry. It directly affects the tension and form adaptation during the simulation.
- **U and V Pattern Division Numbers:** the number of divisions along the U and V directions of the origami pattern. These are critical parameters, as they influence the aspect ratio of the pattern cells, the structural performance of the surface, and the visual expression of the final form.
- **Shrink Factor:** the amount of shrinkage applied to the surface in the longitudinal direction, representing the contraction experienced by the final vault form. It is particularly important for assessing the flexibility and adaptability of different origami configurations.
- **Members Stiffness:** the stiffness of the origami pattern's linear elements within the Kangaroo simulation; how much each member resists deformation (stretching or compression) under applied forces.

The process of altering these parameters was not a linear process. It required continuous, iterative refinement—a back-and-forth workflow—since any change in one parameter directly influenced the overall deformation behaviour and its interaction with the target geometry. Each adjustment demanded re-evaluation of previous steps, reinforcing the responsive and interconnected nature of the parametric design system.

5.2.1 Fixed Parameters and Comparative Framework

To conduct a meaningful and consistent comparison between the three different origami-based patterns, a set of fixed parameters was established. These parameters were applied equally across all simulations, allowing the analysis to focus specifically on the impact of U/V division and shrinkage factor. The fixed parameters used in this study are as follows:

- Base Surface Dimensions: 18 meters × 13 meters
- Target Vault Radius: 4.3 meters
- Target Deformation Strength: 5
- Fold Intensity: 0.99 (maximum folding state)
- Member Stiffness: 60 (it could be between zero to infinity, higher number mean less deformation)

By holding these parameters constant, only two variables were changed in the simulations: U/V Division and Shrink Factor.

This approach provides a clear framework for evaluating the geometric and structural behaviour of each pattern under controlled conditions. The following sections will explore the performance of each pattern individually, followed by a comparative analysis.

5.2.2 Unit Aspect Ratio

The Unit Aspect Ratio (UAR) is calculated based on the actual dimensions of each base unit after division, rather than simply using the ratio of division counts. The formula is:

$$UAR = \left(\frac{Sd_U}{U_{div}}\right) / \left(\frac{Sd_V}{V_{div}}\right)$$

For example, if the surface dimension in the U direction is 13 units divided into 3 segments, and the surface dimension in the V direction is 18 units divided into 4 segments, then:

$$UAR = \left(\frac{13}{3}\right) / \left(\frac{18}{4}\right) \approx 0.96$$

Simply taking the ratio of U and V division numbers does not accurately reflect the actual proportions of the base units because the overall surface shape affects their size. For instance, the same U and V division counts applied to rectangular versus square surfaces produce units with different dimensions and aspect ratios. By using the actual physical dimensions of each unit (i.e., the length of the surface divided by the number of divisions in each direction), this method ensures that the calculated aspect ratio truly represents the geometric proportions of the base units. This leads to more accurate predictions of surface performance and behavior.

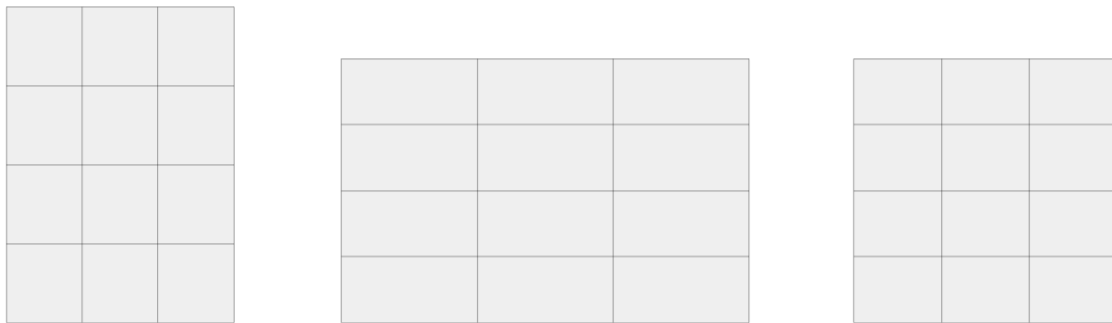


Fig 5.14: Effect of Base Surface Dimensions on Unit Ratio: Surfaces with identical subdivisions (U:3, V:4) but different base shapes—vertical rectangle, horizontal rectangle, and square (from left to right)—demonstrate how unit proportions vary depending on the overall surface dimensions.

5.3 Patterns Behaviour

With the key variables defined and the simulation process established, the next phase of the study involved testing and comparing three different origami-based patterns. Each pattern was analysed through a series of controlled tests, focusing on its behaviour under varying U and V divisions, shrinkage factors and member deformation ranges. The goal of this comparative approach was to identify how different geometric configurations affect the surface's adaptability and responsiveness, structural performance, and visual expression.

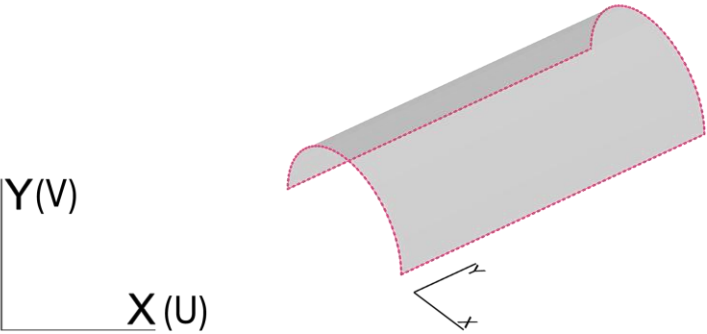
The result was divided in three categories:

- Successful Vault + Shrinkage Adaptation
- Successful Vault Adaptation
- Both Failed

Yoshimura Pattern Behaviour

V 40	9.63	5.78	3.21	2.63	2.06	1.44	0.96	9.63
V 30	7.22	4.33	2.41	1.97	1.55	1.08	0.72	7.22
V 20	4.81	2.89	1.60	1.31	1.03	0.72	0.48	4.81
V 14	3.37	2.02	1.12	0.92	0.72	0.51	0.34	3.37
V 11	2.65	1.59	0.88	0.72	0.57	0.40	0.26	2.65
V 9	2.17	1.30	0.72	0.59	0.46	0.33	0.22	2.17
V 7	1.69	1.01	0.56	0.46	0.36	0.25	0.17	1.69
V 5	1.20	0.72	0.40	0.33	0.26	0.18	0.12	1.20
V3	0.72	0.43	0.24	0.20	0.15	0.11	0.07	0.72
	U 3	U 5	U 9	U 11	U 14	U 20	U 30	U40

Unit Aspect Ratio



- Successful Vault + Shrinkage Adaptation
- Successful Vault Adaptation
- Failed in both

V 40

V 30

V 20

V 14

V 11

V 9

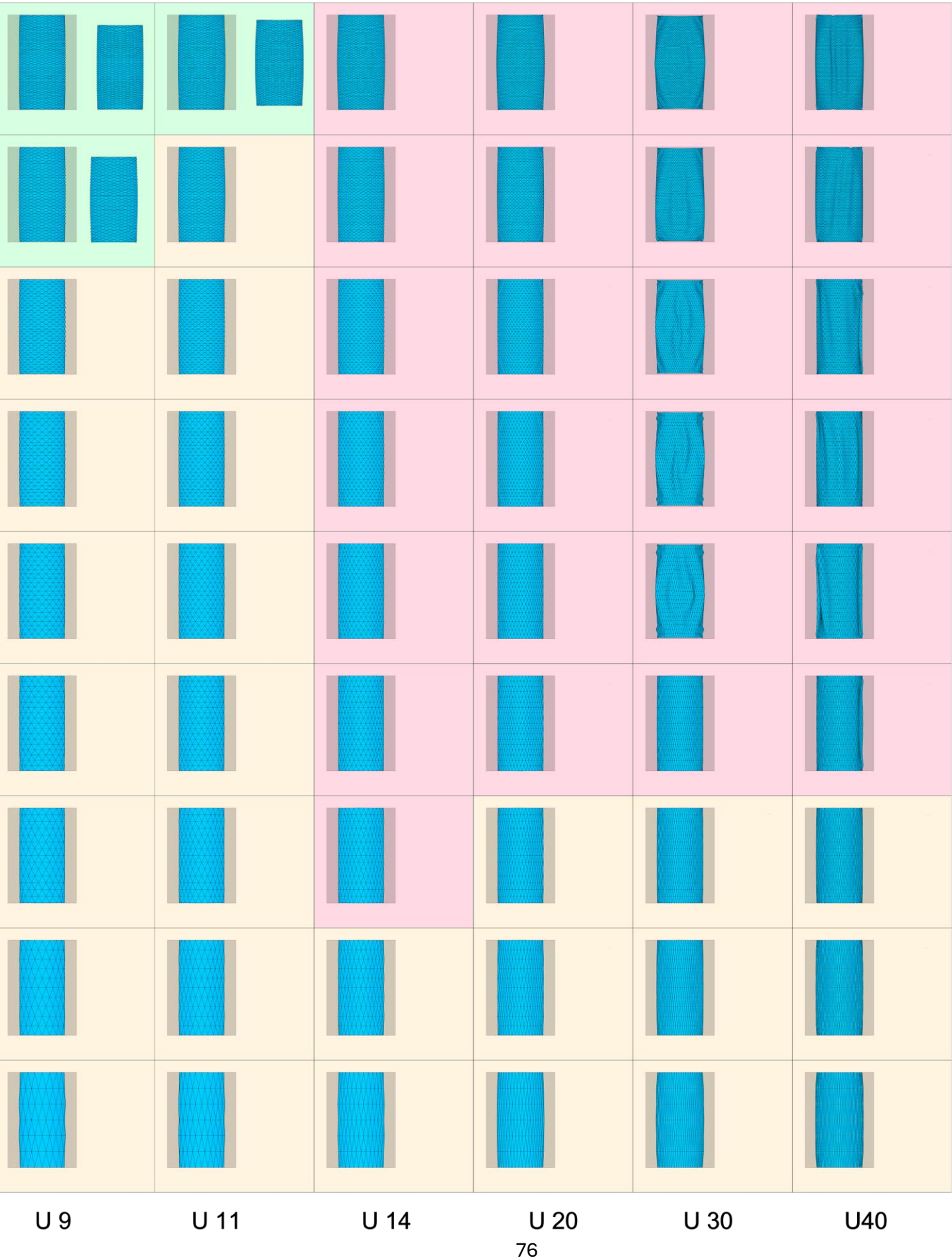
V 7

V 5

V3

U 3

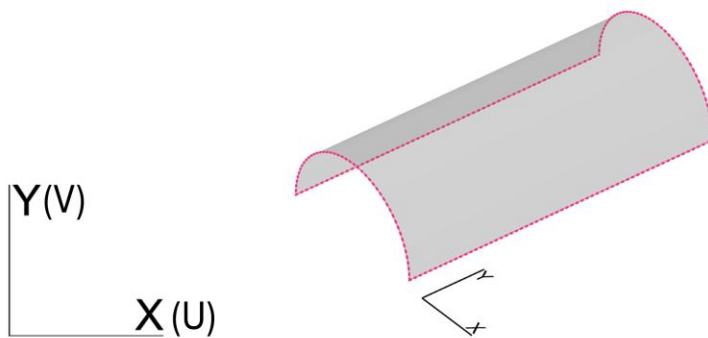
U 5



Kresling Pattern Behaviour

V 40	9.63	5.78	3.21	2.63	2.06	1.44	0.96	9.63
V 30	7.22	4.33	2.41	1.97	1.55	1.08	0.72	7.22
V 20	4.81	2.89	1.60	1.31	1.03	0.72	0.48	4.81
V 14	3.37	2.02	1.12	0.92	0.72	0.51	0.34	3.37
V 11	2.65	1.59	0.88	0.72	0.57	0.40	0.26	2.65
V 9	2.17	1.30	0.72	0.59	0.46	0.33	0.22	2.17
V 7	1.69	1.01	0.56	0.46	0.36	0.25	0.17	1.69
V 5	1.20	0.72	0.40	0.33	0.26	0.18	0.12	1.20
V 3	0.72	0.43	0.24	0.20	0.15	0.11	0.07	0.72
	U 3	U 5	U 9	U 11	U 14	U 20	U 30	U 40

Unit Aspect Ratio



- Successful Vault + Shrinkage Adaptation
- Successful Vault Adaptation
- Failed in both

V 40

V 30

V 20

V 14

V 11

V 9

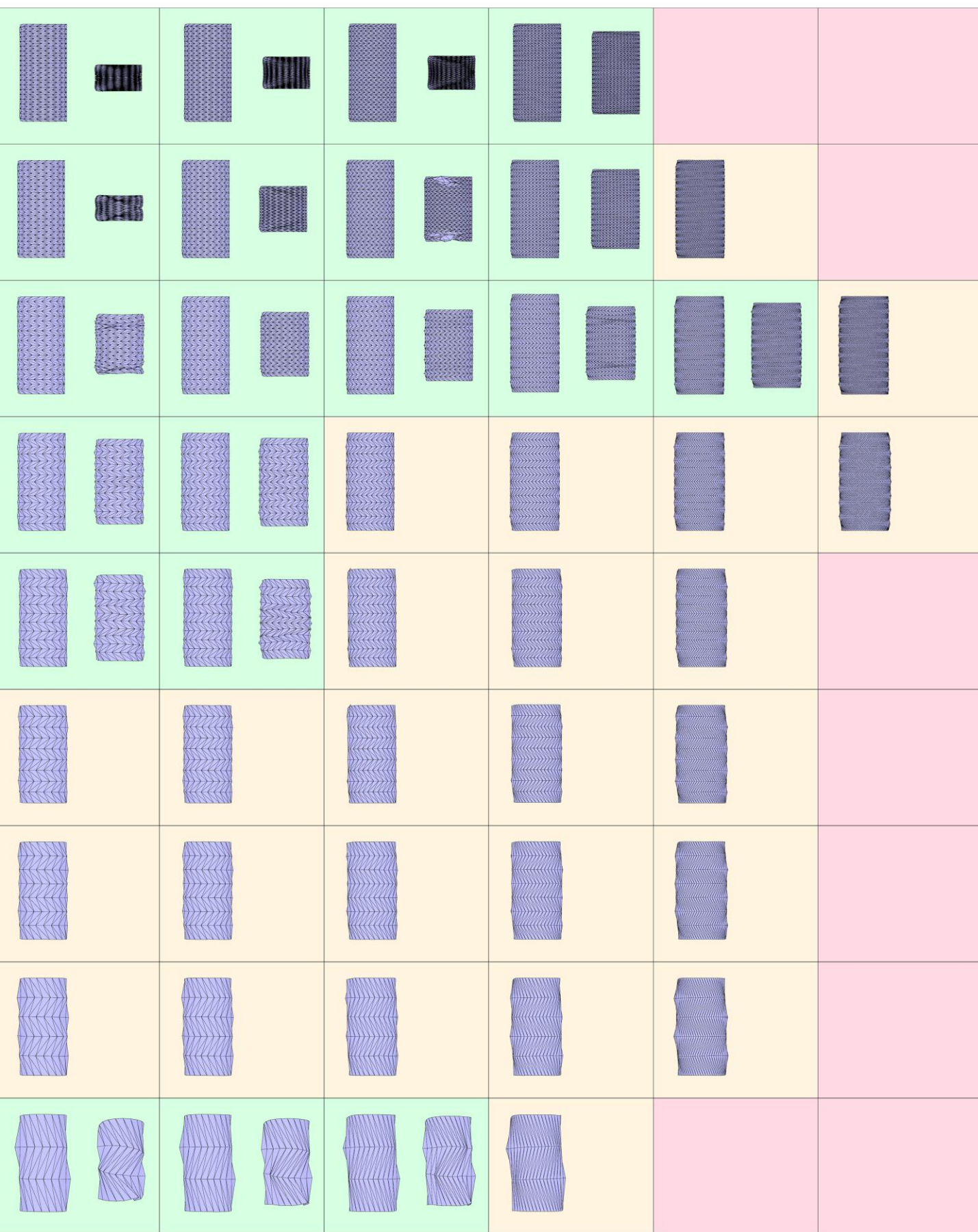
V 7

V 5

V 3

U 3

U 5



U 9

U 11

U 14

U 20

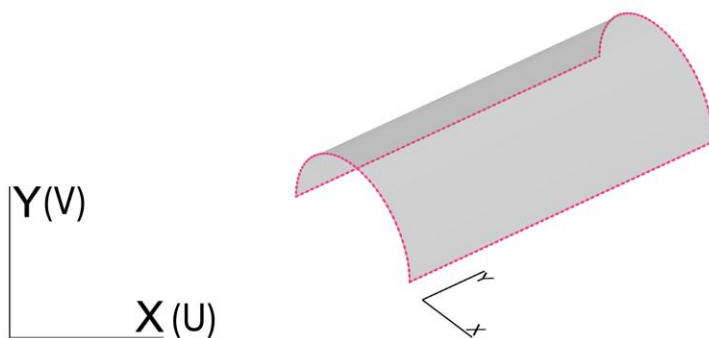
U 30

U 40

Waterbomb Pattern Behaviour

V 40	9.63	5.78	3.21	2.63	2.06	1.44	0.96	9.63
V 30	7.22	4.33	2.41	1.97	1.55	1.08	0.72	7.22
V 20	4.81	2.89	1.60	1.31	1.03	0.72	0.48	4.81
V 14	3.37	2.02	1.12	0.92	0.72	0.51	0.34	3.37
V 11	2.65	1.59	0.88	0.72	0.57	0.40	0.26	2.65
V 9	2.17	1.30	0.72	0.59	0.46	0.33	0.22	2.17
V 7	1.69	1.01	0.56	0.46	0.36	0.25	0.17	1.69
V 5	1.20	0.72	0.40	0.33	0.26	0.18	0.12	1.20
V 3	0.72	0.43	0.24	0.20	0.15	0.11	0.07	0.72
	U 3	U 5	U 9	U 11	U 14	U 20	U 30	U 40

Unit Aspect Ratio



- Successful Vault + Shrinkage Adaptation
- Successful Vault Adaptation
- Failed in both

V 40

V 30

V 20

V 14

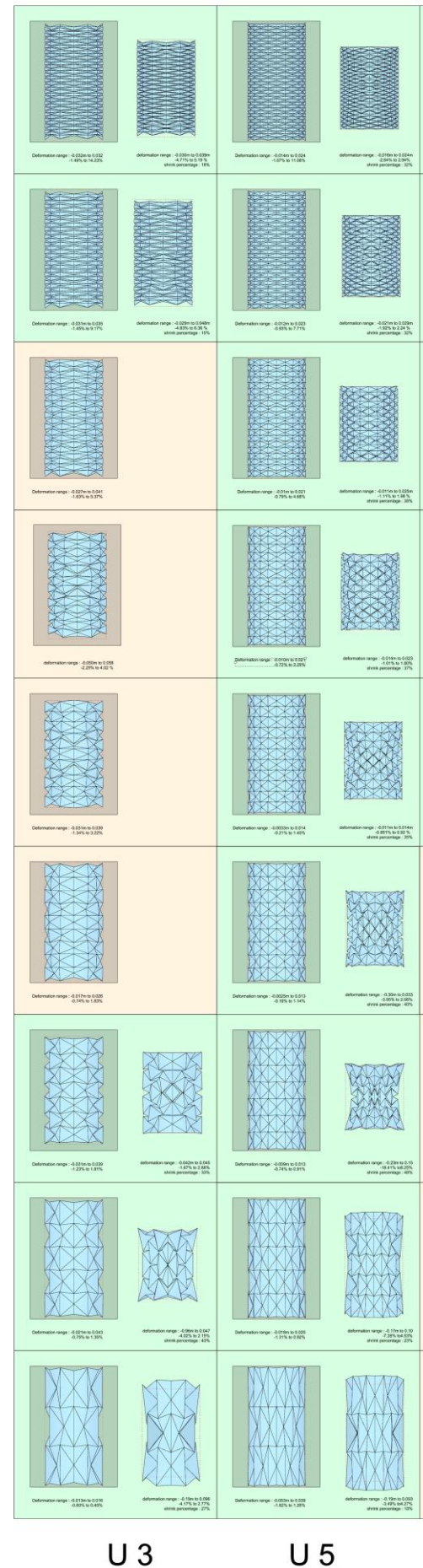
V 11

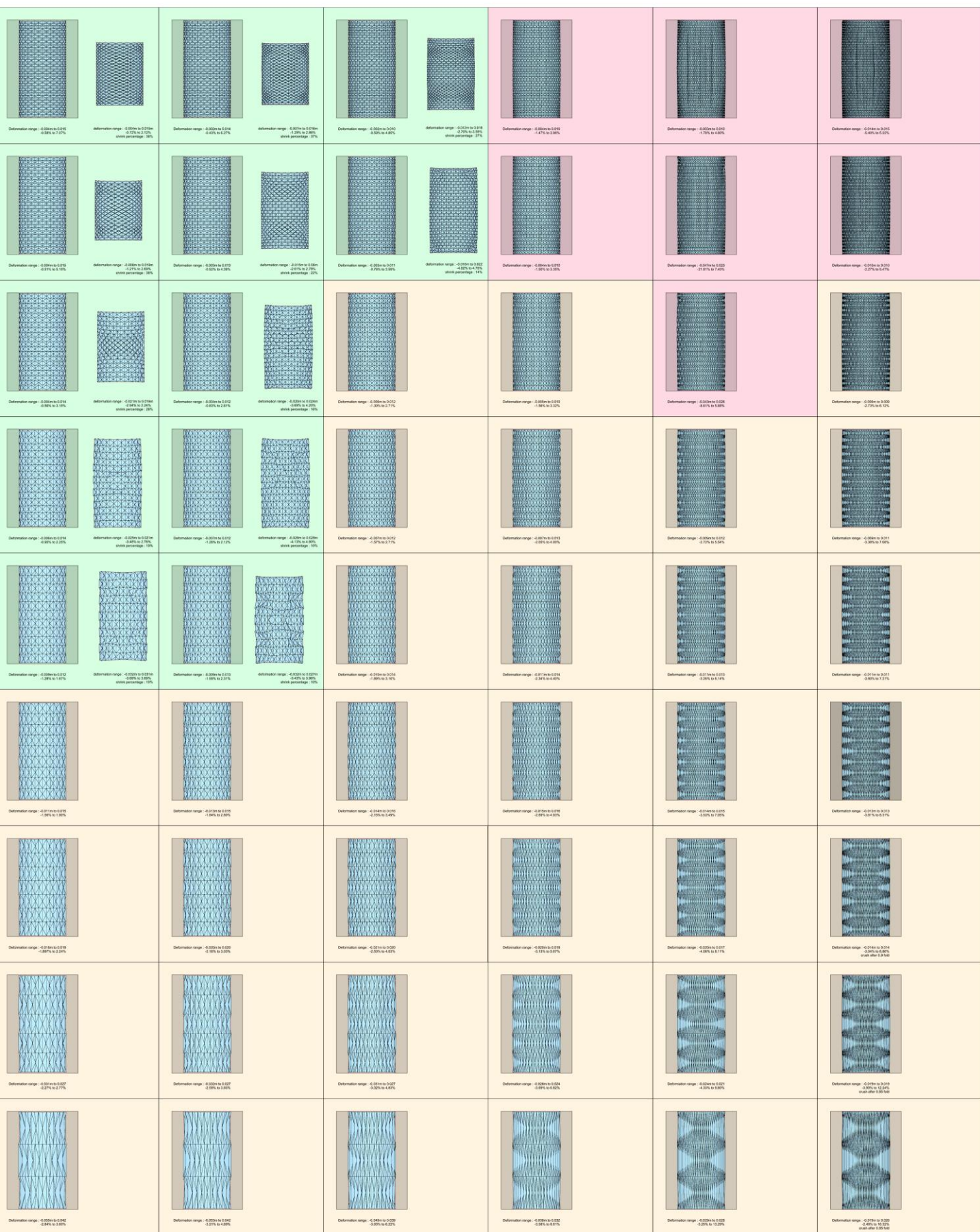
V 9

V 7

V 5

V 3





5.3.1 Patterns Adaptability

Based on the performance tables developed for each pattern, where individual simulation results were evaluated and classified according to vault formation and shrinkage adaptation, the final outcomes were consolidated and summarized in **Fig 5.14**. This summary provides a comparative understanding of the adaptability of the Yoshimura, Kresling, and Waterbomb patterns. Among the three, the Kresling pattern demonstrates the highest overall adaptability, achieving successful vault and shrinkage adaptation in 52.78% of cases. The Waterbomb pattern follows with 36.11%, while the Yoshimura pattern records 20.84% in this combined category. When focusing solely on vault formation, the Waterbomb pattern performs best (54.17%), reflecting its strong geometric flexibility despite lower shrinkage responsiveness. The Yoshimura pattern, while less adaptable overall, still achieves 43% success rate in vault formation. The “Failed in both” category further reinforces these tendencies, with Yoshimura showing the highest failure rate (36.11%) compared to Kresling (12.5%) and Waterbomb (9.72%). Overall, these results indicate that the Kresling pattern provides the most balanced performance between structural adaptability and shrinkage behaviour.

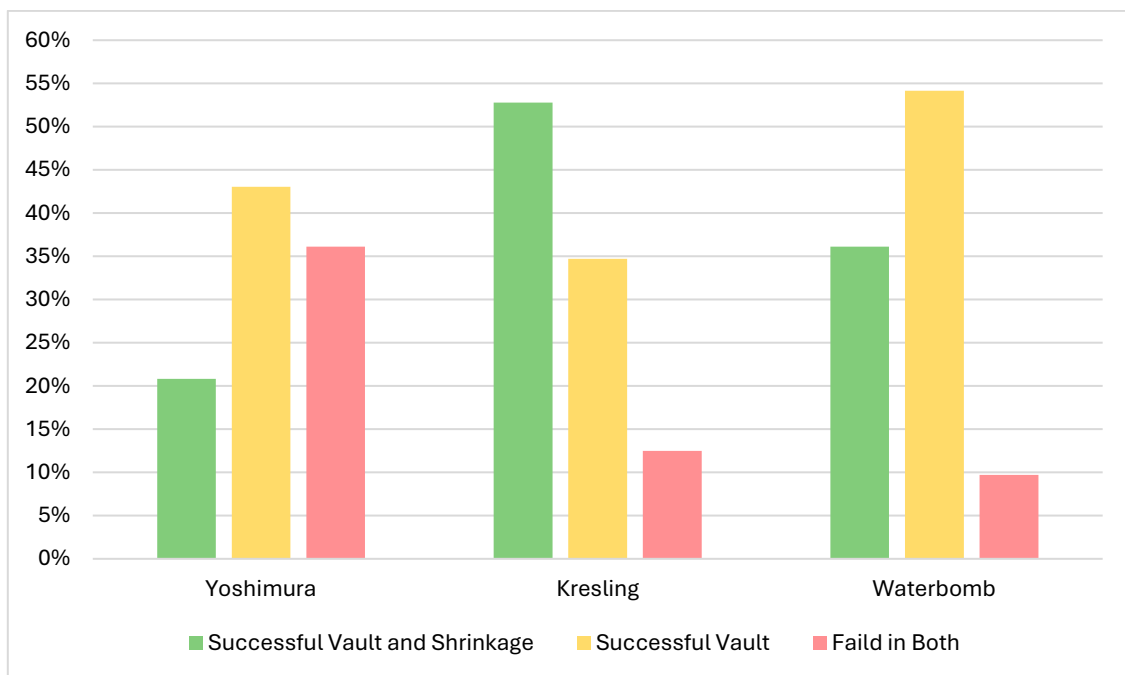
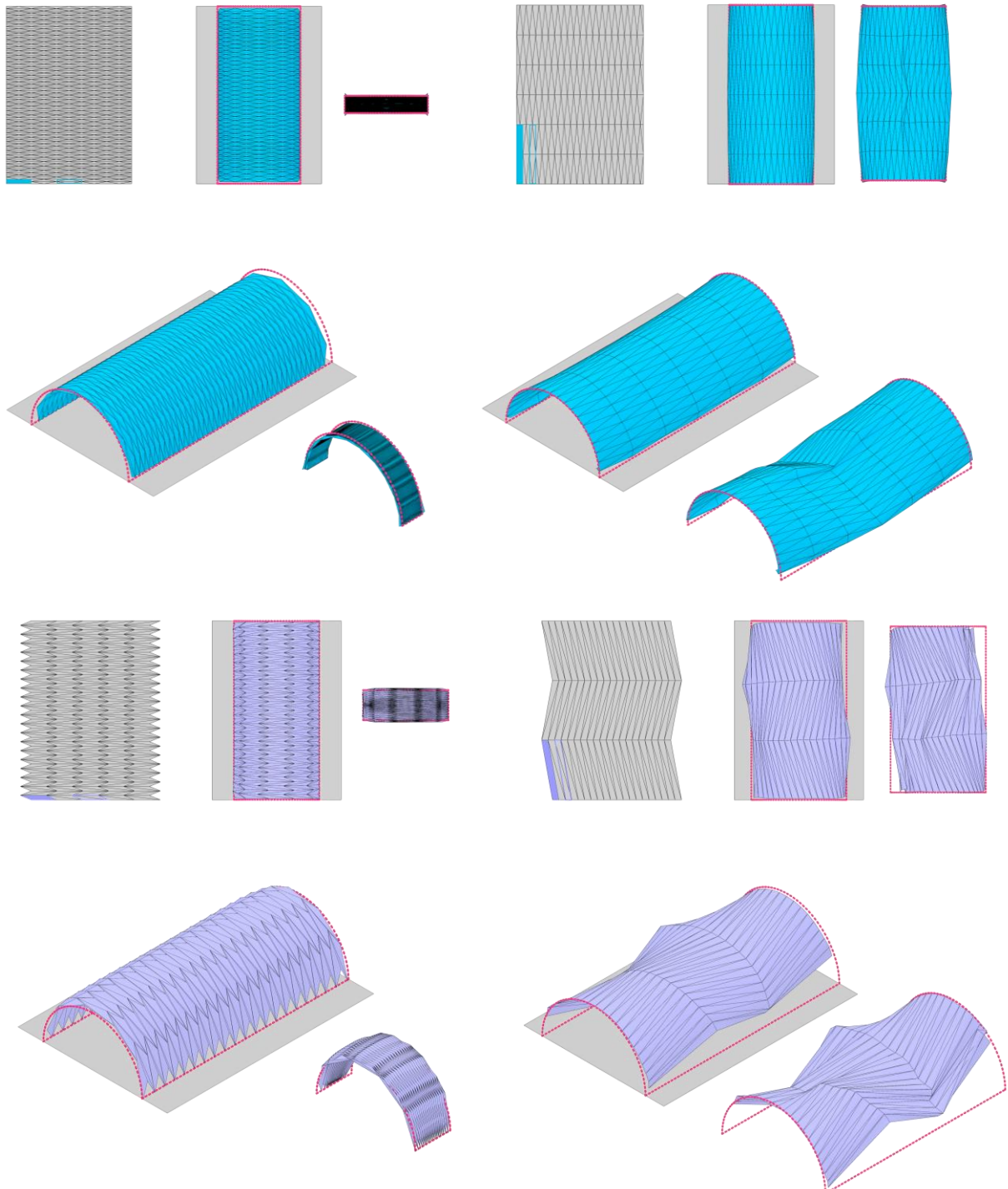


Fig 5.14: Summary of pattern adaptability results

5.3.2 Aspect Ratio Influence on Performance

Going deeper into the simulation outcomes presented in both the aspect ratio table and the performance maps, it becomes evident that the unit aspect ratio plays a decisive role in influencing both vault formation and shrinkage adaptation. Higher aspect ratios—for instance, in configuration U5–V40 (ratio 5.78) across all patterns—generate horizontally wider units that consistently exhibit stable vault formation and effective shrinkage response. In contrast, lower aspect ratios—such as U20–V3 (ratio 0.11)—produce vertically elongated units that may succeed in forming a vault but generally fail to accommodate shrinkage deformation effectively.



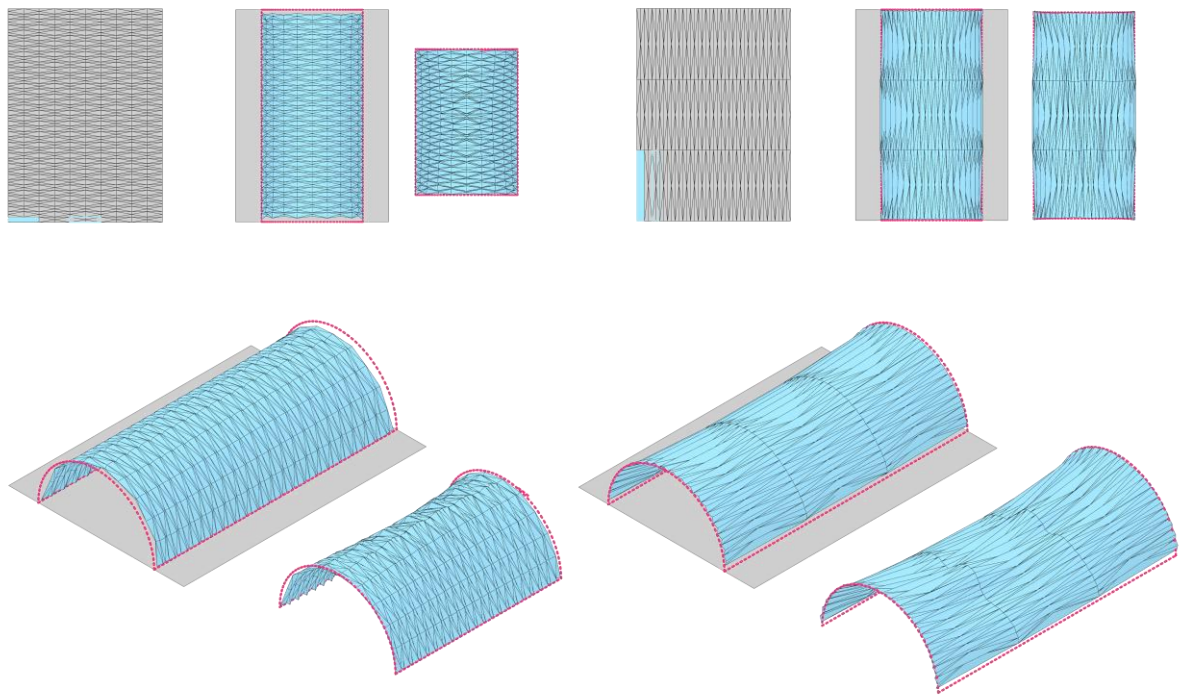


Fig 5.15: Top and Parallel Views of U5-V40 and U20-V40 Surfaces in Different Origami Patterns. From top to bottom: Yoshimura, Kresling, and Waterbomb patterns. The U5-V40 surface (left), characterized by a horizontally wider base unit, demonstrates excellent shrinkage performance — achieving up to 90% contraction in both Yoshimura and Kresling configurations and up to 35% contraction in the Waterbomb pattern — all without structural deformation. In contrast, the U20-V40 surface (right), with a vertically taller base unit, adapts well to the vault-like curvature but exhibits significant deformation and structural collapse when subjected to shrinkage beyond 5%.

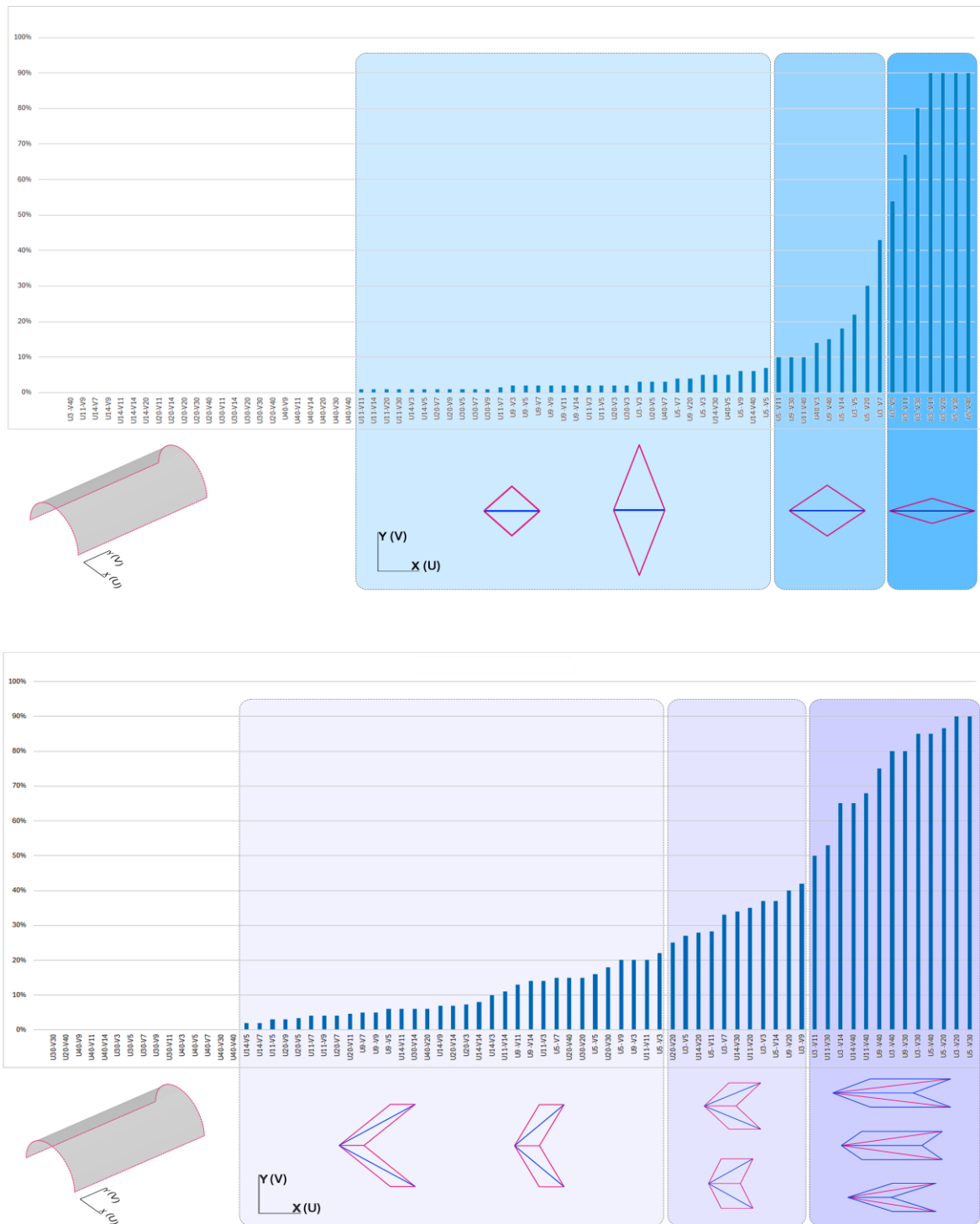


Fig 5.16: The shrinkage charts for the Yoshimura (top) and Kresling (bottom) patterns, arranged from low to high values, demonstrate that horizontally elongated units consistently exhibit superior shrinkage performance.

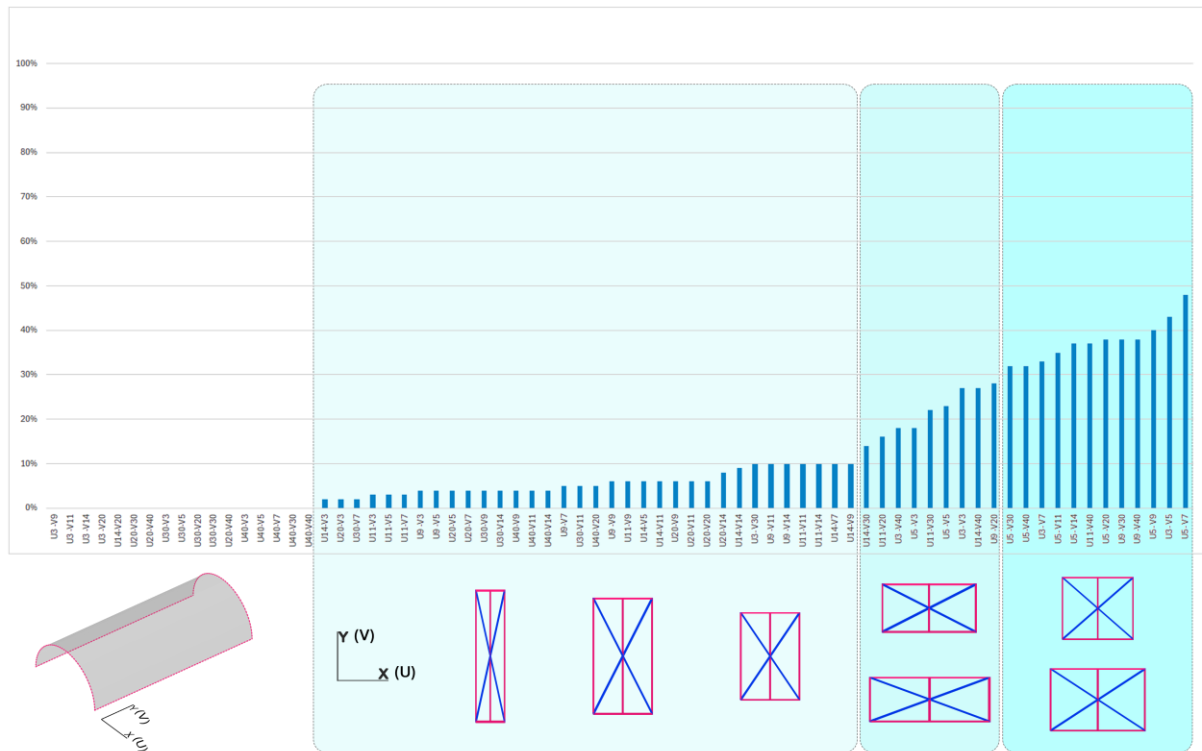


Fig 5.17: The shrinkage chart of the Waterbomb pattern, arranged from low to high values, shows that units with more square proportions—or slightly horizontally elongated shapes—achieve better shrinkage performance.

5.3.3 Influence of Subdivision Density on Surface Performance

Beyond the aspect ratio, the number of subdivisions plays a crucial role in determining the structural behavior of origami-based surfaces. For instance, in the Yoshimura pattern, referring to Fig. 5.19, the surfaces U14–V40 (aspect ratio 2.06) and U3–V9 (aspect ratio 2.17) exhibit nearly identical aspect ratios but markedly different performances. The surface with more subdivisions (U14–V40) contains smaller units with a reduced fold height of only 2.3 cm, causing the structure to behave more like a flexible mesh rather than a rigid folded surface. Since the stiffness and load-bearing capacity of origami structures are closely linked to fold height, the surface U3–V9—with its significantly taller folds of 109 cm—retains high structural stiffness and preserves its arched shape under ~54% shrinkage. In contrast, the low fold height of U14–V40 severely limits its stiffness, leading to noticeable deformation and restricting its shrinkage capacity to approximately 6%.

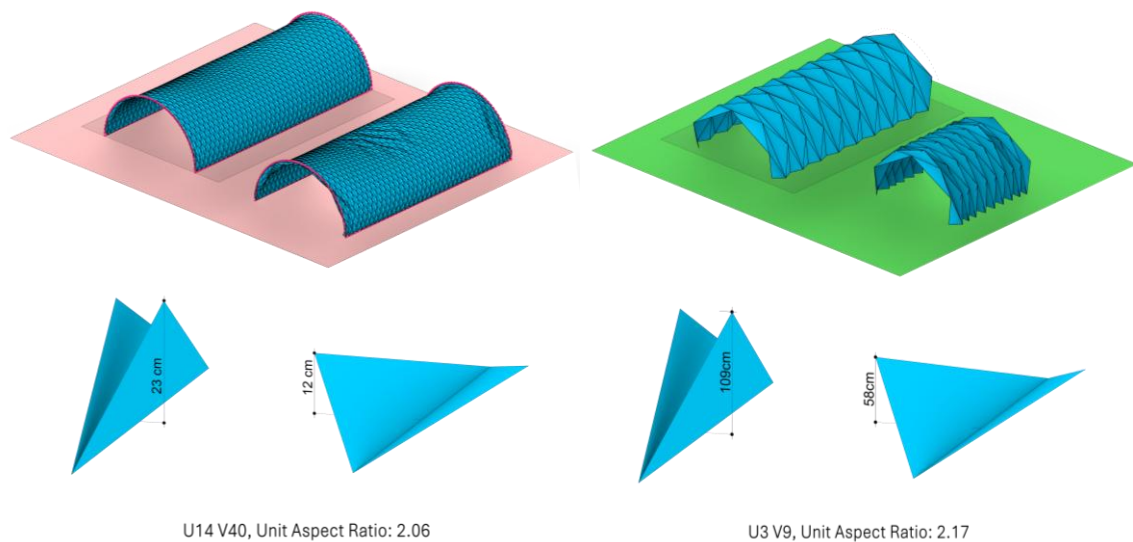
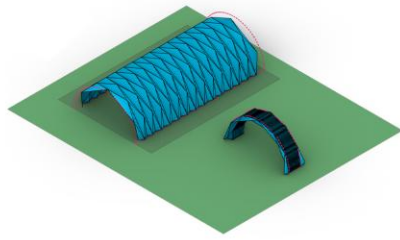


Fig 5.19: Comparison of Fold Height Effects on Surface Behavior in Yoshimura pattern.

A similar trend is observed in the Kresling pattern: both U3–V11 and U40–V11 share an aspect ratio of 2.65, yet their behavior diverges. The surface with fewer subdivisions (U3–V11) successfully maintains the vault shape and achieves a high shrinkage performance, while the more subdivided U40–V11 fails to form a stable vault due to the pronounced reduction in surface stiffness caused by lower fold height.

In the Waterbomb pattern, a comparable effect occurs between U5–V7 (aspect ratio 1.01) and U20–V30 (aspect ratio 1.08). Despite their nearly identical ratios, the surface with fewer and larger units (U5–V7) achieves both a stable vault formation and effective shrinkage, whereas the denser configuration (U20–V30) loses structural rigidity and fails in both aspects.

Shrinkage Positive Result In Yoshimura Pattern

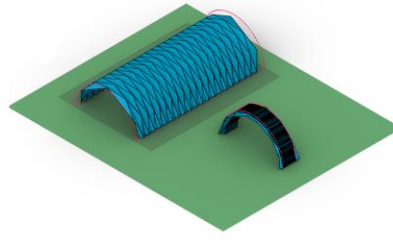


U3 V14

Shrinkage : 90%

Deformation range before shrinkage: -0.055m to 0.058m
-1.28% to 2.57%

Deformation range after shrinkage: -0.012m to 0.013m
-0.56% to 0.30%

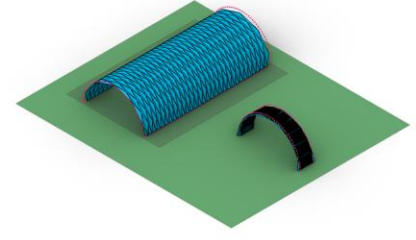


U3 V20

Shrinkage : 90%

Deformation range before shrinkage: -0.060m to 0.063m
-1.40% to 2.87%

Deformation range after shrinkage: -0.026m to 0.022m
-0.62% to 1.02%

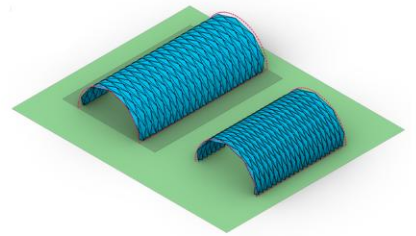
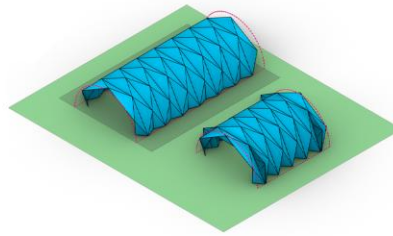
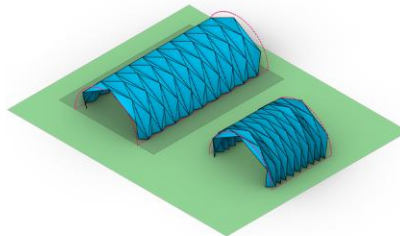


U5 V30

Shrinkage : 90%

Deformation range before shrinkage: -0.024m to 0.026m
-0.94% to 2.94%

Deformation range after shrinkage: -0.016m to 0.020m
-1.23% to 0.80%



U3 V9

Shrinkage : 54%

Deformation range before shrinkage: -0.044m to 0.045m
-1.02% to 1.88%

Deformation range after shrinkage: -0.074m to 0.093m
-3.12% to 2.15%

U3 V7

Shrinkage : 43%

Deformation range before shrinkage: -0.034m to 0.035m
-0.80% to 1.39%

Deformation range after shrinkage: -0.039m to 0.048m
-1.57% to 1.11%

U5 V20

Shrinkage : 30%

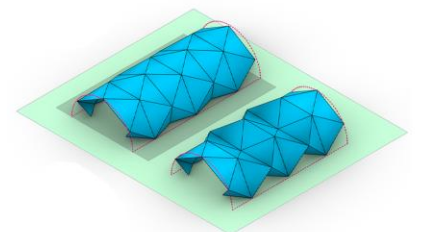
Deformation range before shrinkage: -0.020m to 0.021m
-0.79% to 1.85%

Deformation range after shrinkage: -0.022m to 0.025m
-1.63% to 0.98%

60% to 100% Shrinkage

30% to 60% Shrinkage

10% to 30% Shrinkage



In this study, the shrinkage level stabilized at 90%. However, if material thickness is not considered, surface shrinkage could potentially reach up to 100%.

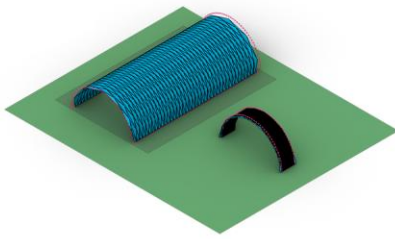
U3 V3

Shrinkage : 13%

Deformation range before shrinkage: -0.0086m to 0.011m
-0.20% to 0.30%

Deformation range after shrinkage: -0.033m to 0.45m
-0.9% to 1.06%

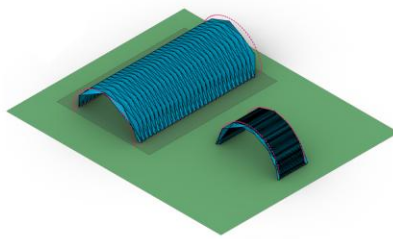
05| Design Process



U5 V40 Shrinkage : 90%

Deformation range before shrinkage: -0.025m to 0.029m
-0.99% to 4.17%

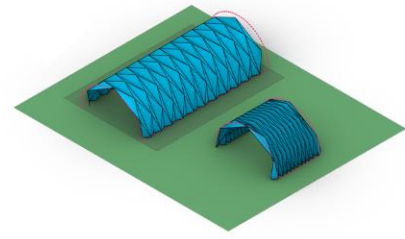
Deformation range after shrinkage: -0.005m to 0.011m
-0.44% to 0.45%



U3 V30 Shrinkage : 80%

Deformation range before shrinkage: -0.063m to 0.064m
-1.45% to 4.57%

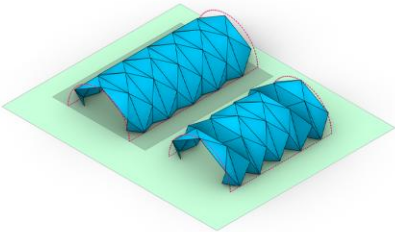
Deformation range after shrinkage: -0.047m to 0.042m
-1.09% to 1.93%



U3 V11 Shrinkage : 67%

Deformation range before shrinkage: -0.050m to 0.01m
-1.16% to 2.23%

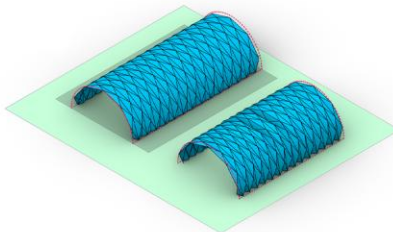
Deformation range after shrinkage: -0.057m to 0.04m
-2.50% to 1.12%



U5 V5 Shrinkage : 22%

Deformation range before shrinkage: -0.022m to 0.021m
-0.50% to 0.76%

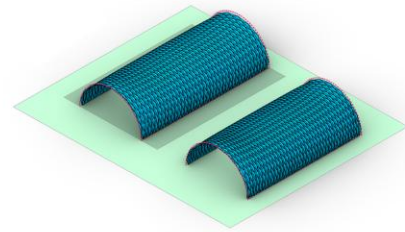
Deformation range after shrinkage: -0.018m to 0.029m
-0.67% to 0.68%



U5 V14 Shrinkage : 18%

Deformation range before shrinkage: -0.015m to 0.017m
-0.61% to 1.22%

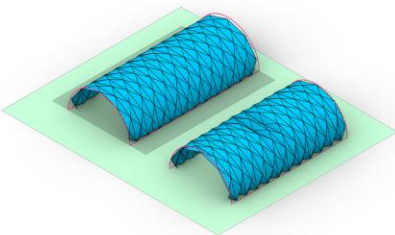
Deformation range after shrinkage: -0.036m to 0.42m
-2.55% to 1.62%



U9 V40 Shrinkage : 15%

Deformation range before shrinkage: -0.010m to 0.026m
-0.73% to 2.98%

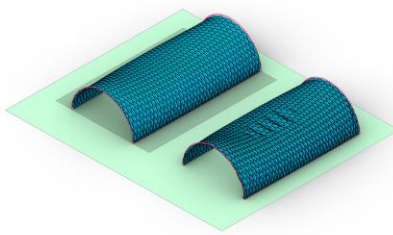
Deformation range after shrinkage: -0.013m to 0.028m
-1.76% to 1.99%



U5 V11 Shrinkage : 10%

Deformation range before shrinkage: -0.013m to 0.016m
-0.53% to 0.94%

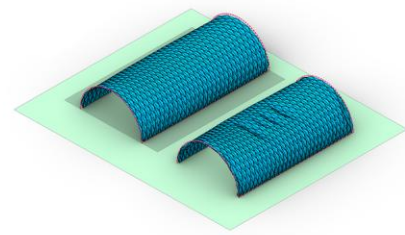
Deformation range after shrinkage: -0.028m to 0.031m
-1.84% to 1.22%



U11 V40 Shrinkage : 10%

Deformation range before shrinkage: -0.009m to 0.025m
-1.05% to 2.69%

Deformation range after shrinkage: -0.013m to 0.031m
-2.10% to 2.67%

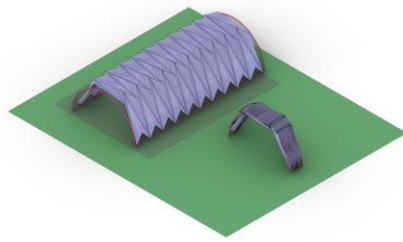


U9 V30 Shrinkage : 10%

Deformation range before shrinkage: -0.010m to 0.026m
-0.73% to 2.20%

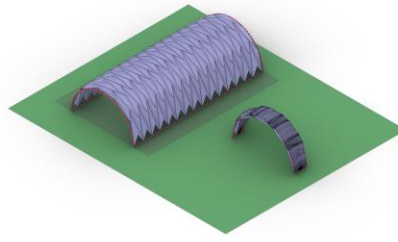
Deformation range after shrinkage: -0.012m to 0.032m
-1.56% to 2.25%

Shrinkage Positive Result In Kresling Pattern



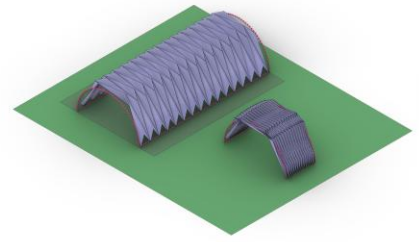
U3 V20
Shrinkage : 90%

Deformation range before shrinkage: -0.049m to 0.074m
-0.89% to 5.24%
Deformation range after shrinkage: -0.035m to 0.013m
-0.82% to 0.54%



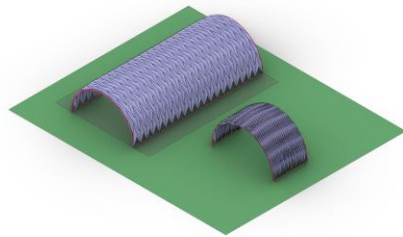
U5 V30
Shrinkage : 90%

Deformation range before shrinkage: -0.030m to 0.041m
-0.82% to 3.33%
Deformation range after shrinkage: -0.030m to 0.10m
-1.18% to 0.28%



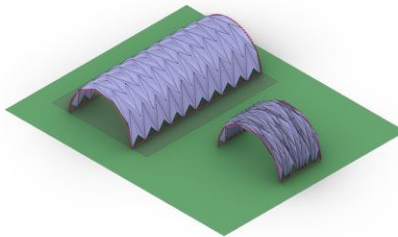
U3 V30
Shrinkage : 85%

Deformation range before shrinkage: -0.024m to 0.026m
-0.94% to 2.94%
Deformation range after shrinkage: -0.016m to 0.020m
-1.23% to 0.80%



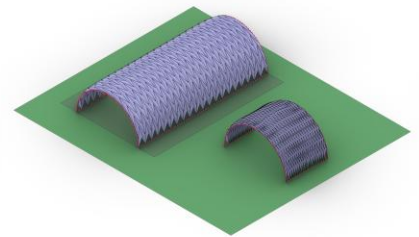
U9 V40
Shrinkage : 75%

Deformation range before shrinkage: -0.019m to 0.026m
-1.16% to 2.27%
Deformation range after shrinkage: -0.025m to 0.009m
-1.79% to 0.69%



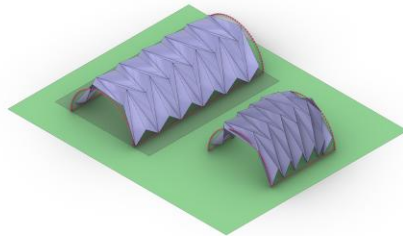
U5 V20
Shrinkage : 68%

Deformation range before shrinkage: -0.027m to 0.040m
-0.76% to 3.21%
Deformation range after shrinkage: -0.077m to 0.029m
-5.46% to 0.847%



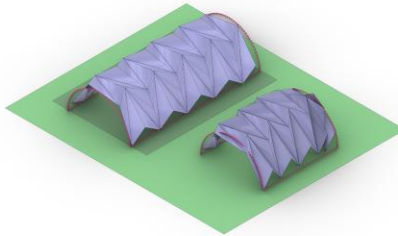
U11 V40
Shrinkage : 68%

Deformation range before shrinkage: -0.017m to 0.024m
-1.3% to 2.07%
Deformation range after shrinkage: -0.023m to 0.01m
-2.00% to 0.81%



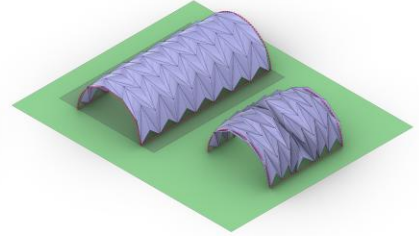
U3 V11
Shrinkage : 50%

Deformation range before shrinkage: -0.035m to 0.073m
-0.63% to 3.72%
Deformation range after shrinkage: -0.11m to 0.044m



U3 V9
Shrinkage : 42%

Deformation range before shrinkage: -0.031m to 0.064m
-0.53% to 2.85%
Deformation range after shrinkage: -0.014m to 0.06m
-6.40% to 1.04%



U5 V1
Shrinkage : 42%

Deformation range before shrinkage: -0.023m to 0.038m
-0.066% to 2.27%
Deformation range after shrinkage: -0.12m to 0.062m
-5.77% to 2.40%

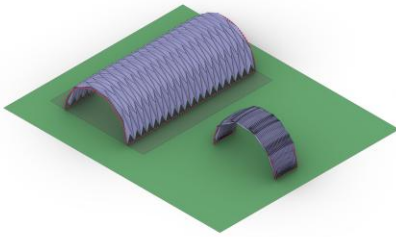
60% to 100% Shrinkage

30% to 60% Shrinkage

10% to 30% Shrinkage

In this study, the shrinkage level stabilized at 90%. However, if material thickness is not considered, surface shrinkage could potentially reach up to 100%.

05| Design Process

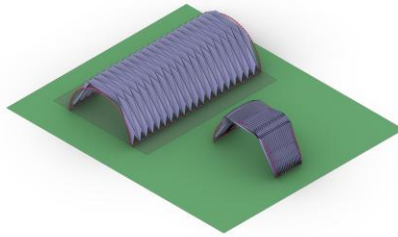


U5 V40

Shrinkage : 85%

Deformation range before shrinkage: -0.031m to 0.040m
-0.84% to 3.39%

Deformation range after shrinkage: -0.022m to 0.018m
-0.86% to 1.58%

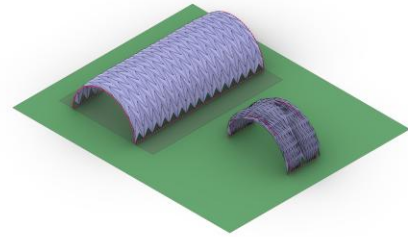


U3 V40

Shrinkage : 80%

Deformation range before shrinkage: -0.053m to 0.084m
-0.98% to 7.13%

Deformation range after shrinkage: -0.036m to 0.702m
-1.34% to 5.99%

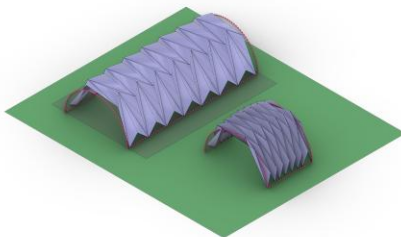


U9 V30

Shrinkage : 80%

Deformation range before shrinkage: -0.019m to 0.027m
-1.14% to 2.22%

Deformation range after shrinkage: -0.039m to 0.019m
-2.76% to 0.92%

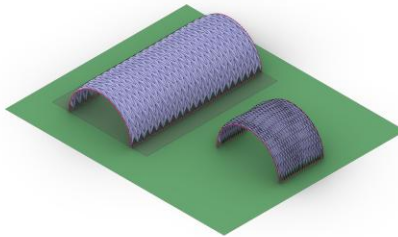


U5 V14

Shrinkage : 65%

Deformation range before shrinkage: -0.042m to 0.068m
-0.76% to 4.04%

Deformation range after shrinkage: -0.077m to 0.037m
-4.57% to 0.74%

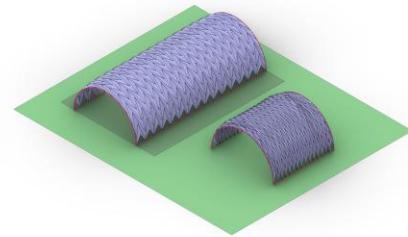


U14 V40

Shrinkage : 65%

Deformation range before shrinkage: -0.017m to 0.021m
-1.83% to 1.85%

Deformation range after shrinkage: -0.021m to 0.009m
-2.20% to 0.89%

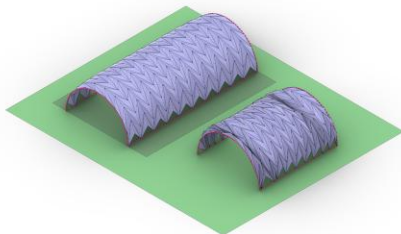


U11 V30

Shrinkage : 53%

Deformation range before shrinkage: -0.016m to 0.025m
-1.43% to 2.04%

Deformation range after shrinkage: -0.034m to 0.016m
-2.74% to 0.97%

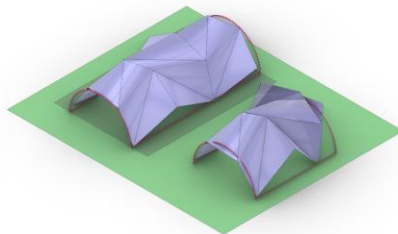


U9 V20

Shrinkage : 40%

Deformation range before shrinkage: -0.017m to 0.027m
-1.17% to 1.96%

Deformation range after shrinkage: -0.096m to 0.028m
-6.81% to 1.83%

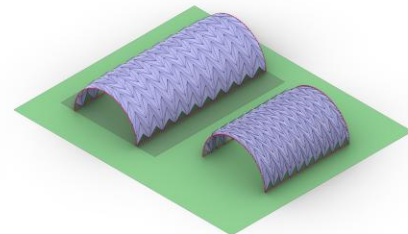


U3 V3

Shrinkage : 37%

Deformation range before shrinkage: -0.027m to 0.036m
-0.63% to 0.59%

Deformation range after shrinkage: -0.065m to 0.035m
-1.51% to 0.57%

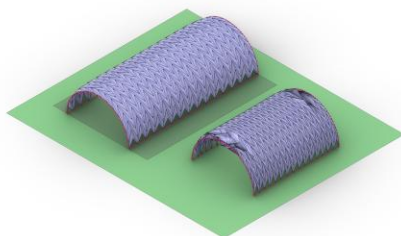


U11 V20

Shrinkage : 35%

Deformation range before shrinkage: -0.017m to 0.025m
-1.45% to 1.79%

Deformation range after shrinkage: -0.038m to 0.017m
-3.26% to 0.93%

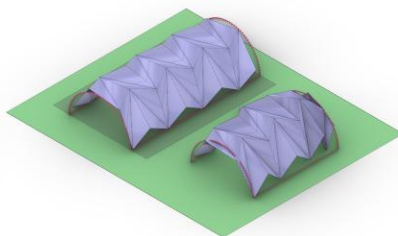


U14 V30

Shrinkage : 34%

Deformation range before shrinkage: -0.017m to 0.022m
-1.8% to 1.84%

Deformation range after shrinkage: -0.023m to 0.013m
-2.40% to 1.02%

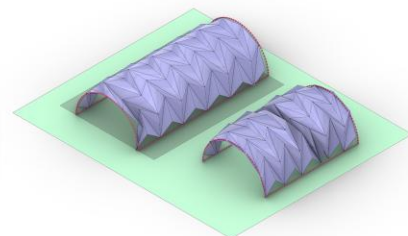


U3 V7

Shrinkage : 33%

Deformation range before shrinkage: -0.025m to 0.054m
-0.57% to 1.94%

Deformation range after shrinkage: -0.014m to 0.070m
-5.61% to 1.17%



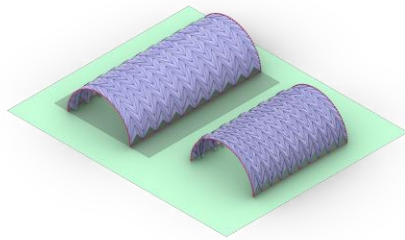
U5 V11

Shrinkage : 28%

Deformation range before shrinkage: -0.020m to 0.036m
-0.73% to 1.83%

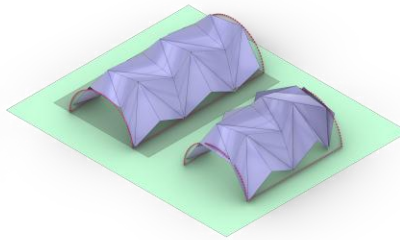
Deformation range after shrinkage: -0.13m to 0.07m
-6.73% to 2.77%

Shrinkage Positive Result In Kresling Pattern



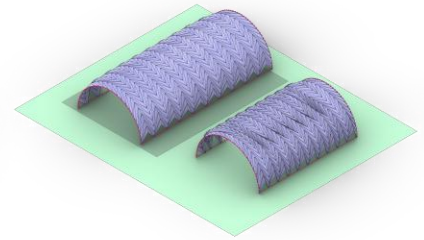
U14 V20
Shrinkage : 28%

Deformation range before shrinkage: -0.020m to 0.025m
-2.17% to 1.76%
Deformation range after shrinkage: -0.039m to 0.015m
-4.25% to 1.25%



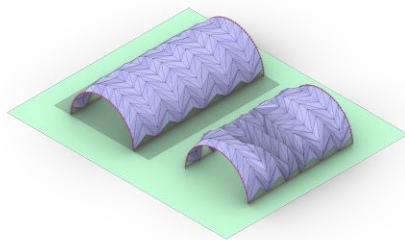
U3 V5
Shrinkage : 27%

Deformation range before shrinkage: -0.026m to 0.042m
-0.60% to 1.13%
Deformation range after shrinkage: -0.014m to 0.068m
-3.76% to 1.05%



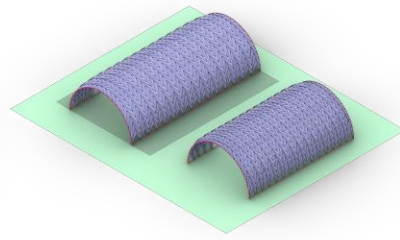
U20 V20
Shrinkage : 25%

Deformation range before shrinkage: -0.016m to 0.020m
-2.50% to 2.23%
Deformation range after shrinkage: -0.035m to 0.014m
-5.42% to 2.19%



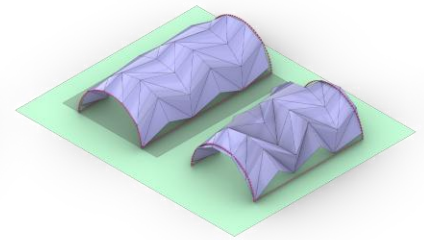
U11 V11
Shrinkage : 20%

Deformation range before shrinkage: -0.018m to 0.024m
-1.53% to 1.25%
Deformation range after shrinkage: -0.047m to 0.024m
-3.92% to 2.27%



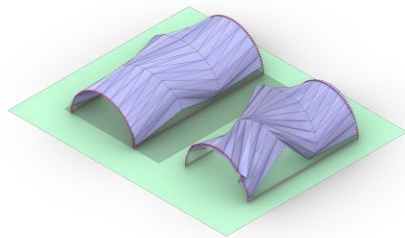
U20 V30
Shrinkage : 18%

Deformation range before shrinkage: -0.017m to 0.020m
-2.73% to 2.14%
Deformation range after shrinkage: -0.023m to 0.012m
-3.57% to 1.48%



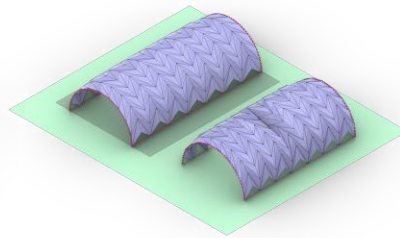
U5 V5
Shrinkage : 16%

Deformation range before shrinkage: -0.020m to 0.025m
-0.77% to 0.067%
Deformation range after shrinkage: -0.13m to 0.066m
-3.66% to 2.20%



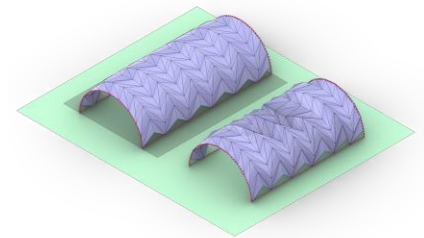
U11 V3
Shrinkage : 14%

Deformation range before shrinkage: -0.040m to 0.045m
-3.40% to 1.14%
Deformation range after shrinkage: -0.014m to 0.061m
-8.35% to 4.02%



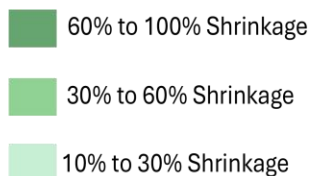
U9 V14
Shrinkage : 14%

Deformation range before shrinkage: -0.016m to 0.027m
-1.14% to 1.62%
Deformation range after shrinkage: -0.045m to 0.022m
-3.17% to 1.55%



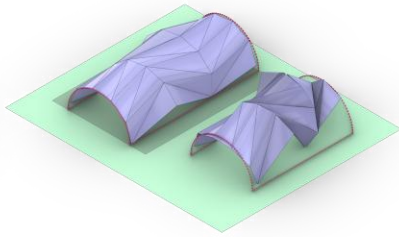
U9 V11
Shrinkage : 13%

Deformation range before shrinkage: -0.018m to 0.026m
-1.27% to 1.34%
Deformation range after shrinkage: -0.049m to 0.020m
-2.46% to 1.45%



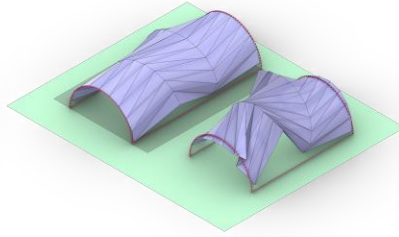
In this study, the shrinkage level stabilized at 90%. However, if material thickness is not considered, surface shrinkage could potentially reach up to 100%.

05| Design Process



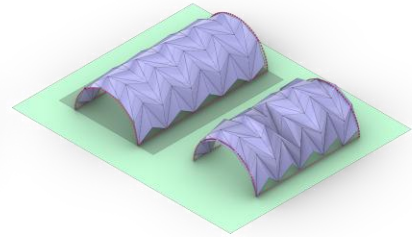
U5 V3
Shrinkage : 22%

Deformation range before shrinkage: -0.023m to 0.030m
-0.88% to 0.49%
Deformation range after shrinkage: -0.09m to 0.003m
-2.27% to 0.50%



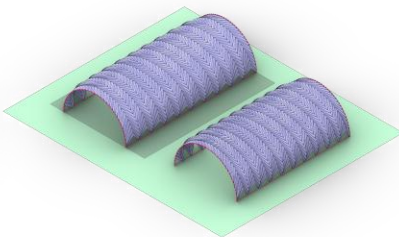
U9 V3
Shrinkage : 20%

Deformation range before shrinkage: -0.033m to 0.040m
-2.29% to 0.87%
Deformation range after shrinkage: -0.15m to 0.067m
-6.50% to 1.135%



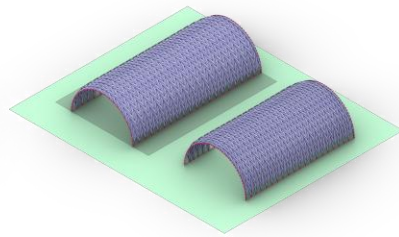
U5 V9
Shrinkage : 20%

Deformation range before shrinkage: -0.019m to 0.033m
-0.75% to 1.46%
Deformation range after shrinkage: -0.094m to 0.007m
-4.13% to 2.22%



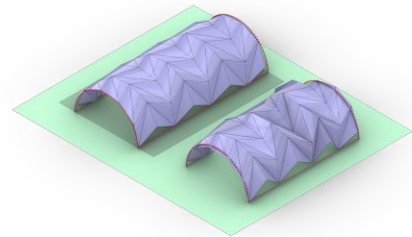
U30 V20
Shrinkage : 15%

Deformation range before shrinkage: -0.017m to 0.018m
-3.98% to 3.36%
Deformation range after shrinkage: -0.020m to 0.010m
-4.78% to 2.32%



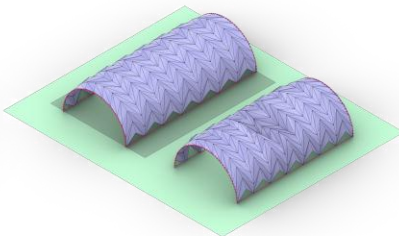
U20 V40
Shrinkage : 15%

Deformation range before shrinkage: -0.019m to 0.018m
-3.00% to 1.91%
Deformation range after shrinkage: -0.020m to 0.014m
-3.10% to 1.71%



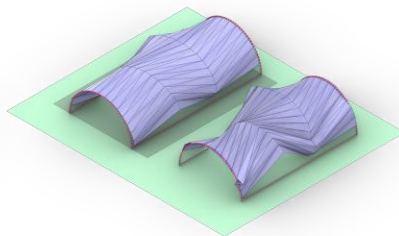
U5 V7
Shrinkage : 15%

Deformation range before shrinkage: -0.019m to 0.030m
-0.76% to 1.07%
Deformation range after shrinkage: -0.093m to 0.0048m
-3.36% to 1.87%



U11 V14
Shrinkage : 11%

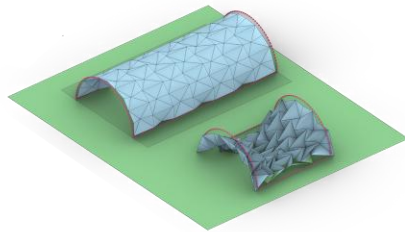
Deformation range before shrinkage: -0.016m to 0.025m
-1.42% to 1.50%
Deformation range after shrinkage: -0.027m to 0.013m
-2.33% to 0.81%



U14 V3
Shrinkage : 10%

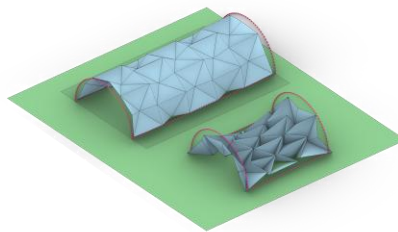
Deformation range before shrinkage: -0.050m to 0.062m
-5.39% to 1.89%
Deformation range after shrinkage: -0.010m to 0.048m
-9.12% to 3.88%

Shrinkage Positive Result In Waterbomb Pattern



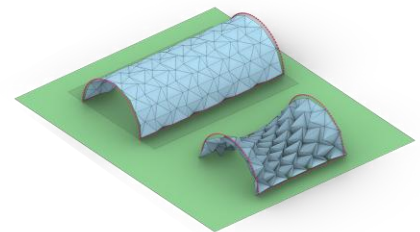
U5 V7
Shrinkage : 48%

Deformation range before shrinkage: -0.009m to 0.013m
-0.74% to 0.91%
Deformation range after shrinkage: -0.023m to 0.015m
-18.41% to 8.25%



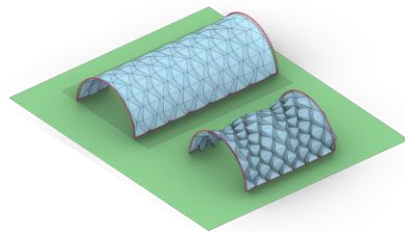
U3 V5v
Shrinkage : 43%

Deformation range before shrinkage: -0.021m to 0.043m
-0.75% to 1.353%
Deformation range after shrinkage: -0.96m to 0.047m
-4.02% to 2.15%



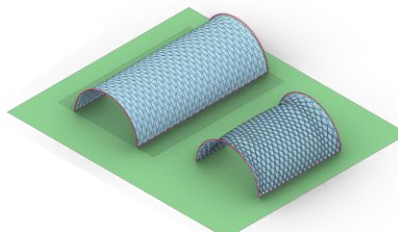
U5 V9
Shrinkage : 40%

Deformation range before shrinkage: -0.025m to 0.013m
-0.19% to 1.14%
Deformation range after shrinkage: -0.30m to 0.033m
-3.9% to 2.06%



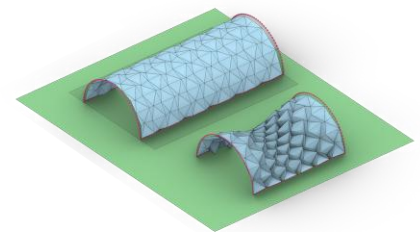
U5 V14
Shrinkage : 37%

Deformation range before shrinkage: -0.010m to 0.021m
-0.72% to 3.9%
Deformation range after shrinkage: -0.014m to 0.023m
-1.01% to 1.80%



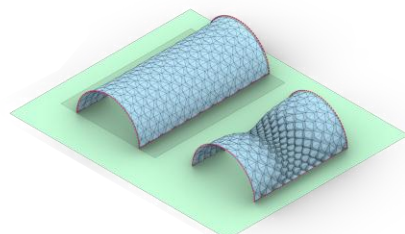
U11 V40
Shrinkage : 37%

Deformation range before shrinkage: -0.002m to 0.014m
-0.43% to 6.27%
Deformation range after shrinkage: -0.007m to 0.016m
-1.29% to 2.86%



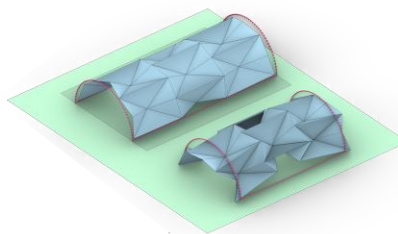
U5 V11
Shrinkage : 35%

Deformation range before shrinkage: -0.0033m to 0.014m
-0.21% to 1.40%
Deformation range after shrinkage: -0.011m to 0.014m
-0.85% to 0.92%



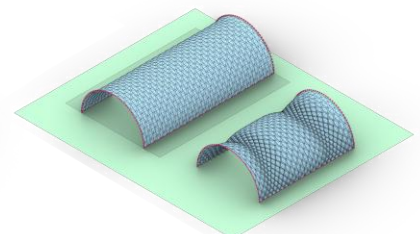
U9 V20
Shrinkage : 28%

Deformation range before shrinkage: -0.004m to 0.014m
-0.56% to 3.15%
Deformation range after shrinkage: -0.021m to 0.024m



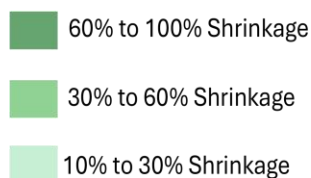
U3 V3
Shrinkage : 27%

Deformation range before shrinkage: -0.013m to 0.016m
-0.60% to 0.45%
Deformation range after shrinkage: -0.19m to 0.096m
-4.17% to 2.77%

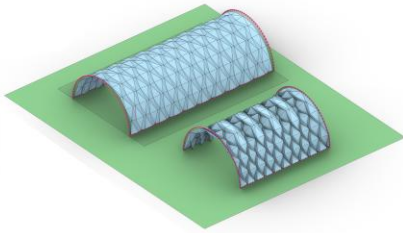


U14 V40
Shrinkage : 27%

Deformation range before shrinkage: -0.002m to 0.010m
-0.59% to 4.85%
Deformation range after shrinkage: -0.012m to 0.016m
-2.70% to 3.59%

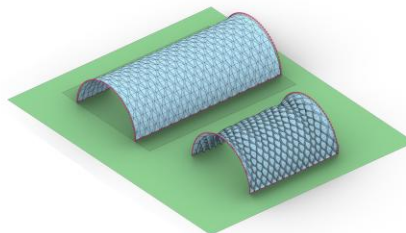


In this study, the shrinkage level stabilized at 90%. However, if material thickness is not considered, surface shrinkage could potentially reach up to 100%.



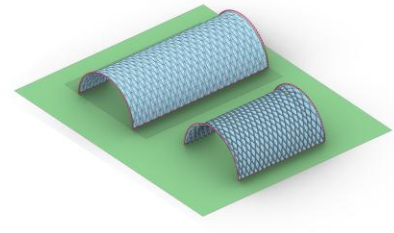
U5 V20 Shrinkage : 38%

Deformation range before shrinkage: -0.01m to 0.021m
-0.79% to 4.68%
Deformation range after shrinkage: -1.11m to 1.98m
-0.86% to 1.58%



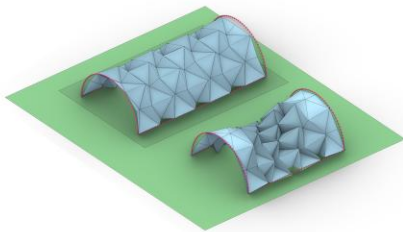
U9 V30 Shrinkage : 38%

Deformation range before shrinkage: -0.004m to 0.015m
-0.518% to 5.15%
Deformation range after shrinkage: -0.008m to 0.019m
-1.21% to 2.69%



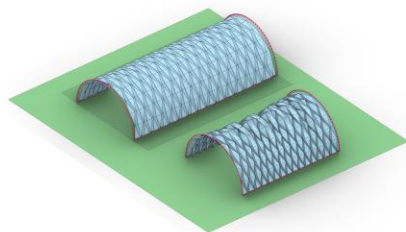
U9 V40 Shrinkage : 38%

Deformation range before shrinkage: -0.004m to 0.015m
-0.58% to 7.07%
Deformation range after shrinkage: -0.004m to 0.015m
-0.72% to 2.12%



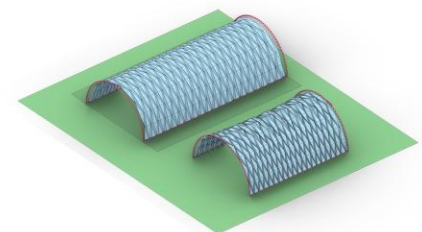
U3 V7 Shrinkage : 33%

Deformation range before shrinkage: -0.031m to 0.039m
-1.23% to 1.81%
Deformation range after shrinkage: -0.042m to 0.045m
-1.67% to 2.88%



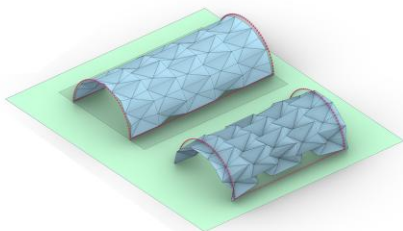
U5 V30 Shrinkage : 32%

Deformation range before shrinkage: -0.012m to 0.023m
-0.93% to 7.71%
Deformation range after shrinkage: -0.021m to 0.029m
-1.92% to 2.24%



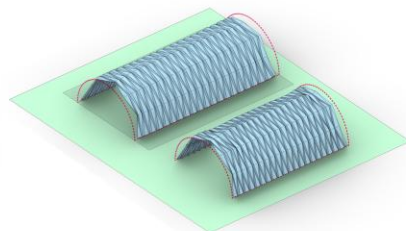
U5 V40 Shrinkage : 32%

Deformation range before shrinkage: -0.014m to 0.024m
-1.07% to 11.08%
Deformation range after shrinkage: -0.016m to 0.024m
-2.64% to 2.94%



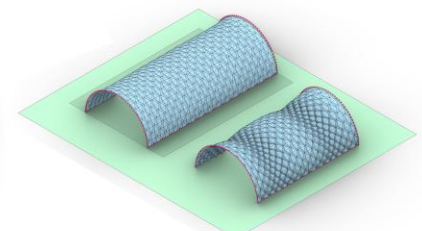
U5 V5 Shrinkage : 23%

Deformation range before shrinkage: -0.018m to 0.020m
-1.31% to 0.92%
Deformation range after shrinkage: -0.17m to 0.10m
-7.26% to 4.53%



U3 V40 Shrinkage : 18%

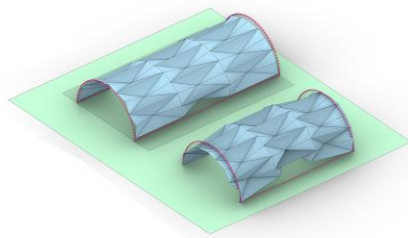
Deformation range before shrinkage: -0.032m to 0.032m
-1.49% to 14.23%
Deformation range after shrinkage: -0.030m to 0.039m
-4.71% to 5.197%



U11 V30 Shrinkage : 22%

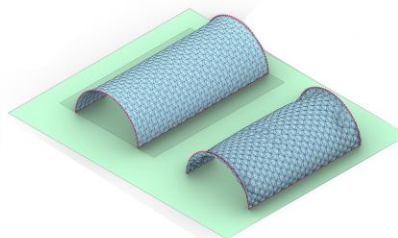
Deformation range before shrinkage: -0.003m to 0.013m
-0.52% to 4.38%
Deformation range after shrinkage: -0.015m to 0.060m
-2.61% to 2.78%

05| Design Process



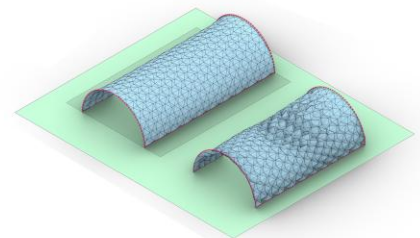
U5 V3
Shrinkage : 18%

Deformation range before shrinkage: -0.053m to 0.039m
-1.823% to 1.26%
Deformation range after shrinkage: -0.019m to 0.093m
-3.49% to 4.27%



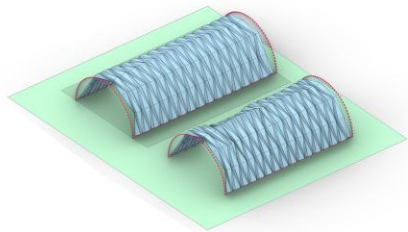
U14 V30
Shrinkage : 14%

Deformation range before shrinkage: -0.003m to 0.011m
-0.76% to 3.58%
Deformation range after shrinkage: -0.016m to 0.022m
-4.02% to 4.76%



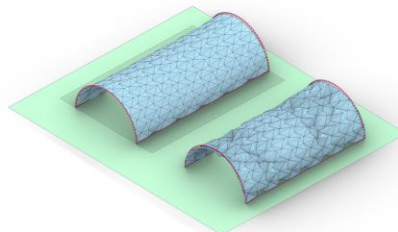
U11 V20
Shrinkage : 16%

Deformation range before shrinkage: -0.004m to 0.012m
-0.83% to 2.81%
Deformation range after shrinkage: -0.020m to 0.024m
-3.693% to 4.20%



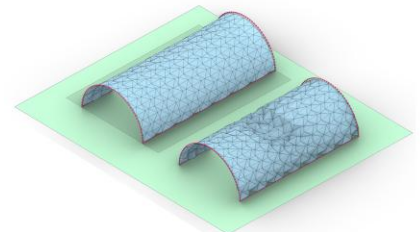
U3 V30
Shrinkage : 10%

Deformation range before shrinkage: -0.031m to 0.035m
-1.45% to 9.17%
Deformation range after shrinkage: -0.029m to 0.048m
-4.83% to 6.36%



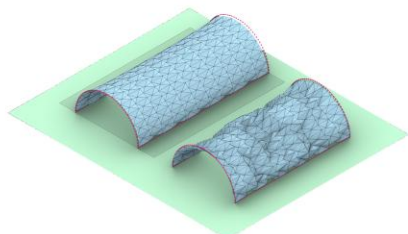
U9 V11
Shrinkage : 10%

Deformation range before shrinkage: -0.009m to 0.012m
-1.28% to 1.67%
Deformation range after shrinkage: -0.032m to 0.031m
-3.69% to 3.69%



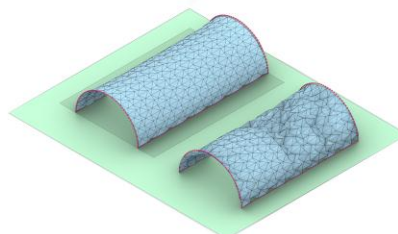
U9 V14
Shrinkage : 10%

Deformation range before shrinkage: -0.006m to 0.014m
-0.95% to 2.25%
Deformation range after shrinkage: -0.025m to 0.021m
-3.48% to 2.78%



U11 V11
Shrinkage : 10%

Deformation range before shrinkage: -0.009m to 0.013m
-1.59% to 2.31%
Deformation range after shrinkage: -0.032m to 0.027m
-3.43% to 3.96%



U11 V14
Shrinkage : 10%

Deformation range before shrinkage: -0.007m to 0.012m
-1.280% to 2.12%
Deformation range after shrinkage: -0.026m to 0.029m
-4.13% to 4.90%

60% to 100% Shrinkage

30% to 60% Shrinkage

10% to 30% Shrinkage

In this study, the shrinkage level stabilized at 90%. However, if material thickness is not considered, surface shrinkage could potentially reach up to 100%.

5.4 Deformation in members

At this stage of the project, the deformation results were analyzed based on the main parameters available in the dataset. Although no consistent or strong trend were identified, three parameters were considered potentially influential:

- **Shrinkage:** Evaluated at two levels—first, by comparing deformation between cases with and without shrinkage, and second, by considering whether a greater degree of shrinkage leads to more deformation.
- **Total Number of Units (Subdivision Density):** The number of units within the structure was taken into account to see if higher U/V subdivision density had an effect on deformation behavior.
- **Unit Aspect Ratio:** Differences in unit proportions were analyzed to explore whether aspect ratio influences how deformation occurs.

5.4.1 Deformation Analysis Based on Shrinkage Levels

To improve understanding of the simulation results, the deformation data were converted into charts for each folding pattern, illustrating compression (–) and tension (+) values in percentages. Each chart represents deformation at two stages: before shrinkage (shown as bars, corresponding to the vault position) and after shrinkage (represented by lines). The members were arranged from left to right according to increasing shrinkage levels, allowing for easier identification of potential trends between shrinkage and deformation behavior.

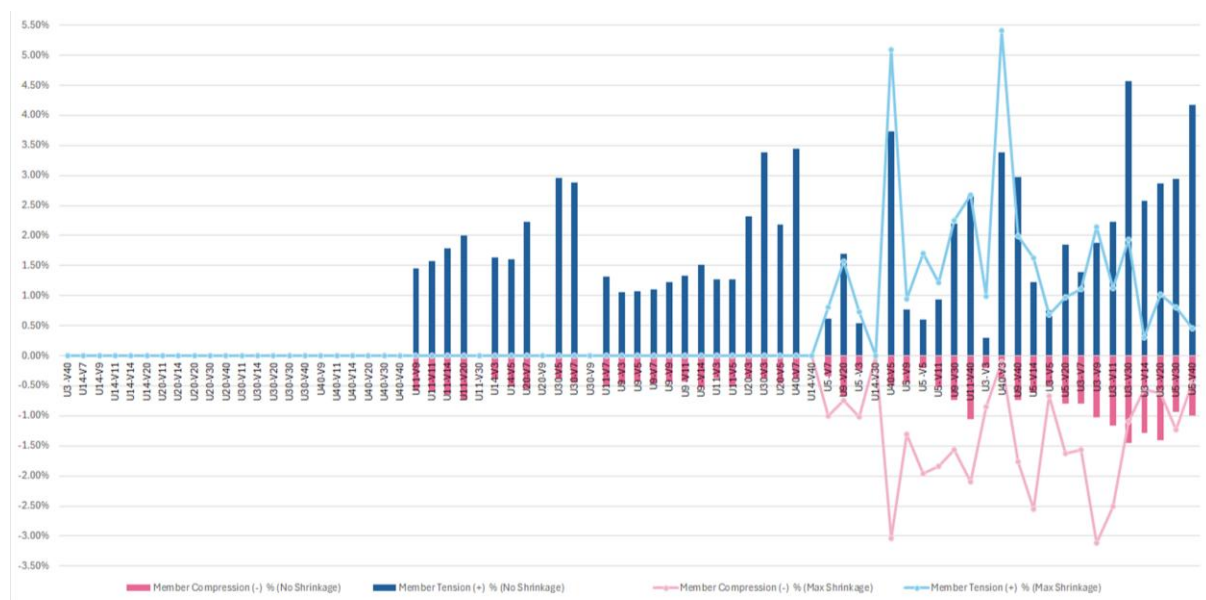


Fig 5.20: Member Deformation Before vs. After Shrinkage in Yoshimura Pattern (Ordered (left to right) by Shrinkage level: Low to High)

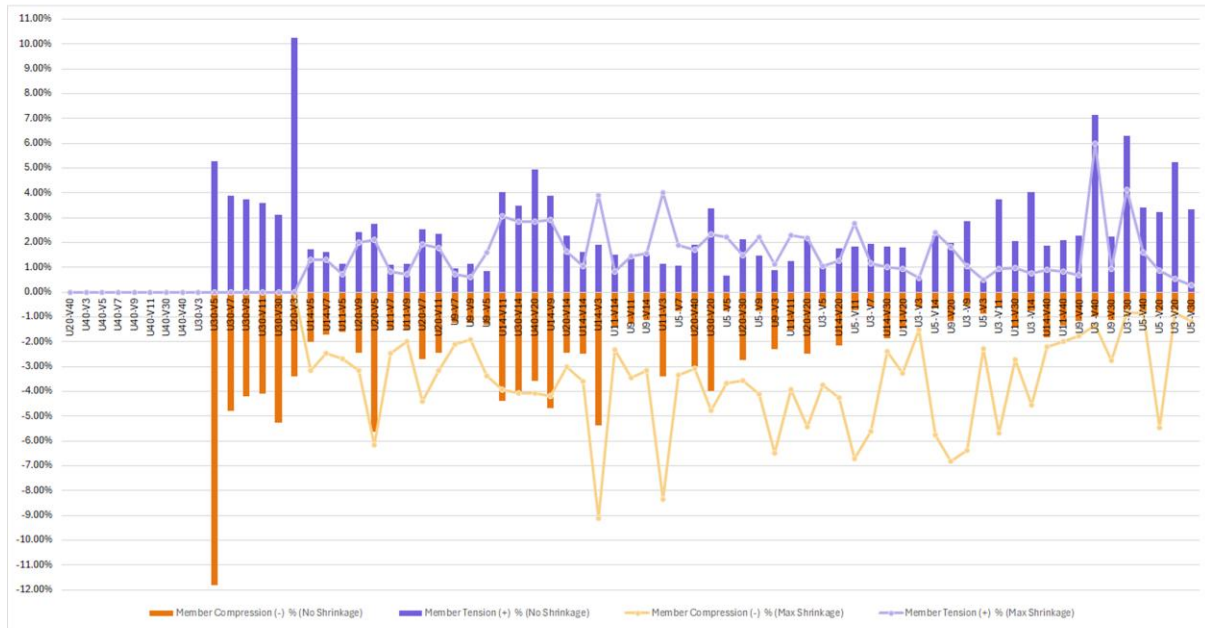


Fig5.21: Member Deformation Before vs. After Shrinkage in Kresling Pattern (Ordered (left to right) by Shrinkage level: Low to High)

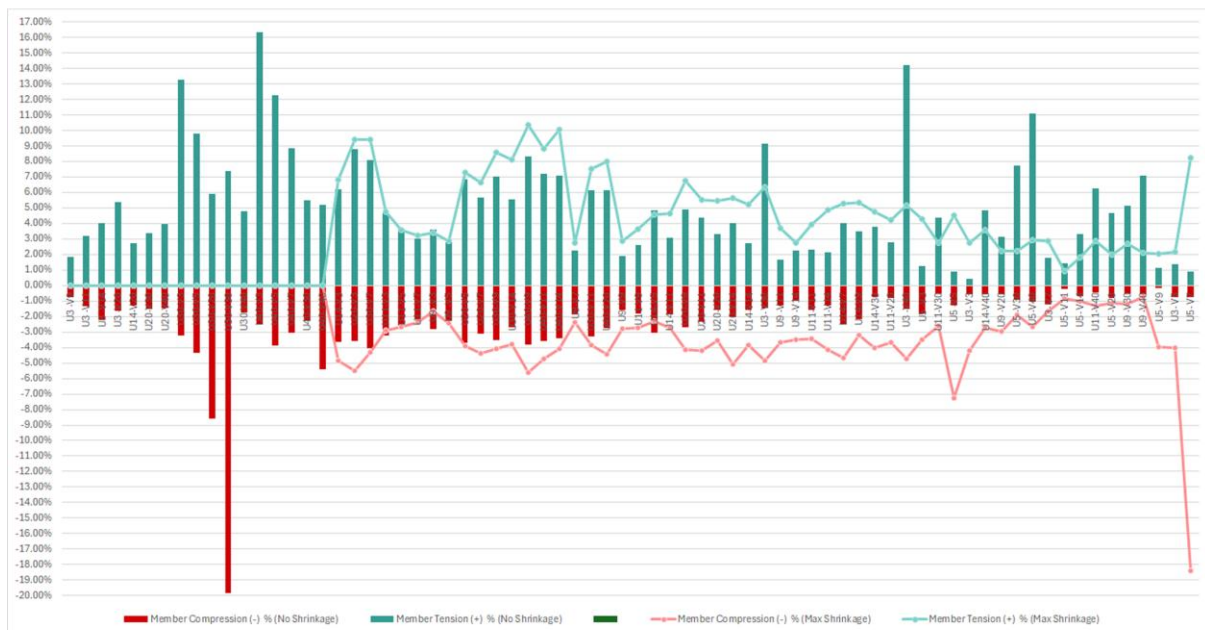
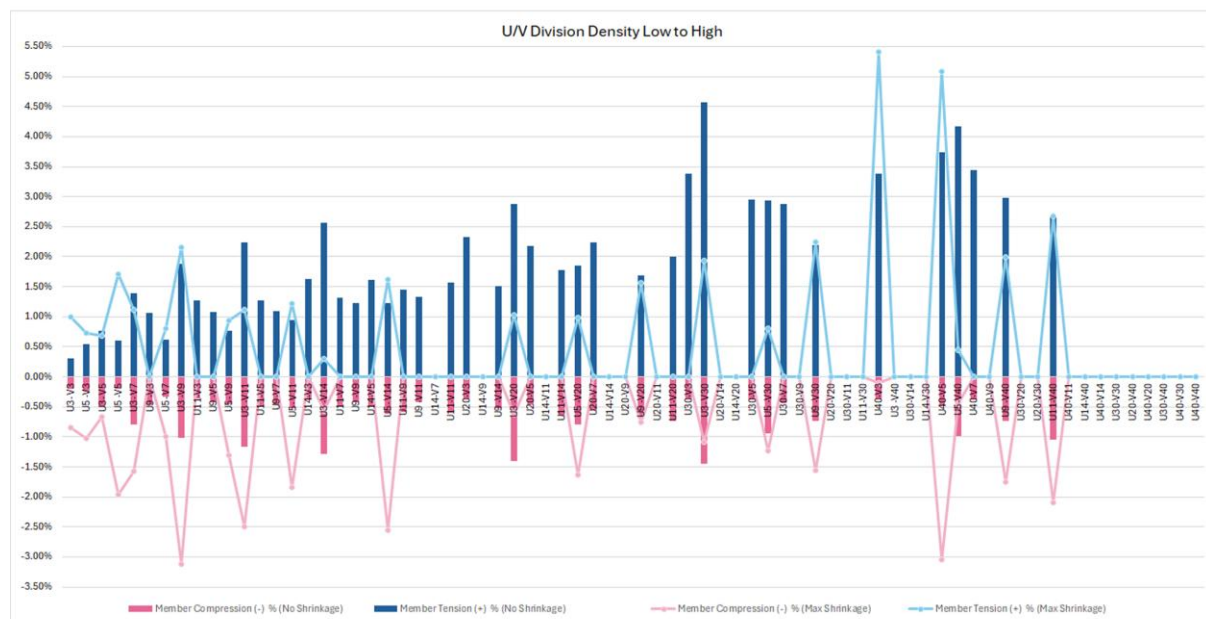


Fig5.22: Member Deformation Before vs. After Shrinkage in Waterbomb Pattern (Ordered (left to right) by Shrinkage level: Low to High)

However, the results did not reveal any consistent or strong correlation between shrinkage magnitude and deformation response in any of the patterns. Both tensile and compressive deformations appeared scattered across the shrinkage spectrum, with similar deformation magnitudes occurring at both low and high shrinkage values. This suggests that shrinkage alone does not exert a significant or predictable influence on member deformation within this dataset. Consequently, it is likely that other structural parameters—such as geometric configuration, fold height, or subdivision density—play a more dominant role in governing the observed deformation behavior.

5.4.2 Deformation Analysis Based on U/V Subdivision Density

In a subsequent analysis aimed at identifying factors influencing member deformation, the data were reorganized according to the U/V subdivision density, arranged from lowest to highest. The charts maintained the same visual language as in the previous stage, with bars representing the vault-stage deformation and lines indicating post-shrinkage deformation, where compression is shown as negative and tension as positive. This reordering was intended to evaluate whether an increase in the number of structural units (i.e., higher subdivision density) corresponded to greater or lesser deformation.



05| Design Process

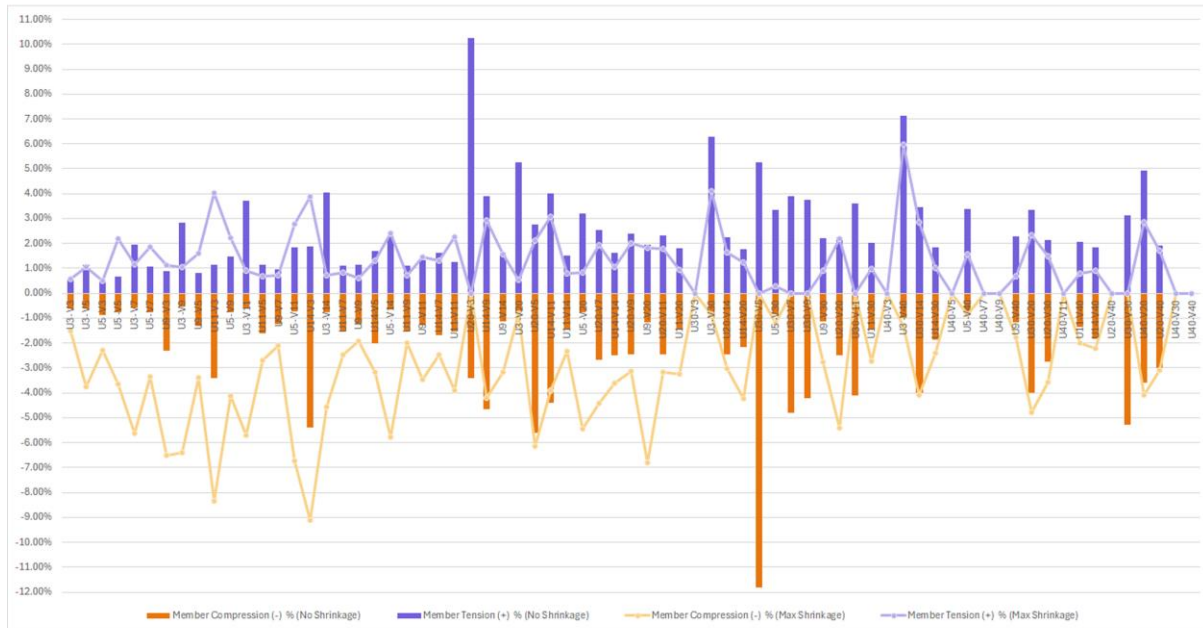


Fig5.24: Member Deformation Before vs. After Shrinkage in Kresling Pattern (Ordered (left to right) by U/V division density: Low to High)

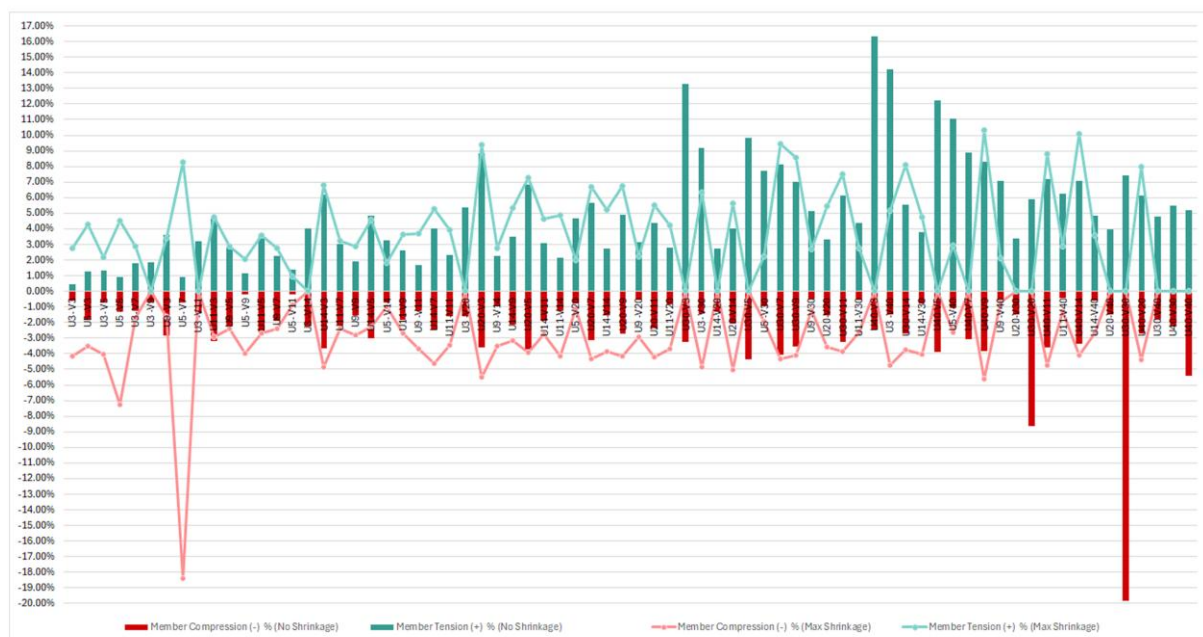


Fig5.25 Member Deformation Before vs. After Shrinkage in Waterbomb Pattern (Ordered (left to right) by U/V division density: Low to High)

5.4.3 Deformation Analysis Based on Unit Aspect Ratio

In the final stage of the analysis, the data were reorganized according to the unit aspect ratio to examine whether the geometric proportions and shapes of individual units influence member deformation. It was hypothesized that more elongated or irregular units might exhibit different deformation behaviors due to variations in stiffness or force distribution. However, consistent with the findings from the previous analyses based on shrinkage level and subdivision density, the deformation results did not reveal any clear or systematic trend across the range of aspect ratios.

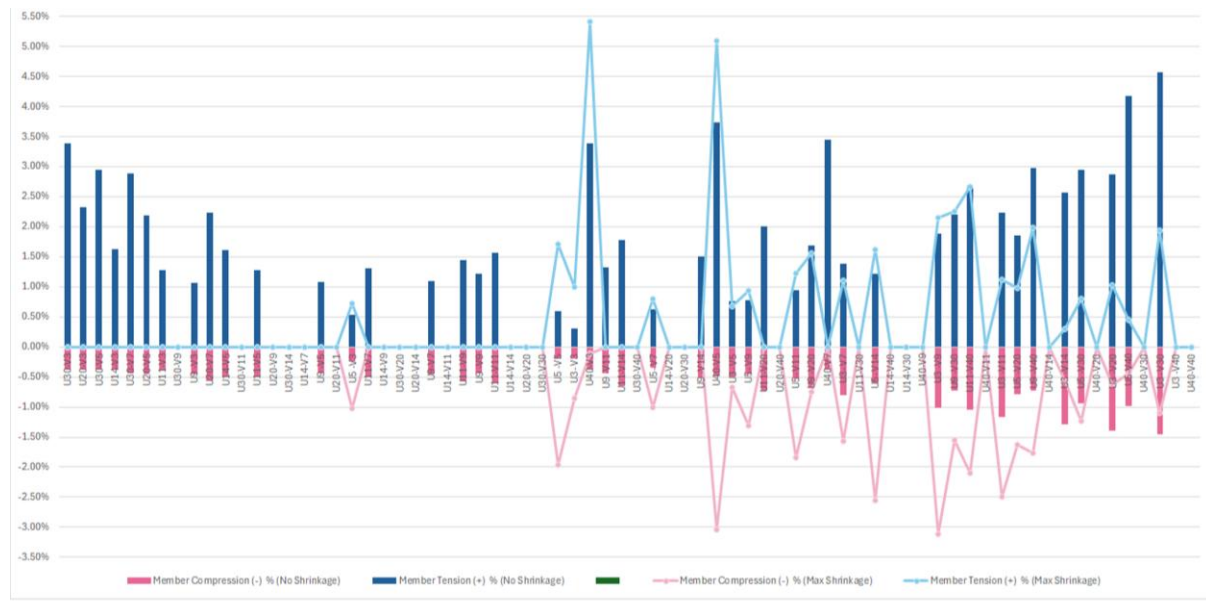


Fig5.26 Member Deformation Before vs. After Shrinkage in Yoshimura Pattern (Ordered (left to right) by Unit Aspect Ratio: Low to High)

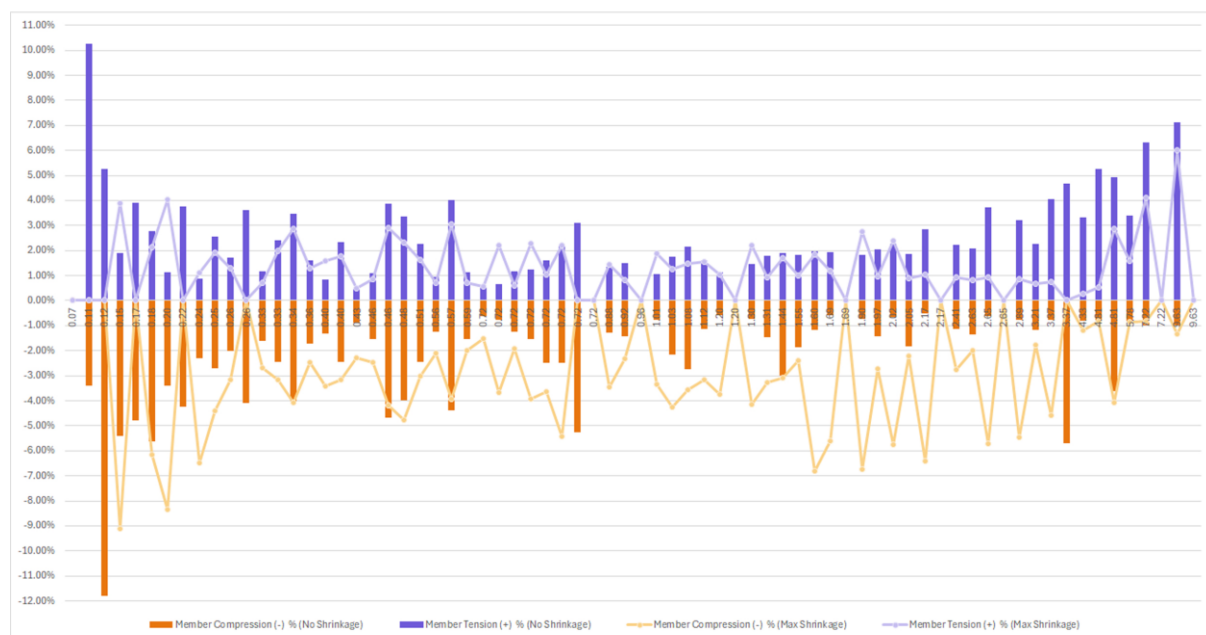
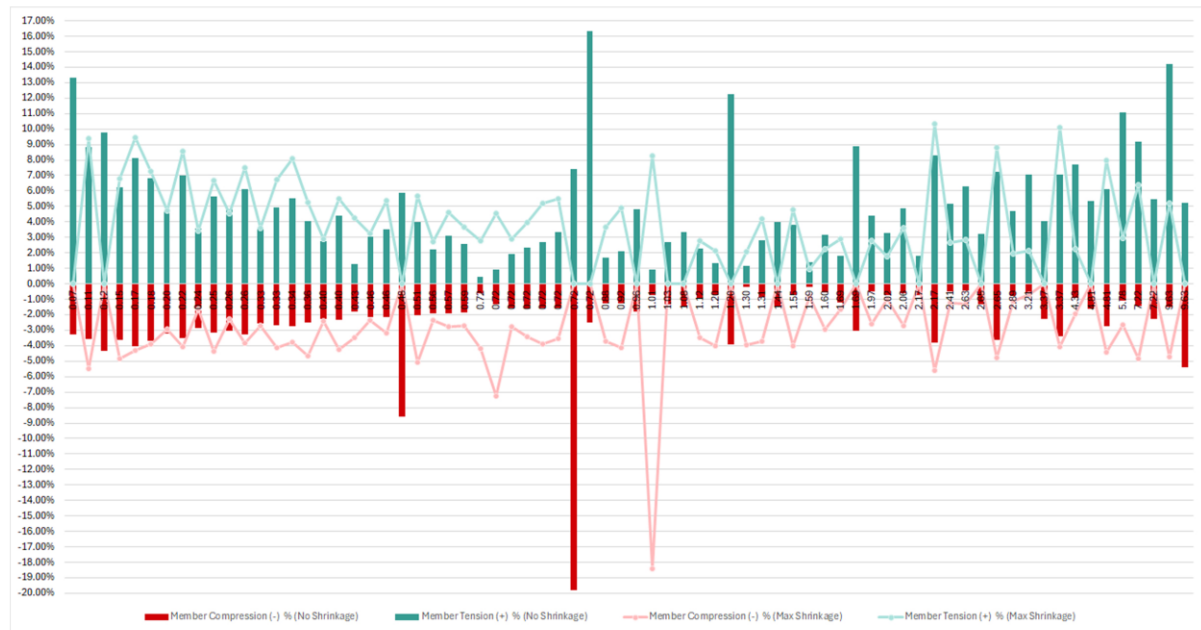


Fig5.27 Member Deformation Before vs. After Shrinkage in Kresling Pattern (Ordered (left to right) by Unit Aspect Ratio: Low to High)



Fif5.28: Member Deformation Before vs. After Shrinkage in Waterbomb Pattern (Ordered (left to right) by Unit Aspect Ratio: Low to High)

5.4.4 Overall Interpretation

While the analysis did not reveal any strong or consistent patterns linking shrinkage, subdivision density, or unit aspect ratio individually to member deformation, this does not necessarily imply that these factors have no influence on structural behavior. It is possible — and even likely — that member deformation results from a complex interplay of multiple factors, including but not limited to the three explored in this study. These variables may interact in ways that mask direct correlations when assessed independently. Therefore, it is important to recognize that the absence of clear individual trends does not rule out their combined or indirect effects. Future research could benefit from exploring these interactions more deeply, possibly through multivariable or parametric analyses that account for the hybrid nature of structural responses.

5.5 Conclusion

The comparative analysis in this section provides a comprehensive understanding of how different folding patterns respond to varying geometric and structural conditions. By systematically examining the outcomes of multiple configurations, it highlights the ranges that lead to successful performance as well as those that result in failure or excessive deformation. This structured approach helps reduce trial and error in the design process, enabling more efficient exploration of possible configurations and allowing potential issues to be anticipated before physical or digital prototyping. Even in the absence of a single predictive formula, the analysis serves as a practical framework for interpreting the complex interactions within origami-inspired surfaces, offering insights that support informed decision-making and contribute to the development of reliable, functional structures.

06| Design Implementation

6.1 Integration into Real-World Applications

6.2 Selected Case Studies

6.3 Form Finding through Clustering

6.4 Design Strategies for Responsiveness and Adaptation

6.5 Possible Applications

6.6 Material and Construction

6.7 Imaginary Scenario of Application

6.1 Integration into Real-World Applications

Building on the positive results obtained in Section 5, where both geometry and form demonstrated adaptive and responsive behavior, this stage of the research focuses on exploring how these findings can be applied toward design implementation. By identifying the factors that influence simulation outcomes and developing a collection of positive configurations, it becomes possible to move beyond experimentation toward practical applications. The aim is to achieve a design that maximizes control over the final results while maintaining responsiveness and adaptability.

Based on the research objectives—including aesthetics, spatial efficiency, dimensional organization, structural performance, and the level of responsiveness—this stage allows for a deeper exploration of design options and the introduction of informed modifications. From each pattern studied previously, one positive case is selected as a case study to investigate the implementation of the surface in real-world contexts, focusing on its interaction with users and its functional potential.

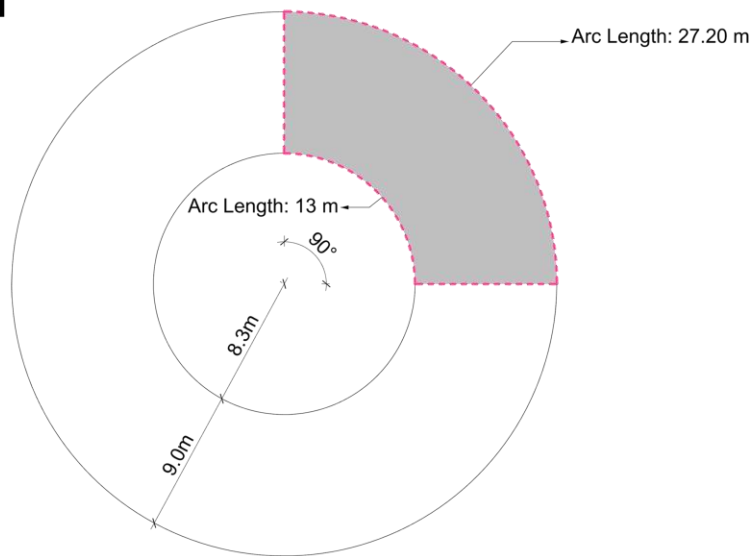
The criteria considered for selecting the final surface were as follows: the surface needed to demonstrate effective shrinkage behavior, allowing for maximum adaptability. Second, it was important that the surface exhibited an appropriate unit density, enabling partial or localized transformations. Third, the dimensions of the individual units were chosen to achieve an optimal folding height, ensuring both functional usability and sufficient positive elevation for user interaction. Finally, from an aesthetic perspective, the surface was selected to express the inherent qualities of the origami pattern and to emphasize the conceptual idea of folding in its purest form.

6.2 Selected Case Studies

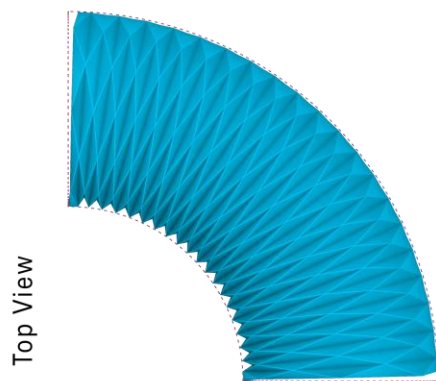
Based on the criteria outlined above, three surface configurations were selected for further analysis: the Yoshimura pattern (U3 V20), the Kresling pattern (U5 V20), and the Waterbomb pattern (U5 V11). Among all the simulated cases presented in Section 5, these configurations demonstrated the most promising performance. Both the Yoshimura and Kresling models exhibited up to 90% shrinkage with excellent shape adaptability, while the Waterbomb pattern achieved approximately 35% shrinkage with stable deformation behaviour. In all selected cases, a high number of units in the V-direction allowed the surfaces to undergo partial and localized shape transformations, ensuring improved adaptability and responsiveness. The following pages present the results of simulations incorporating the new target curve.

From a visual and aesthetic perspective, the selected surfaces also provide a strong fold expression, with clearly visible mountains and valleys that emphasize the conceptual idea of folding. This visual depth is perceptible from both the interior and exterior, particularly in semi-folded and fully shrunken states, effectively conveying the dynamic and transformative nature of the structure.

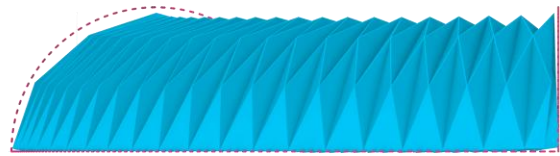
Target Curve 01



Yoshimura | U3 V20



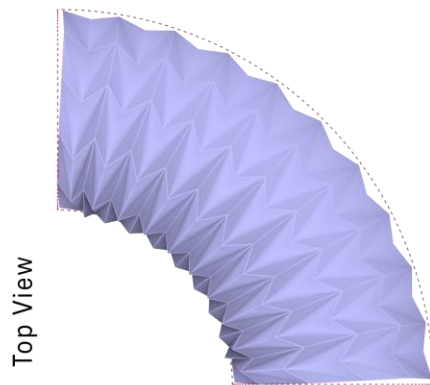
Back View



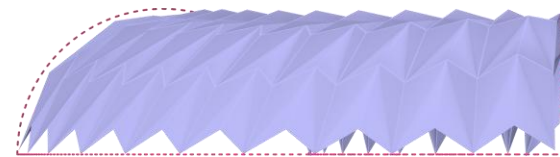
Left View



Kresling | U5 V20



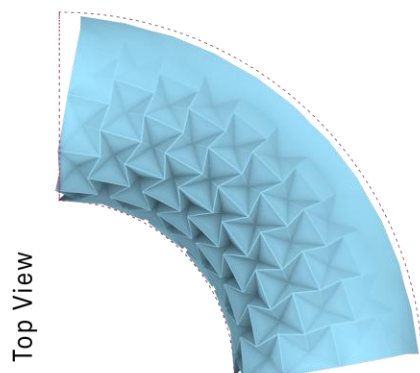
Back View



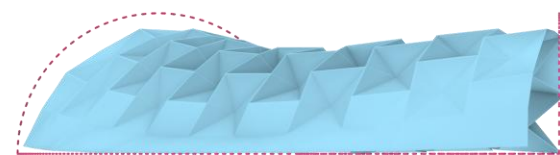
Left View



Waterbomb | U5 V11

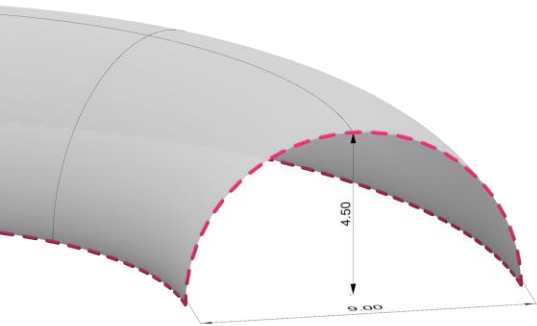


Back View



Left View





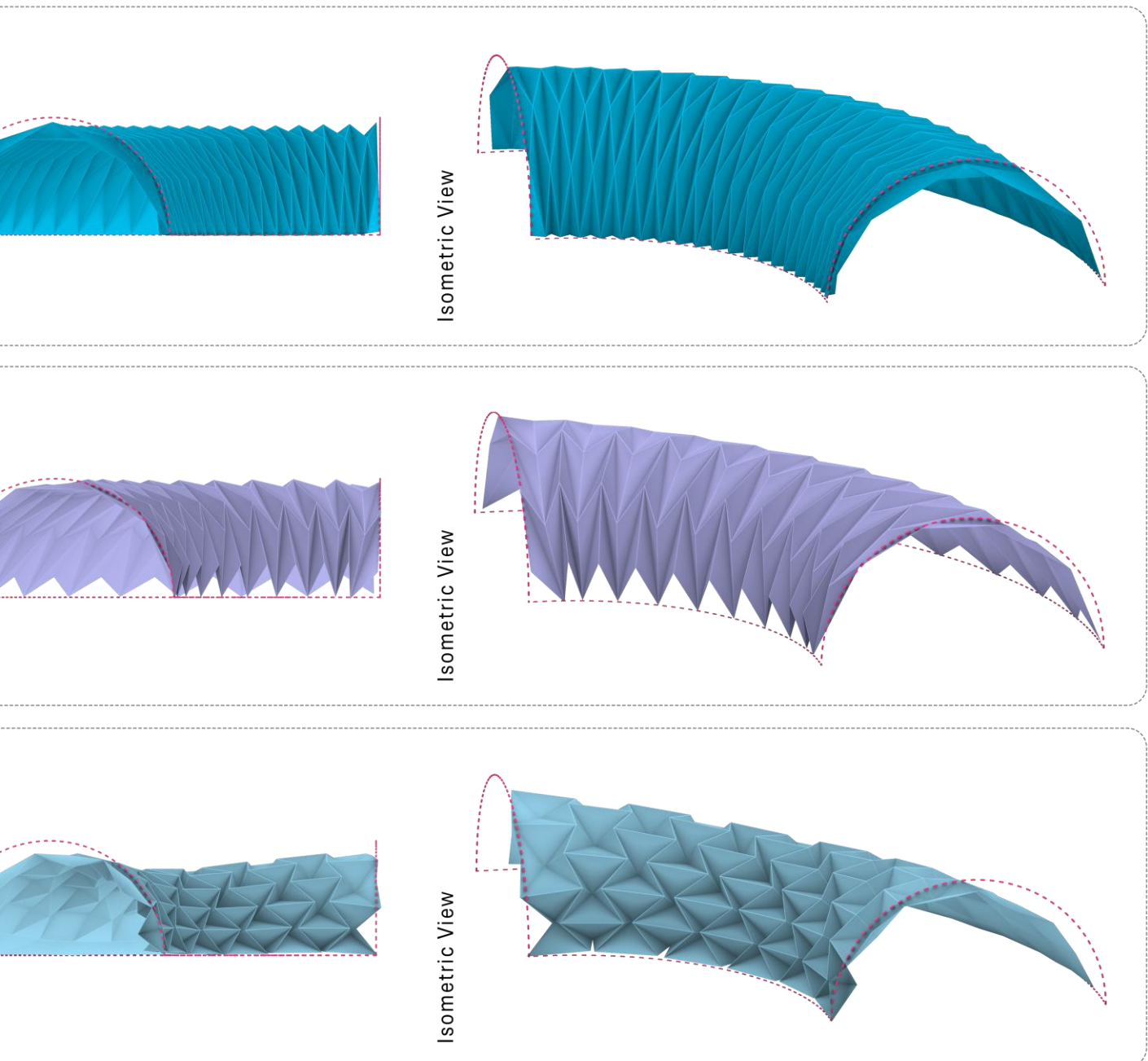
In these simulations, a quarter of a full circular ring was considered as the geometry. The outer arc length was set to 27 meters, while the inner arc length was 13 meters. This defines a sector-shaped annular domain representing the target curve region. All other parameters were kept constant throughout the simulations as:

Target Vault Radius: 4.5 meters

Target Deformation Strength: 5

Fold Intensity: 0.99 (maximum folding state)

Member Stiffness: 60



As illustrated in Figure 6.1, the dimensions of the units and their corresponding folding heights are presented to clarify the geometric behaviour of each configuration. Regarding the folding height, it is important to note that the surface features folds extending both inward and outward relative to its vault-shaped geometry. In some patterns, the dimensions of these inward and outward folds differ. For the purposes of this study, the inward fold height is of primary interest, as it directly influences the usable interior height of the space. Fold height changes based on the fold's state, with more advanced folding leading to greater height.

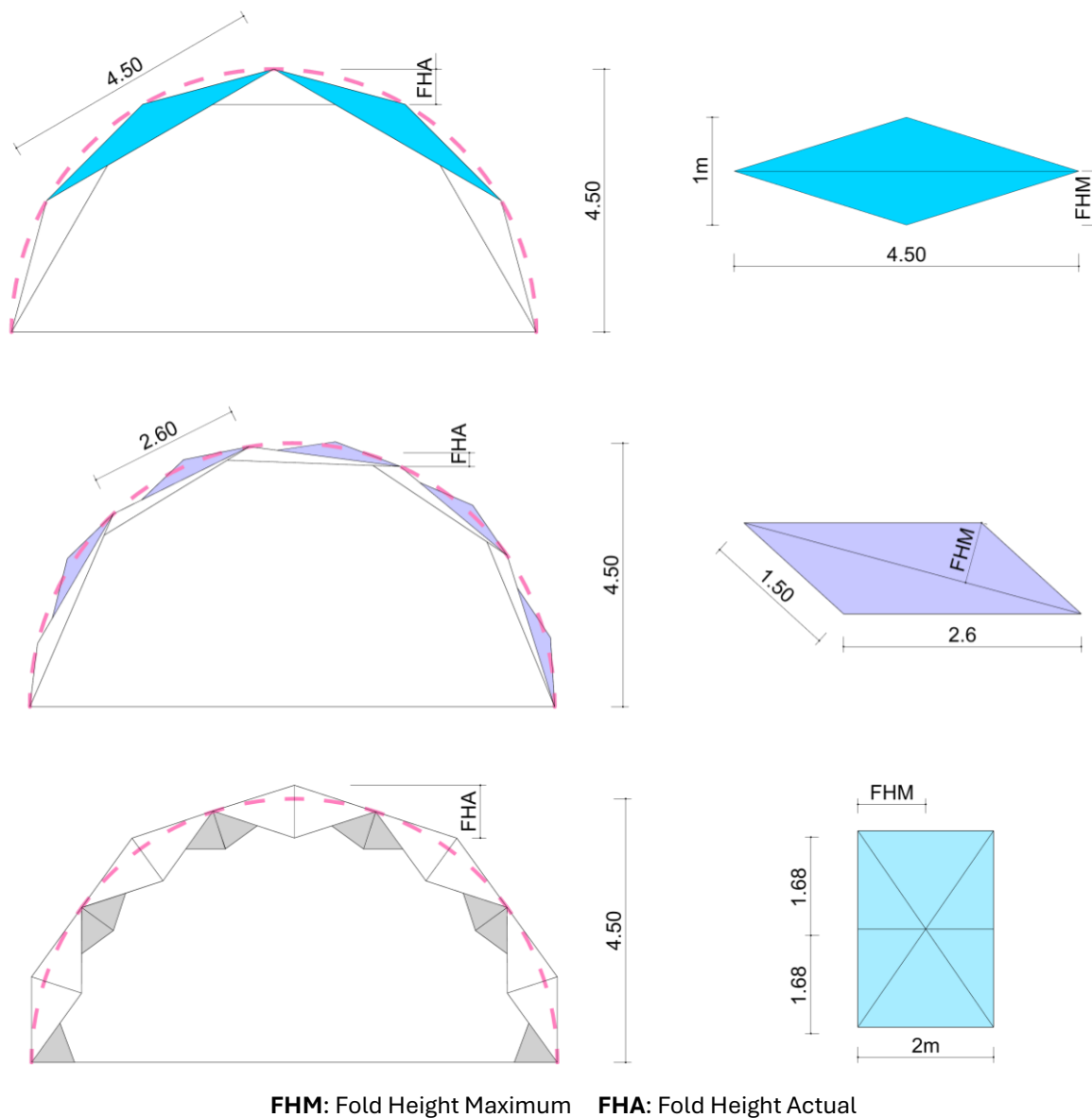


Fig 6.1: Demonstration of unit dimensions and fold heights for the patterns shown from top to bottom: Yoshimura U3 V20, Kresling U5 V20 and Waterbomb U5 V11

6.3 Form Finding through Clustering

As we explored the possibility of employing different target curves in the form-finding process, an alternative approach involves clustering: rather than designing complex surfaces as continuous forms, they can be constructed from assemblies of simpler modular surface units. This methodology enables greater flexibility and localized control over distinct regions of the geometry. For instance, a toroidal surface can be approximated by assembling four quarter-toroid units, rather than generating the entire form as a single piece. By composing complex forms from simpler elements, the structural and fabrication complexity is reduced, while the behavior of individual segments can be more systematically analyzed and optimized. Moreover, this approach provides the opportunity to expand or reduce the form in the future, which is particularly advantageous in the context of temporary and portable structures. Using modular surface units allows transformations to be achieved with reduced cost and complexity during both assembly and disassembly. Overall, this clustering strategy provides an effective framework for exploring intricate surface geometries while maintaining practical control over both form and structural performance.

By referring to our two previous curve targets, it is possible—through simple geometric compositions of these forms—to achieve a wide variety of spatial configurations. Although the dimensions represented in this study were intended for small to mid-scale spaces, they can be adjusted according to the building's purpose and performance goals, allowing for both expansion and reduction as needed.

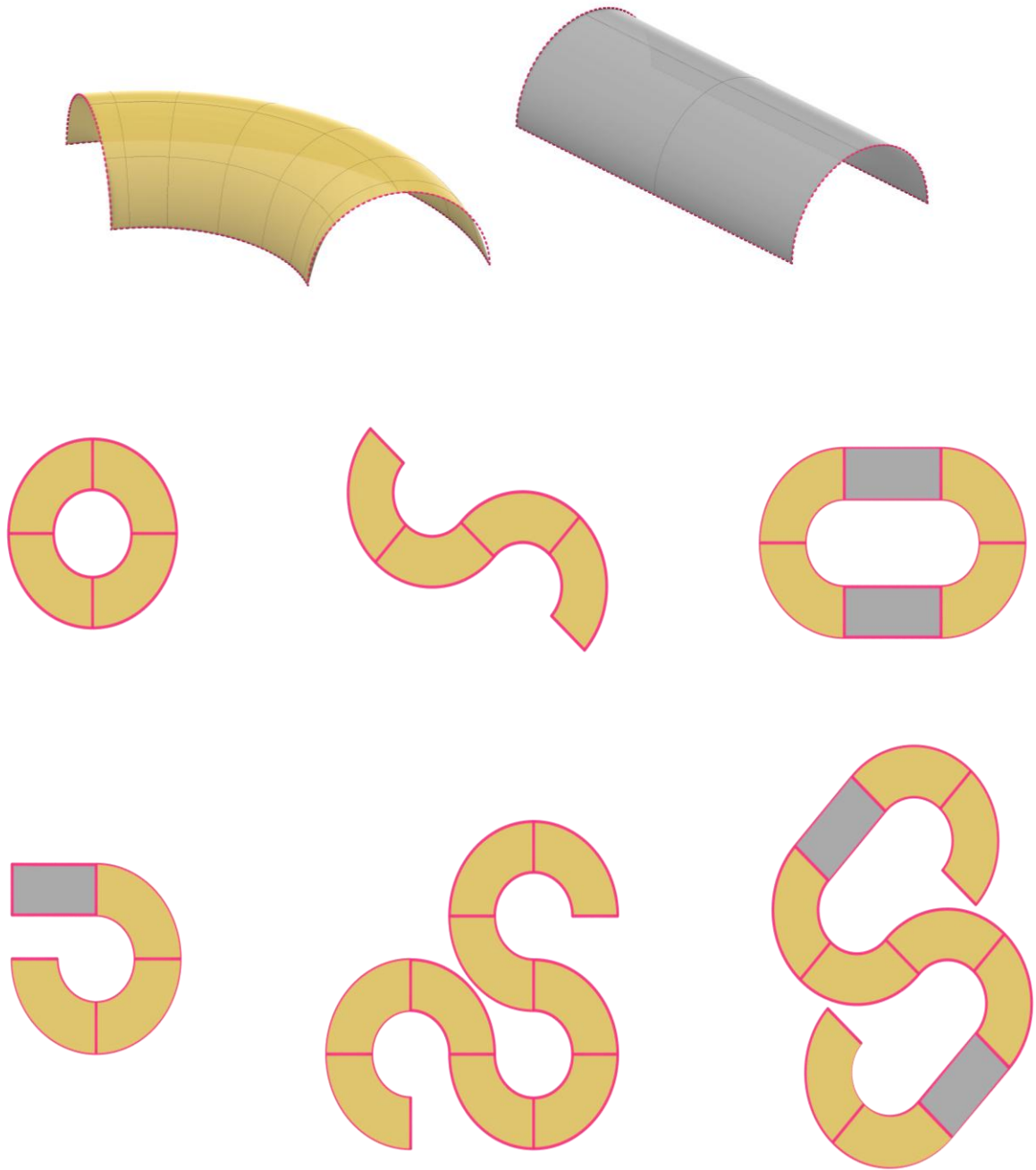


Fig 6.2 From top to bottom: Two Proposed Target Curve, Possible Clustering Configuration in Form Finding

6.4 Design Strategies for Responsiveness and Adaptation

Up to this point, we have explored form-finding processes and the various possibilities and opportunities that the mentioned origami pattern can provide in surface design. However, this study also has another important objective: investigating responsiveness and user interaction in surface design. To address this, two possible responsive actions were proposed: Shrinkage and Lateral Opening, which will be explained in detail in the following sections.

In section 5, the concept of shrinkage within the surface was examined, focusing on its behaviour across different origami patterns and the associated limitations and opportunities. However, when considering the real-world implementation of origami-based surfaces, it becomes essential to explore more deeply the potential applications of shrinkage in surface design.

Lateral opening, on the other hand, refers to the introduction of openings along the sides of a vault-shaped surface. This approach represents a geometric transformation made possible by origami principles. As previously discussed, the selected pattern allows for partial deformation, giving the surface the ability to open laterally without compromising its overall structural integrity. Beyond enhancing adaptability and user interaction, the inclusion of lateral openings adds a higher level of formal complexity and visual richness to the design. It expands the potential for form-finding and exploration of aesthetic qualities, while also generating semi-open intermediary spaces that create stronger connections between the interior and the surrounding environment.

For the sake of clarity, from this point onward, we will focus on one final combination of surfaces to continue exploring the use of shrinkage and lateral opening.

- **Shrinkage and lateral opening for pathways and circulation:** Shrinkage can be used to create temporary openings within a closed surface, providing flexible points of entry and exit for users. This allows pathways to adapt dynamically during occupancy, enabling the entrance and exit locations to be changed according to functional needs or user preferences.
- **Shrinkage and lateral opening for Space Expansion and Contraction:** Another key application of shrinkage is the ability to adapt the dimensions of a space in real time. A surface can be compressed to its minimum size and then expanded as needed, allowing the spatial volume to respond to changing functional requirements.
- **Shrinkage and lateral opening for experience change:** Shrinkage allows a surface or structure to redefine space for multiple uses. The geometry of the surface, along with the varying degrees of folding, can reintroduce new spatial qualities and shape user experience, enabling the same physical space to adapt and transform according to the desired impact on its users.

6.5 Possible Applications

The adaptive folding systems explored in this thesis demonstrate how origami geometry can enable surfaces to expand, contract, and transform in response to spatial, functional, or environmental demands. The ability of these forms to reconfigure—while remaining materially efficient and structurally stable—positions them as promising components within contemporary architecture. Below are key domains where such systems present clear potential:

- **Temporary and Mobile Installations:** Origami-based adaptive structures are ideal for non-permanent, deployable architectural interventions. Their ability to fold into compact volumes for transportation and unfold into spatially rich environments allows for:
 - Urban pop-up installations that respond to shifting cultural events:
 - Mobile pavilions that can be assembled in one location today and relocated the next day.
 - Flexible exhibition or performance spaces that adapt to different urban sites without the need for heavy logistical systems.
- **Dynamic Market and Public Space Infrastructure:** Many urban contexts host daily or weekly markets, fairs, and temporary communal activities. Origami-inspired surfaces can serve as:
 - Retractable canopies and stalls that open during market hours and fold away when not in use.
 - Shading and spatial dividers that adjust based on crowd density or flow.
 - The ability to reconfigure allows one system to serve multiple spatial scales, from individual vendor booths to larger communal coverings.
- **Extensions to Existing Buildings:** Adaptive origami surfaces can operate as temporary or seasonal architectural extensions, adding functional flexibility to build environments:
 - Retractable balconies, terraces, or outdoor rooms that expand when needed and fold back to reduce footprint.
 - Pop-out study or work modules for educational campuses or co-working spaces.
 - Temporary circulation or waiting areas, especially in contexts with fluctuating user density (e.g., museums, hospitals).
- **Emergency and Humanitarian Deployable Shelters:** The lightweight, compact, and rapidly deployable nature of origami-based systems makes them well-suited for:
 - Disaster relief shelters that can be transported efficiently and assembled quickly.
 - Expandable modular units that can adapt to family size or specific site conditions.
 - Climate-responsive shelters that open for ventilation or close for protection depending on needs.

- **Environmental Control: Shading, Ventilation, and Light Modulation:** Origami forms inherently create variable porosity and dynamic apertures, making them useful as environmental regulators:
 - Adaptive shading systems for public spaces, façades, or courtyards.
 - Foldable greenhouse skins that facilitate efficient installation, dismantling, or mobility for temporary growing zones, control solar gain, humidity, and airflow.
 - Responsive skylights that alter geometry to regulate daylight penetration or night-time insulation.

- **Event Architecture and Festival Infrastructure:** Due to their speed of deployment and sculptural quality, these systems are highly suited for:
 - Festival stages, domes, and audience shelters.
 - Interactive public art installations where movement and transformation become part of the experiential design.

6.6 Material and Construction

The structural and material strategies of this project are fundamentally shaped by the geometric logic of origami and by the need for controlled, reversible transformation. Because the proposed surface is designed to fold, expand, and contract, its material system must balance rigidity and flexibility, while its structural framework must support both local deformation and global movement. This section examines the architectural precedents and technical principles that inform the proposal, focusing on how adaptive materials, lightweight composite assemblies, and kinetic structural mechanisms can be integrated to create a responsive vault-like surface.

The structural concept of this project is organized around two primary components:

- **the material system that forms the adaptive surface.**
- **the Structure that enables its shrinkage, expansion, and movement.**

6.7.1 Unit's Material

For the surface material itself, two primary options are under consideration, inspired by precedents discussed in Section 4.

- **Plywood:** A lightweight, affordable material that is easy to machine—by cutting, drilling, or CNC milling. It offers a warm, natural finish while maintaining durable performance over time, making it ideal for modular applications. These qualities are clearly demonstrated in projects such as the *Resonant Chamber*, the *HygroSkin Pavilion*, and *Translated Geometry*. Standard panels—typically around 1.2×2.4 m and 12–18 mm thick—simplify both design and assembly, and when produced under strict quality control plywood provides consistent structural behaviour..(Sandoval *et al.*, 2025)

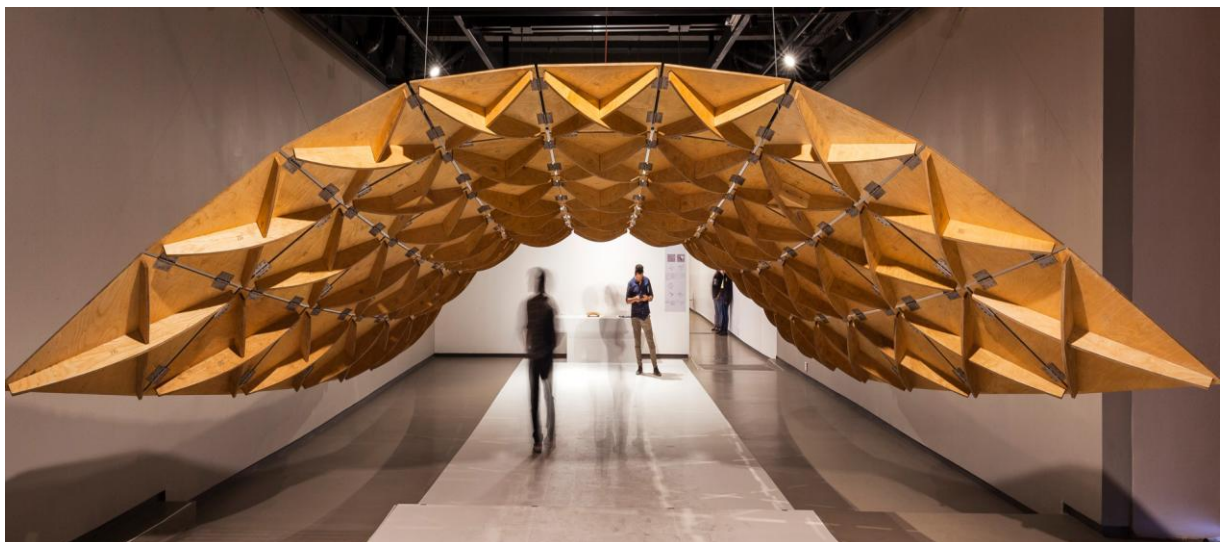


Fig 6.7: Rigid Origami Inspired Pavilion in Plywood Material(Skidmore, 2018)

- **PTFE:** commonly known by its commercial name Teflon, is a high-performance fluoropolymer characterized by exceptional chemical inertness, very low surface energy, and outstanding thermal stability. When used in architectural membranes, a woven glass-fibre base cloth is coated with PTFE to produce a material that is both strong and durable. This makes it especially suitable for long-span tensile or membrane structures. PTFE fabrics resist cracking under repeated flexural stress, endure exposure to UV radiation, and maintain performance over decades. In addition to durability, PTFE membranes are relatively self-cleaning due to their low surface tension, and they can transmit diffused daylight, offering both functional and aesthetic benefits. (Ansell, Hill and Allgood, 1983)

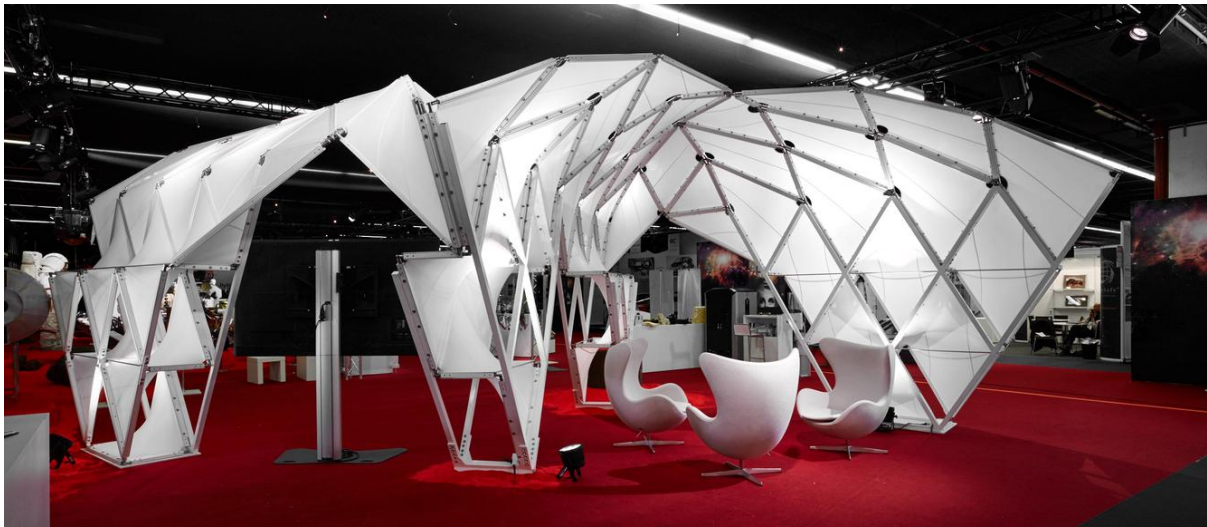


Fig 6.8: Pavilion with PTFE material (Archdaily, 2017)

6.7.2 Joints

Each origami unit in the system is fabricated separately and then connected to form the whole adaptive surface. While there are many possible connection strategies, hinges represent the most straightforward and economical solution: they allow the panels to rotate relative to one another, enabling folding and unfolding behaviour without excessively complex joints.

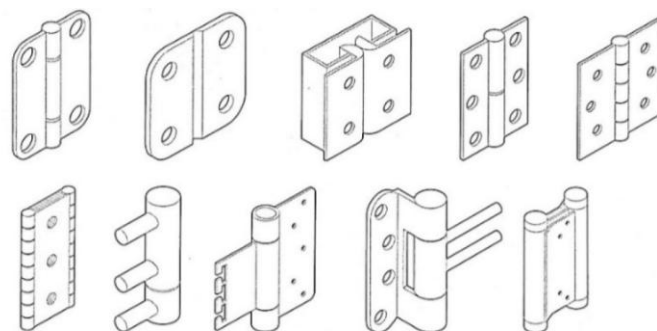


Fig 6.8: Hinge Examples (Schumacher, Schaeffer and Vogt, 2010)

6.7.3 Movement Structure

The movement mechanism of the adaptive surface is primarily inspired by the portable façade system of The Shed in New York. While the scale of that project is significantly larger than the scope of this thesis, the underlying concept is simple and adaptable to a shrinkage/expansion strategy. The system relies on **rails** and **rollers** as the main components of motion: rails are fixed along the ground, providing a defined path and structural stability, while rollers are attached at the boundaries of the surface to allow smooth translation. By constraining the vault along the rails, the form remains stable under lateral forces while enabling controlled movement. For shrinkage or expansion, a driving force is applied to the structure to slide the panels along the rails, allowing the surface to contract or extend as needed.



Fig 6.9: The Shed, Diller Scofidio + Renfro; External surface with possibility of movement.(Archdaily, 2019)

Anchor points play a critical role in this system. Some can be fixed to provide stability and braking at specific positions, while others remain movable to accommodate transformations, ensuring both safety and flexibility according to functional or spatial requirements. This design also allows the anchor points to be adjusted in real time, adapting to changing needs as they arise.



Fig 6.10: The Shed, Diller Scofidio + Renfro System of Rail and Rollers.(Archdaily, 2019)

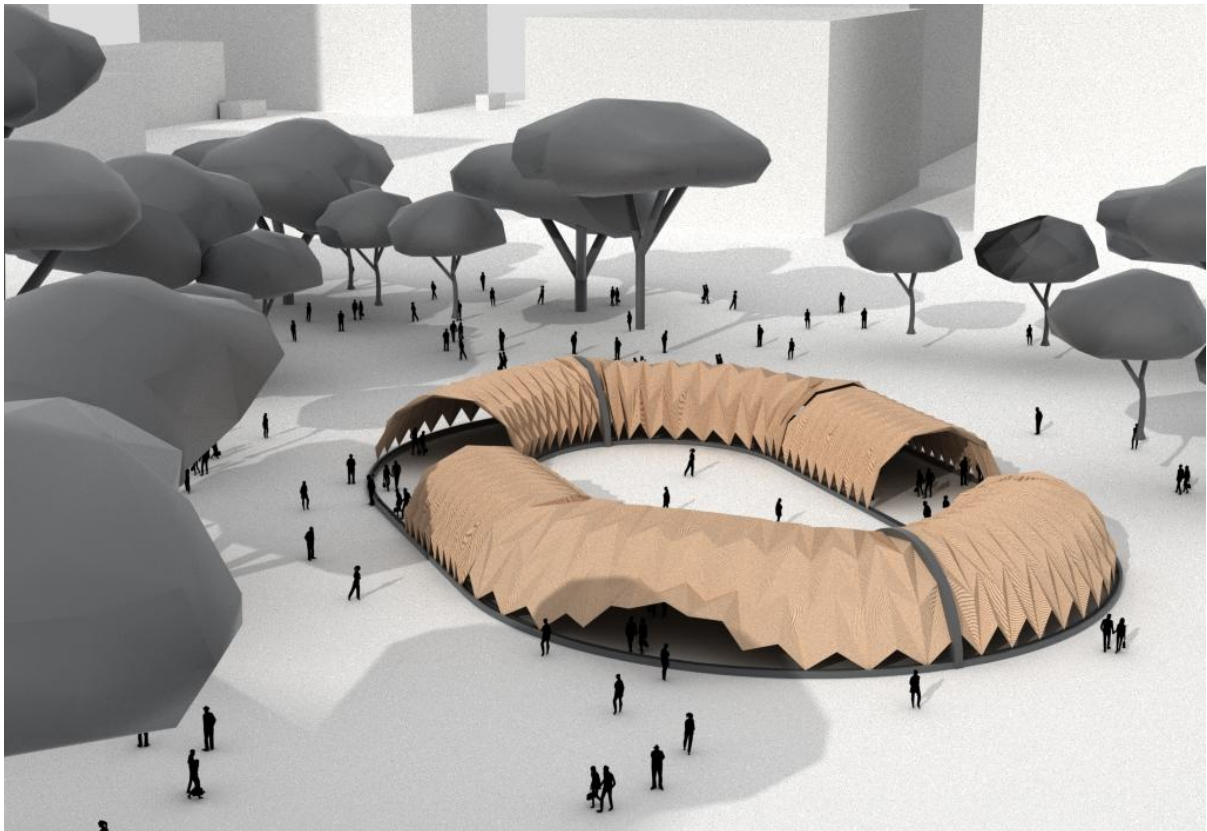
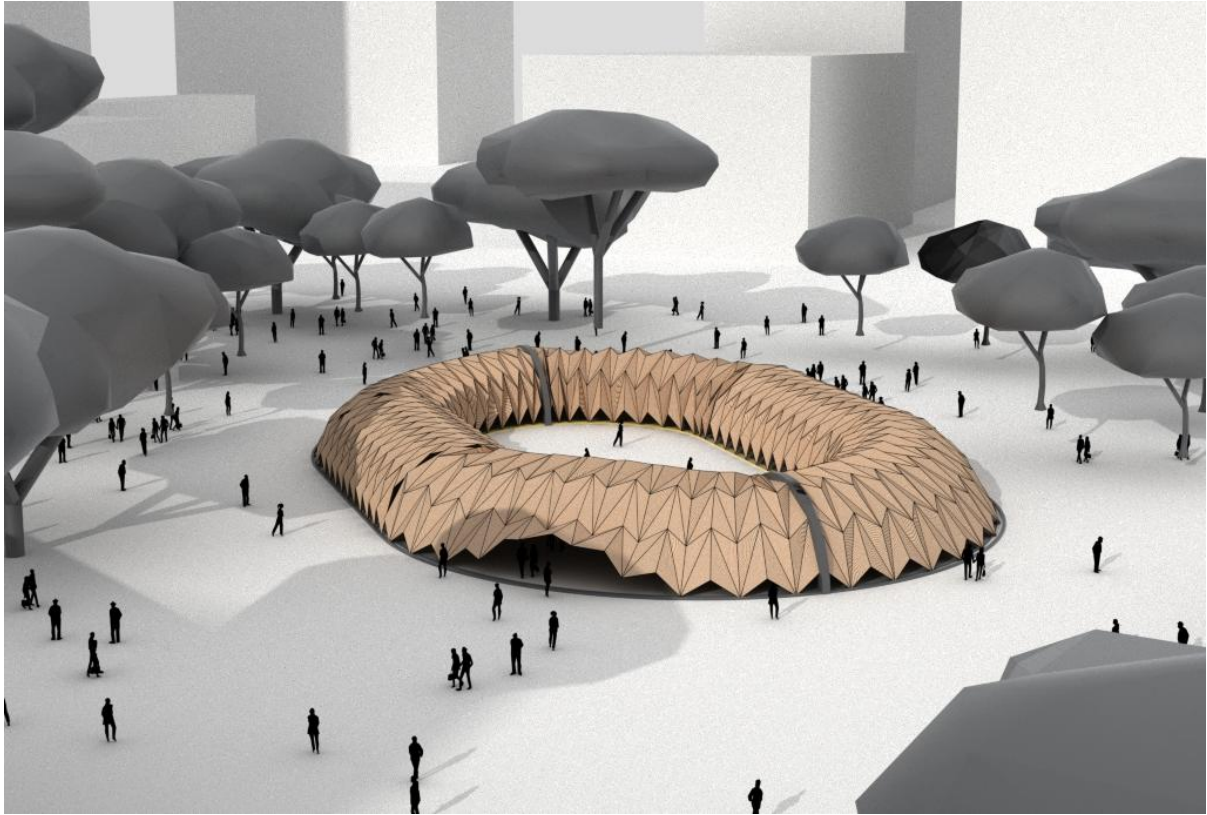
6.7.4 Actuator

Any mechanical system needs a source of energy in order to move. The source can be direct actuation by a user (manual actuation) or it can have other energy sources.(Schumacher, Schaeffer and Vogt, 2010)

For the shrinkage behavior of the surfaces studied in this thesis, the structure's low weight in many applications allows actuation simply through human pressure. For larger-scale applications, however, hydraulic or pneumatic actuators positioned along the edges of the surface can provide the necessary force to achieve controlled deformation efficiently.

Hydraulic and pneumatic actuators use pressurized fluids or gases to generate motion. They offer high power relative to their size . At their core, these actuators rely on motorized pumps that create pressure through blades, gears, screws, or pistons. In architecture, pneumatic actuators are particularly notable: pneumatic muscles, such as tensairities, consist of tubular or cushion-like chambers that expand and contract as gas pressure changes.(Osorio, Paio and Oliveira, 2023)

6.7 Imaginary Scenario of Application





07| Conclusion

This thesis has explored the potential of origami geometry as a tool for responsive architecture, demonstrating how folding patterns and adaptive surfaces can expand the possibilities of design. Through a review of responsiveness in architecture, the examination of relevant technologies, and the analysis of origami forms, the study established a framework for understanding how geometry, mechanics, and design intersect to produce adaptable structures.

The case studies provided a comprehensive understanding of which technologies and strategies have been most effectively implemented within responsive design, highlighting areas where responsiveness has been most actively explored. These investigations informed the subsequent simulations and analyses, which focused on three key origami patterns—Yoshimura, Kresling, and Waterbomb—and their behavior under vault shaping and shrinkage conditions. While no single pattern emerged as universally optimal, each displayed unique strengths, offering multiple pathways for design depending on specific functional requirements. This approach emphasizes flexibility: rather than producing a single final design, the research generated a diverse set of options, enabling tailored responses to varying needs and design goals.

The simulation and implementation phases further illustrated the richness of origami-inspired surfaces. By employing clustering strategies and targeting specific curves, it was possible to generate a wide variety of configurations from simple inputs, demonstrating the potential for large-scale adaptability and complex form-finding. Although this thesis primarily explored standard geometric patterns, the findings suggest that future studies could expand into more intricate manipulations, varying density, exaggerating local deformations, or combining patterns to enhance responsiveness and aesthetic expression.

Overall, this work reinforces that origami geometry offers a versatile and powerful approach to responsive architecture. While the technology itself is not entirely new and significant research already exists, the methods and comparative analyses presented here contribute to a deeper understanding of pattern behavior and deformation, providing a foundation for more informed design decisions. The maps, simulations, and flexible frameworks developed in this thesis serve as a tool for anticipating performance, reducing trial and error, and exploring the vast design space that origami forms can unlock. Future research can build on these insights to push the boundaries of adaptive structures, combining creativity, geometry, and engineering to open new possibilities in architecture.

References

{ArchDaily} (2013) Q1, ThyssenKrupp Quarter Essen / JSWD Architekten + Chaix & Morel et Associés. Available at: <https://www.archdaily.com/326747/q1-thyssenkrupp-quarter-essen-jswd-architekten-chaix-morel-et-associes> (Accessed: 05 Nov).

Akgün, Y., Erkarlan, Ö.E. and Kavuncuoğlu, C. (2022) 'Tectonics of kinetic architecture: Moving envelope, changing space and the shades of the shed', *Frontiers in Built Environment*, Volume 8 - 2022 Available at: 10.3389/fbuil.2022.1006300

Ansell, M., Hill, C. and Allgood, C. (1983) 'Architectural PTFE-Coated Glass Fabrics--Their Structure and Limitations', *Textile Research Journal - TEXT RES J*, 53, pp. 692-700. Available at: 10.1177/004051758305301110

Archdaily (2017) Teflon Pavilion. Available at: https://www.archdaily.com/872182/unstudio-designs-teflon-pavilion-to-test-concepts-for-extraterrestrial-living/5926ed85e58ece88db0003bd-unstudio-designs-teflon-pavilion-to-test-concepts-for-extraterrestrial-living-photo?next_project=no (Accessed: 18 Oct).

Archdaily (2019) The Shed. Available at: <https://www.archdaily.com/914639/the-shed-a-center-for-the-arts-diller-scofidio-plus-renfro> (Accessed: 04 Sep).

Chen, Y., Feng, H., Ma, J., Peng, R. and You, Z. (2016) 'Symmetric waterbomb origami', *Proceedings of the Royal Society A: Mathematical, Physical and Engineering Science*, 472, p. 20150846. Available at: 10.1098/rspa.2015.0846

Davis, E., Demaine, E., Demaine, M. and Ramseyer, J. (2014) 'Reconstructing David Huffman's Origami Tessellations'.

Evans, T., Lang, R., Magleby, S. and Howell, L. (2015) 'Rigidly Foldable Origami Gadgets and Tessellations', *Royal Society Open Science*, 2 Available at: 10.1098/rsos.150067

Foschi, R. (2022) *Origami Design Strategies for Architects and Designers: Analysis and Design of Folded Surfaces Through Algorithmic Modelling*. Bononia University Press.

Fox, M. (2016) *Interactive Architecture: Adaptive World*. Princeton Architectural Press.

Fox, M. and Kemp, M. (2009) *Interactive Architecture*. Princeton Architectural Press.

References

Fujimoto, S. (1978) *Twist Origami 1*. Self-published.

Haitong, L., Guangbo, H., Olszewski, O., Jiang, Z. and Zhang, K. (2023) 'Design of a foldable origami mechanism with helical motion inspired by the Resch Triangular Tessellation', *Mechanism and Machine Theory*, 179, p. 105101. Available at: <https://doi.org/10.1016/j.mechmachtheory.2022.105101>

Hardingham, S. (2003) *Cedric Price: Opera*. Wiley.

Hatori, K. (2011) 'History of Origami in the East and the West before Interfusion', in., pp. 3-11. doi: 10.1201/b10971-3.

Herdt, T. (2021) 'From Cybernetics to an Architecture of Ecology', *FOOTPRINT*, 15 Available at: 10.59490/FOOTPRINT.15.1.4946

Hernández Vargas, J. (2015) 'From the Fun Palace to the Generator Cedric Price and the conception of the first intelligent building', *ARQ*, pp. 48-57.

Jackson, P. (2011) *Folding Techniques for Designers: From Sheet to Form*. Quercus.

Karakoç, E. and Çağdaş, G. (2021) 'Adaptive Architecture Based on Environmental Performance: An Advanced Intelligent Façade (AIF) Module', *Gazi University Journal of Science*, 34(3), pp. 630-650. Available at: 10.35378/gujs.725902

Karanouh, A. and Kerber, E. (2015) 'Innovations in dynamic architecture', *Journal of Facade Design and Engineering*, 3, pp. 185-221. Available at: 10.3233/FDE-150040

Kresling, B. (2012) 'Origami-structures in nature: Lessons in designing "smart" materials', *MRS Proceedings*, 1420 Available at: 10.1557/opl.2012.536

Kronenburg, R., Lim, J. and Chii, W.Y. (2003) *Transportable Environments 2*. Taylor & Francis.

L, G. (2008) 'Cedric Price's Generator and the Frazers' systems research', *Technoetic Arts*, 6, pp. 55-72. Available at: 10.1386/tear.6.1.55_1

Lang, R. and Hull, T. (2011) 'Origami design secrets: mathematical methods for an ancient art', *The Mathematical Intelligencer*, 27, pp. 92-95. Available at: 10.1007/BF02985811

References

Lang, R.J. (2011) *Origami Design Secrets: Mathematical Methods for an Ancient Art, Second Edition*. Taylor & Francis.

Lang, R.J., Wang-Iverson, P. and Yim, M. (2016) *Origami 5: Fifth International Meeting of Origami Science, Mathematics, and Education*.

Lee, J. and Ostwald, M. (2021) 'Characterizing Smart Environments as Interactive and Collective Platforms: A Review of the Key Behaviors of Responsive Architecture', *Sensors*, 21, p. 3417. Available at: 10.3390/s21103417

Lee, J.H., Ostwald, M.J. and Kim, M.J. (2021) 'Characterizing Smart Environments as Interactive and Collective Platforms: A Review of the Key Behaviors of Responsive Architecture', *Sensors (Basel)*, 21(10) Available at: 10.3390/s21103417

Liu Cheng, A. (2023) *The Intelligent Built-Environment as Cyber-Physical System*. doi: 10.7480/abe.2023.24.

Maden, F. (2019) *Kinetic Architecture: Responsive Facades and Structures*.

Mathews, S. (2007) *From Agit-prop to Free Space: The Architecture of Cedric Price*. Black Dog Pub. Limited.

Megahed, N. (2016) 'Understanding kinetic architecture: typology, classification, and design strategy', *Architectural Engineering and Design Management*, 13, pp. 1-17. Available at: 10.1080/17452007.2016.1203676

Meloni, M., Cai, J., Zhang, Q., Lee, D.S.-H., Li, M., Ruijun, M., Parashkevov, T. and Feng, J. (2021) 'Engineering Origami: A Comprehensive Review of Recent Applications, Design Methods, and Tools', *Advanced Science*, 8 Available at: 10.1002/advs.202000636

Miura, K. and Kenkyūjo, U.K. (1985) *Method of Packaging and Deployment of Large Membranes in Space*. Institute of Space and Astronautical Sciences.

O'Neil, J., Deleo, A.A., Yasuda, H., Salviato, M. and Yang, J. (2018) *Deployable Structures Constructed from Composite Origami*.

Osorio, F. (2014) *Geometry of Kinetic Folded Surfaces*.

References

Osorio, F., Paio, A. and Oliveira, S. (2023) 'A kinetic origami surfaces methodology', *Architectural Science Review*, 67, pp. 1-24. Available at: 10.1080/00038628.2023.2182270

Price, C. (1960-1964) Fun Palace: interior perspective. Available at: <https://www.cca.qc.ca/en/search/details/collection/object/378817> (Accessed: 10 February).

Price, C. (1964) Fun Palace: typical short section. Available at: <https://www.cca.qc.ca/en/search/details/collection/object/309793>.

Price, C. (1976-1979) Generator: Site plan showing initial layout of bases. Available at: <https://www.cca.qc.ca/en/search/details/collection/object/322218> (Accessed: 10 February).

Price, C. (1978) Generator: Axonometrics showing typical assembly details. Available at: <https://www.cca.qc.ca/en/search/details/collection/object/456288> (Accessed: 10 February).

Resch, R.D. (1967) Made With Paper. Available at: <http://www.ronresch.org/ronresch/gallery/made-with-paper-show-nov-1967/madepaper7.Crp.png/view.html> (Accessed: 25 Sep).

Resch, R.D. (1968) *Self-supporting structural unit having a three-dimensional surface* Patent no. 3407558A. Available at: <https://patents.google.com/patent/US3407558A/en> (Accessed: 30 July 2025).

Resch, R.D. (1976) *Self-supporting structural unit having a three-dimensional surface*. Patent no. 4059932A. Available at: <https://patents.google.com/patent/US4059932A/en#patentCitations> (Accessed: 30 July 2025).

Sachithanandan, J., Uriol Balbin, I. and Solano López, P. (2023) 'Preliminary Design of a CubeSat Demonstrator for an Origami-inspired Deployable Structure', *International Astronautical Congress (IAC)* Baku, Azerbaijan, 2-6 October. IAF.

Sandoval, M., Javadi, M., Soto-Zúñiga, P., Cárdenas-Ramírez, J.P., Arnett, M., Oñate, A., Cancino, R., Flores, E. and Tuninetti, V. (2025) 'Full Orthotropic Mechanical Characterization of *Pinus radiata* Plywood Through Tensile, Compression and Shear Testing with Miniaturized Specimens', *Forests*, p. 1676. Available at: 10.3390/f16111676

References

Schmidt, R. and Austin, S. (2016) *Adaptable Architecture: Theory and practice*. Taylor & Francis.

Schumacher, M., Schaeffer, O. and Vogt, M.M. (2010) *MOVE: Architecture in Motion - Dynamic Components and Elements*. Birkhäuser Basel.

Skidmore, O.M.L.S. (2018) Kinematic Pavilion. Available at: <https://www.som.com/ideas/> (Accessed: 20 Oct).

Stachel, H. (2009) 'Remarks on Miura-ori, a Japanese folding method', *JIDEG: Journal of Industrial Design and Engineering Graphics*, 52.

Tachi, T. (2013) *Designing Freeform Origami Tessellations by Generalizing Resch's Patterns* (135).

Tateishi, K. (2016) 'Deictic properties of origami technical terms and translatability: Cross-linguistic differences between english and Japanese', in., pp. 13-28.

Wang, X., Qu, H., Zhao, K., Yang, X. and Guo, S. (2024) 'Kresling origami derived structures and inspired mechanical metamaterial', *Smart Materials and Structures*, 33 Available at: 10.1088/1361-665X/ad5a5a

Wiener, N. (2019) *Cybernetics or Control and Communication in the Animal and the Machine*. The MIT Press.

Xia, X., Spadaccini, C. and Greer, J. (2022) 'Responsive materials architected in space and time', *Nature Reviews Materials*, 7, pp. 1-19. Available at: 10.1038/s41578-022-00450-z

Xing, D. and You, Z. (2023) 'Origami Claw Tessellation and Its Stacked Structure', *Journal of Mechanisms and Robotics*, 16 Available at: 10.1115/1.4056828

Yamaki, N. and Kodama, S. (1976) 'Postbuckling behavior of circular cylindrical shells under compression', *International Journal of Non-Linear Mechanics*, 11(2), pp. 99-111. Available at: [https://doi.org/10.1016/0020-7462\(76\)90008-1](https://doi.org/10.1016/0020-7462(76)90008-1)

Yin, P., Han, H., Tang, L., Tan, X., Guo, M., Xia, C. and Aw, K. (2024) 'Kresling origami-inspired electromagnetic energy harvester with reversible nonlinearity', *Smart Materials and Structures*, 33 Available at: 10.1088/1361-665X/ad27fb

Yogesh, S., Yogalakshmi, M., Abishek, M., Prasath, R.A. and Madhusudanan, G. (2021) 'Origami based folding techniques for solar panel applications', *IJEET*, 12(3), pp. 158-164.

References

Yoshimura, Y. (1955) *On the Mechanism of Buckling Pattern of a Circular Cylindrical Shell under Axial Compression* (NACA TM-1390). Washington, D.C.: NACA Technical Memorandum 1390. Available at: <https://ntrs.nasa.gov/citations/19930093840> (Accessed: 10 August 2025).

Zuk, W. and Clark, R.H. (1970) *Kinetic Architecture*. Van Nostrand Reinhold.